ISSN
2395-6992

International Journal of Engineering Research & Science

www.ijoer.com
www.adpublications.org

Volume-4! Issue-3! March, 2018 www.ijoer.com ! info@ijoer.com

Preface

We would like to present, with great pleasure, the inaugural volume-4, Issue-3, March 2018, of a scholarly journal, *International Journal of Engineering Research & Science*. This journal is part of the AD Publications series *in the field of Engineering, Mathematics, Physics, Chemistry and science Research Development*, and is devoted to the gamut of Engineering and Science issues, from theoretical aspects to application-dependent studies and the validation of emerging technologies.

This journal was envisioned and founded to represent the growing needs of Engineering and Science as an emerging and increasingly vital field, now widely recognized as an integral part of scientific and technical investigations. Its mission is to become a voice of the Engineering and Science community, addressing researchers and practitioners in below areas

Chemical Engineering	
Biomolecular Engineering	Materials Engineering
Molecular Engineering	Process Engineering
Corrosion Engineering	
Civil Engineering	
Environmental Engineering	Geotechnical Engineering
Structural Engineering	Mining Engineering
Transport Engineering	Water resources Engineering
Electrical Engineering	
Power System Engineering	Optical Engineering
Mechanical Engineering	
Acoustical Engineering	Manufacturing Engineering
Optomechanical Engineering	Thermal Engineering
Power plant Engineering	Energy Engineering
Sports Engineering	Vehicle Engineering
Software Engineering	
Computer-aided Engineering	Cryptographic Engineering
Teletraffic Engineering	Web Engineering
System Engineering	
Mathematics	
Arithmetic	Algebra
Number theory	Field theory and polynomials
Analysis	Combinatorics
Geometry and topology	Topology
Probability and Statistics	Computational Science
Physical Science	Operational Research
Physics	
Nuclear and particle physics	Atomic, molecular, and optical physics
Condensed matter physics	Astrophysics
Applied Physics	Modern physics
Philosophy	Core theories

Chemistry	
Analytical chemistry	Biochemistry
Inorganic chemistry	Materials chemistry
Neurochemistry	Nuclear chemistry
Organic chemistry	Physical chemistry
Other Engineering Areas	
Aerospace Engineering	Agricultural Engineering
Applied Engineering	Biomedical Engineering
Biological Engineering	Building services Engineering
Energy Engineering	Railway Engineering
Industrial Engineering	Mechatronics Engineering
Management Engineering	Military Engineering
Petroleum Engineering	Nuclear Engineering
Textile Engineering	Nano Engineering
Algorithm and Computational Complexity	Artificial Intelligence
Electronics & Communication Engineering	Image Processing
Information Retrieval	Low Power VLSI Design
Neural Networks	Plastic Engineering

Each article in this issue provides an example of a concrete industrial application or a case study of the presented methodology to amplify the impact of the contribution. We are very thankful to everybody within that community who supported the idea of creating a new Research with IJOER. We are certain that this issue will be followed by many others, reporting new developments in the Engineering and Science field. This issue would not have been possible without the great support of the Reviewer, Editorial Board members and also with our Advisory Board Members, and we would like to express our sincere thanks to all of them. We would also like to express our gratitude to the editorial staff of AD Publications, who supported us at every stage of the project. It is our hope that this fine collection of articles will be a valuable resource for *IJOER* readers and will stimulate further research into the vibrant area of Engineering and Science Research.

Mukesh Arora

(Chief Editor)

Board Members

Dr. S.R.Boselin Prabhu

Ph.D, Wireless Sensor Networks, M.E. Network Engineering, Excellent Professional Achievement Award Winner from Society of Professional Engineers Biography Included in Marquis Who's Who in the World (Academic Year 2015 and 2016). Currently Serving as Assistant Professor in the department of ECE in SVS College of Engineering, Coimbatore.

Dr. Maheshwar Shrestha

Postdoctoral Research Fellow in DEPT. OF ELE ENGG & COMP SCI, SDSU, Brookings, SD Ph.D, M.Sc. in Electrical Engineering from SOUTH DAKOTA STATE UNIVERSITY, Brookings, SD.

Zairi Ismael Rizman

Senior Lecturer, Faculty of Electrical Engineering, Universiti Teknologi MARA (UiTM) (Terengganu) Malaysia Master (Science) in Microelectronics (2005), Universiti Kebangsaan Malaysia (UKM), Malaysia. Bachelor (Hons.) and Diploma in Electrical Engineering (Communication) (2002), UiTM Shah Alam, Malaysia

Dr. D. Amaranatha Reddy

Ph.D.(Postdocteral Fellow,Pusan National University, South Korea), M.Sc., B.Sc. : Physics.

Dr. Dibya Prakash Rai

Post Doctoral Fellow (PDF), M.Sc.,B.Sc., Working as Assistant Professor in Department of Physics in Pachhuncga University College, Mizoram, India.

Dr. Pankaj Kumar Pal

Ph.D R/S, ECE Deptt., IIT-Roorkee.

Dr. P. Thangam

BE(Computer Hardware & Software), ME(CSE), PhD in Information & Communication Engineering, currently serving as Associate Professor in the Department of Computer Science and Engineering of Coimbatore Institute of Engineering and Technology.

Dr. Pradeep K. Sharma

PhD., M.Phil, M.Sc, B.Sc, in Physics, MBA in System Management, Presently working as Provost and Associate Professor & Head of Department for Physics in University of Engineering & Management, Jaipur.

Dr. R. Devi Priya

Ph.D (CSE),Anna University Chennai in 2013, M.E, B.E (CSE) from Kongu Engineering College, currently working in the Department of Computer Science and Engineering in Kongu Engineering College, Tamil Nadu, India.

Dr. Sandeep

Post-doctoral fellow, Principal Investigator, Young Scientist Scheme Project (DST-SERB), Department of Physics, Mizoram University, Aizawl Mizoram, India- 796001.

Mr. Abilash

MTech in VLSI, BTech in Electronics & Telecommunication engineering through A.M.I.E.T.E from Central Electronics Engineering Research Institute (C.E.E.R.I) Pilani, Industrial Electronics from ATI-EPI Hyderabad, IEEE course in Mechatronics, CSHAM from Birla Institute Of Professional Studies.

Mr. Varun Shukla

M.Tech in ECE from RGPV (Awarded with silver Medal By President of India), Assistant Professor, Dept. of ECE, PSIT, Kanpur.

Mr. Shrikant Harle

Presently working as a Assistant Professor in Civil Engineering field of Prof. Ram Meghe College of Engineering and Management, Amravati. He was Senior Design Engineer (Larsen & Toubro Limited, India).

Table of Contents

Parameter Configuration Researched of Sludge Drying Treatment System on the Screw Press

Qu Qingwen[1], Hu Xiaoqing[2], Lin Chunmei[3]

Yantai Nanshan University, Machinery Department, Yantai Longkou Shandong P R China

Abstract**—** *The basic idea of modular design is applied to the planning and analysis of the screw press sludge treatment system in this paper. A combination mode of sludge treatment system is obtained. The functional modules of the system are formed. The interface information relation of each module is analyzed by system function. The process parameters of each module were precisely configured according to the dry requirements of sludge treatment and the initial sludge concentration. The transfer relationship between modules is achieved. The control parameters are determined according to the transfer relationship. The parameter basis is provided for the control design of the system.*

Keywords**—** ***Screw Process, Sludge drying treatment system, machinery, sludge concentration, control system.***

I. INTRODUCTION

The disposal of sludge is a prominent problem in current environmental protection management. How do sewage treatment plants face the problem of producing a large amount of surplus sludge every day? Due to its large quantity of production, difficulty in transferring and disposal, and the high cost of disposal, it is the focus of the work of enterprises and environmental protection departments at all levels[1-2].

Improving the concentration and dehydration efficiency of wastewater has become an important issue to realize circular economy and sustainable development. By means of mechanical compression, the mud or viscous liquid mixture is separated into solid and liquid operations, which is called squeezing dehydration. It is an effective method for high dewatering in solid-liquid separation technology. Through the improvement and optimization of the researchers, it has been widely used in the fields of chemical industry, metallurgy, energy, dyestuff, food, pharmacy and sludge treatment[3].The theory of screw squeeze is mainly used in the oil and juicing of crops[4].It is still in the initial stage to use this technology for sludge dewatering in the process of sludge dewatering. Theoretical research is not yet perfect. At present, the research in this field mainly focuses on the design of screw press structure, optimization and improvement of experiments and analysis through simulation software. Many scholars have made great progress. The relationship between the use of flocculant and the effect of dehydration was studied by Jaroslav Boráň. The use of flocculant was found under different working conditions. It is helpful to optimize the performance of screw press[5]. Li tong carried out a flocculant screening test and sludge dewatering test in gaobeidian sewage treatment plant. The following conclusions are drawn. Improving the rate of flocculating agent can improve the dewatering performance of the screw press dehydrator. The speed of the screw can be increased appropriately, and the transmission speed of the sludge in the drum is accelerated. The speed of the screw can be increased appropriately, and the transmission speed of the sludge in the drum is accelerated. So it increases the throughput. But if the speed is too fast, it will cause the export pressure drop. Thus, the moisture content of mud cake increases[6].

In addition to the above research results, some new research directions have been developed in the field of spiral squeezing sludge dewatering. Such as discrete element method, pelease /Thickening theory is applied[7].However, most of the sludge dewatering only analyzes the single equipment, and there is no systematic process analysis[8].In this paper, the function of the system is studied by modularization analysis technique. A modular sludge drying treatment system is designed. The module division and function analysis are carried out for each process of the system. The technical requirements and parameter configuration of the screw pressing technology in the sludge drying system are discussed. A new system of mechanical dehydration was established. Furthermore, the efficiency of sludge dewatering is improved. The dry degree of higher final sludge was obtained.

II. ANALYSIS OF THE DRYING PROCESS SYSTEM OF SCREW PRESS SLUDGE

The sludge drying process is mainly to realize the separation of mud and water. Water can be reused. Sludge can be reused after drying and decrement. The pollution of the sludge was eliminated. The sludge system of this study can deal with muddy water mixture with impurity content of more than 3%.Finally, it is required to get the impurity mud with the dry degree >40%.This will enable the reuse of sludge and filtered water.

The composition of sludge treatment system is shown in 'Figure1'. According to the function of the system, it mainly includes the sludge modulation processing system, the first-level dehydration system, the squeezing dehydration system and the control system.

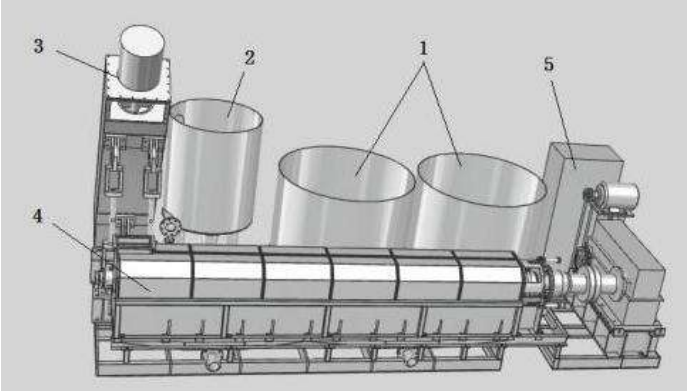

FIGURE1. SCHEMATIC DIAGRAM OF SLUDGE SCREW PRESS PROCESSING SYSTEM
1-Flocculant dissolving system, 2-Flocculation system, 3-Primary dehydration system, 4-Screw extrusion dehydration system, 5-Control system

In addition, it also includes auxiliary systems such as sludge tank and separating water and deweighting sludge. The overall operating condition of the system is shown in 'Figure 2'.

In sludge treatment system, the parameters of sludge are mainly mud content. The parameters associated with the process are fiber content. Fiber content is related to the breakdown of flocculation. In the treatment of sewage, the initial sludge content is generally uncertain, and is changed within a certain range. For example, the amount of sewage in papermaking is above 3%.Therefore, in most cases, the sludge tank is set up. The concentration of the whole pool is used as the basis for analysis. Its concentration is tested online by sensing technology. The measured value is an important parameter of control system design. The sludge modulation system consists of two parts, flocculant modulation system and flocculation process. Flocculant modulation system generally consists of particle flocculant quantification, solvent quantification, dissolving pool, proportioning pump and so on. The flocculant is generally solid, and the dissolution time is long, so the solution pool must be set. Flocculation process is the process of full mixing of sludge and flocculation solution. A variety of flocculators can be used at present. The sludge is agglomerated to form a flocculation with certain strength. The formation is separated from some water. The primary dehydration system is connected with the flocculator. After flocculation, the mixture enters the first stage of dehydration. In this study, the oblique helical device was used as the primary dehydration. The concentration of the outlet sludge is adjusted by adjusting the Angle of oblique helix. The purpose is to adapt to the requirements of subordinates. The screw press system is used as a terminal dewatering.

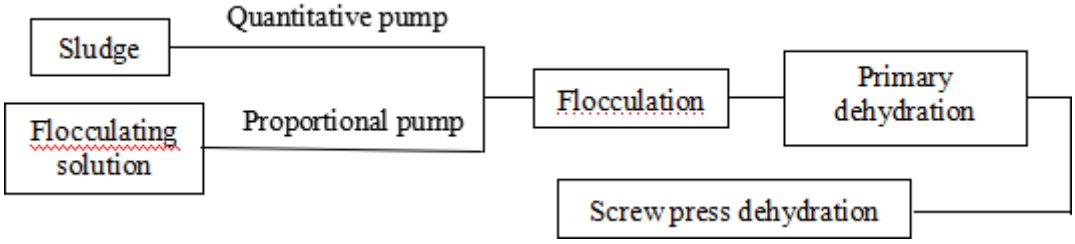

FIGURE 2.SCHEMATIC DIAGRAM OF SYSTEM OPERATION

Quantitative pump

III. MODULAR ANALYSIS OF SLUDGE DEWATERING SYSTEM

Sludg e

According to the function of the ombination by using analysis method of modular design, the whole system is divided into mud storage module, he flocculant module, flocculant adequate supply module, water supply module, flocculation module, the level of de module, interface module, screw press dehydration module and control module, etc. The functions of each module are shown in table 1.

Flocculation system

Proportional pump

Flocculation liquid

TABLE 1
FUNCTION ANALYSIS OF SLUDGE DEWATERING SYSTEM

Module		Function
Water storage		Storage of initial sewage. The storage capacity is designed according to the production capacity of the system.
Water supply		According to the production capacity and the sludge concentration, the pump delivery system is designed with adaptive function and flow control.
The dissolution of the flocculant	Flocculant addition	The flocculant is automatically added according to the solubility requirement.
	The water supply	According to the solubility requirement, the clean water is automatically added according to certain proportion.
	Dissolution time	According to the properties of flocculants, the dissolution time is generally controlled at 45~120min.
Flocculant solution supply		The pump and flow control system is adopted. The adaptive control is realized according to the sewage flow.
Flocculation		The flocculator are used in this module. The full and uniform mixing and mixing time of sludge and flocculant must be guaranteed.
Primary dehydration		The oblique helical device is used. According to the production capacity analysis, the modular design of the module is carried out, single row, double row or row. Water content and yield can be adjusted. The water content will be adjusted by adjusting the oblique Angle of the oblique spiral. The output is obtained by adjusting the rotational speed.
Interface		Through the interface, the sludge transfer between the oblique spiral and the squeeze screw is completed. The continuous and adaptive control of sludge will be realized.
Screw press		The final squeeze of the sludge will be finished. The speed control is realized in the screw system to meet the requirements of different sludge and different drying degree.
Dry mud conveying		The transport and storage of dry mud will be completed.
Control		The whole machine is controlled by PLC or main engine.

IV. DETERMINATION OF SYSTEM PROCESS PARAMETERS

The process parameter is the guarantee of the stable operation of the system. The process parameters are determined according to the actual production capacity requirements. The sludge treatment system is based on the requirement of sludge treatment. The initial amount of sludge or the production capacity of the final squeeze screw can be used as a process control parameter. This provides the basis for control parameter design. At the same time, the parameter design basis of each control point of the system can be provided.

4.1 Production capacity and press screw parameter configuration.

This study is based on the analysis of terminal sludge treatment. The analysis of the squeezing screw, the basic parameters are the rotational speed, compression ratio, inlet and outlet sectional area, and pitch. The compression ratio is determined by the ratio of the water content of the inlet. Its production capacity is defined as the volume of the first spiral.

$$Q = \frac{\pi D_1 A n \gamma \varphi c}{\cos \beta} \tag{1}$$

D_1-The average diameter of spiral first pitch. *A*-The average section area of spiral first pitch. *n*-speed, γ-The bulk of dry mud., φ-Filling coefficient, *c*-The entrance concentration.

Theoretical compression ratio is the ratio of the end to the initial spiral void volume.

$$\alpha = V_1 / V_i \tag{2}$$

Compression ratio is selected in the following analysis, a=4. The control parameters are shown in table 2.

TABLE 2
CONTROL PARAMETERS OF PRESS SCREW

Speed (rpm)	Export production (t/d)	Absolute dry mud (t/d)	The entrance concentration (%)	Flow (t/h)	Flow (m^3/h)	Export concentration (%)
0.29	5	2.5	13.3	0.783	0.766	50
1.47	26	13	13.3	4.073	3.982	50

Note: the data in table 2 is calculated based on the total output analysis. The first line is calculated when the output is 5t/d. The second line is calculated when the output is 26t/d. In the analysis of the screw press module, in addition to the shape of the module itself, the production capacity is determined by the spindle speed. In general, frequency conversion is adopted on the main shaft. The production capacity is related to the selection of the module, and the range of production capacity is related to the change of motor frequency. After the module is determined, the compression ratio is a fixed value. Therefore, it is very important to control the inlet concentration during the design analysis. The squeezing screw module is generally composed of sub-modules, such as press screw, variable frequency motor, transmission (deceleration system), etc. The transmission form can be determined according to the nature of the actual sludge by any combination of belt drive, reducer and chain drive. The speed of the best treatment is obtained. The speed of the optimum sludge treatment is obtained. After the speed is determined, the type of screw is determined according to the yield. The output of this paper is based on the number of tons per day, which means that there is no water pure mud. The flow in the table is expressed in two ways: t/d or m^3/d.

4.2 Primary dehydration system - parameter matching of oblique spiral module

The inlet parameters of the screw press are provided by the first-level dehydration module. The final sludge moisture content is guaranteed by inlet parameters. Compression ratio is the fixed value after the press screw module is determined. At this point, the export concentration is determined by the entrance concentration. Two basic parameters must be guaranteed by the first level dehydration module, i.e., output concentration and output. The control parameters of the oblique spiral module are shown in table 3.

TABLE 3
CONTROL PARAMETERS OF OBLIQUE SPIRAL

The entrance concentration (%)	Inlet mud flow (t/h)	Export concentration (%)	The inner diameter of the screen (mm)	Helical root diameter (mm)	Pitch (mm)	Speed (rpm)	Modular number of modules
4.3	2.39583	13.3	165	65	120	18.42	1
4.3	12.45833	13.3	165	65	120	47.89	2

Note: the data in table 3 is calculated based on the total output analysis. The first line is calculated when the output is 5t/d. The second line is calculated when the output is 26t/d. For example, the inlet concentration is calculated from the two parts of sewage and potion. The outlet concentration must be compatible with the inlet concentration of the press screw. The speed term refers to the use of single row of oblique helical parameters; double row can be reduced double. In the research, the helical screw module has been standardized and can be combined to meet the production capacity requirements. The same combination of modules should be used to facilitate the installation and adjustment of the equipment. By changing the inclination angle of the spiral, the export concentration is corrected. The change of speed is a two-way influence on production capacity and export concentration, which must be adjusted accurately in production.

4.3 Parameter configuration of flocculation module

In the sludge treatment system, the flocculation module is an important module to complete the coagulation of the sludge, so that the sludge mass is separated from the water. The parameters of the flocculation module are shown in table 4.

TABLE 4
PARAMETER CONFIGURATION OF FLOCCULATION MODULE

Enter the concentration of the mud (%)	Flow into the mud (m^3/h)	Drug concentration（%）	Incoming flow（m^3/h）	Postmixed concentration（%）	Outlet flow（t/h）
5	2.08333	0.1	0.4166	4.3	2.39583
5	10.8333	0.1	2.1666	4.3	12.45833

The first line is calculated when the output is 5t/d. The second line is calculated when the output is 26t/d. The mud concentration of the flocculator is the concentration of sludge tank. The inlet flow of sludge is calculated according to the production capacity. The dilution concentration of flocculant was selected as 0.1%, according to the type of flocculant and the actual dosage. The concentration of sludge outlet in flocculator was about 4.3%.The time and uniformity of flocculation must be guaranteed to obtain good flocculation quality. The effect of the dehydration effect on the first stage dewatering helical module is significant.

4.4 The parameter configuration of the dissolving module

The dissolving module of flocculant includes the additive module, the water supply module, the control module, etc. The parameter configuration is shown in table 5.

Note: The first line is calculated when the output is 5t/d. The second line is calculated when the output is 26t/d. Dosage is based on sludge characteristics and flocculation effect to determine. In this paper, flocculant was applied to the sludge treatment by 4kg/t, which was calculated according to the amount of dry mud. The determination of concentration is related to the drug supply flow, and the concentration is determined according to the size and type of the dilution pool. In general, the lower the concentration, the more uniform the mixture of sludge and solution, the shorter the flocculation time.

TABLE 5
PARAMETER CONFIGURATION OF FLOCCULANT DISSOLVING MODULE

Concentration of dissolved（%）	The dosage（m^3/d）	Flow（m^3/h）	Flocculant dosage（kg/d）	Usage time（h/m^3）
0.1	10	0.41667	10	2.4
0.1	52	2.16667	52	0.4615

V. CONCLUSION

Sewage treatment technology is a worldwide technical problem. It is desirable to make full use of the sludge to the environment. Sludge treatment system is used, sludge reduction can be realized. The purpose of the sludge can be determined according to the nature of the sludge. For example, paper sludge containing fiber can be incinerated to generate electricity. The sludge contains less pollutants and can be returned to the field or fertilizer after treatment. Industrial sludge must be treated harmlessly to be used. The process control parameter of this paper is calculated by the parameterized program, which is the result of the comprehensive process analysis, and only provides reference for design module selection. The combined parameter chain of the actual system should be analyzed and calculated according to the requirements of the production process, and the necessary experiments should be carried out to modify the parameters. Through parameter configuration analysis, the design parameters of control system can be determined, and the time of design system can be shortened effectively, and the success rate of system combination design is greatly improved.

REFERENCES

[1] Zhang Y L, Yang L, Liu B Y and C M Zhao 2009 *Heilongjiang Pulp & Paper*. 2 53-56.
[2] Tang L S, Luo Z G, Zhang L J, Song J and L X Deng 2016 *Technology of water treatment* .42 12-17
[3] Ding Q S, Wang W Y, 2000 *New and practical filtering technology* (Beijing: Metallurgical Publishing)
[4] Evon P, Kartika Amalia and Cerny M2013 *Feasibility study*. 47 33-42
[5] Jaroslav B, Lucie H and E Thomas 2010 *Conservation and Recycling*. 54 278-282
[6] Li T, Li J and Liu W Y 2009 *China Water and Wastewater.* 25 66-68
[7] Krishnamurthy S, and Viraraghanan T 2005 *Energy Sources*.27 113-122
[8] Zhang N M, Qu Q W and Chen Y H 2015 *Coal Technology*. 34 241-243.

Measurements of PVC composite with Corn Cob flour additive

Krisztina Roman

Institute of Ceramics and Polymer Engineering, University of Miskolc, Miskolc, Hungary

Abstract— *Mechanical and thermo-analytical analysis carried out on the composites. In order to determine the relationships between structure and properties of composite, it is necessary to carry out different measurements. The tests were: tensile test, hardness test, thermal conductivity SEM, DSC and DMA. The results showed that the mixtures were inhomogeneous. The tensile and hardness test resulted that the composite has stronger structure and an increase in the strength values. From the thermo-analytical analysis the corn cob additive effect in the composite structure can be observed. The result of the DMA shows that the additive works as inactive filler, and does not change the glass transition temperature of the rigid PVC foam.*

Keywords— Composite, PVC, foam, DSC, DMA.

I. INTRODUCTION

Due to continuous development and in order to fulfill the needs of customers the production of polymer composites are becoming highly common [1]. In construction PVC composites are met [2]. PVC is a hardly degradable bulk plastic; with the use of natural additives this ability can be changed. The production of composites propose many advantages such as higher strength and aesthetic [3]. Also many disadvantages rise like weak impact strength due to weak adhesion and water uptake [4]. During PVC composite foaming the corn cob additive differs the structure of the foam highly. Foam structure also differs based on the density of the composite and the presence of additives [5]. In this paper the mechanical and structural abilities of the resulting foam structure is to be determined.

II. MATERIALS

The raw material was the PVC powder. The PVC power's K values are 58 from the BorsodChem Zrt. Company. The mixture contains stabilizers, lubricants, processing aids, foaming agent (azodicarbonamide), filler and corn cob nature filler. The commercial corn cob fillers are grinded and dried (24hour-80 °C). The additives main components are 42% cellulose, 46% hemicelluloses, 7% lignin and 5% organic substances. The average particle sizes are approximately 492 μm. The PVC-corn cob ratio was 100/20 phr in the mixtures.

The composites were made / homogenized in a high-speed mixer at 110°C. During the mixing method the composite should be a homogenous system. After the mixing process, a twin-screw laboratory extruder was used to make the foaming sheets. The extruder parameters were: D=30mm, L/D= 20, compression rate 1:3 and the extruder temperature set at 165°C/170°C/170°C°/175°C/175°C/180°C from hopper to die. The extruded sheets were used for the different examinations. The specimens were cut by pneumatic punching tools.

TABLE 1
DENSITY VALUES OF PVC-CORN COB COMPOSITE

Material	Density [g/cm^3]
PVC-Corn cob composite	1.1252±0.006

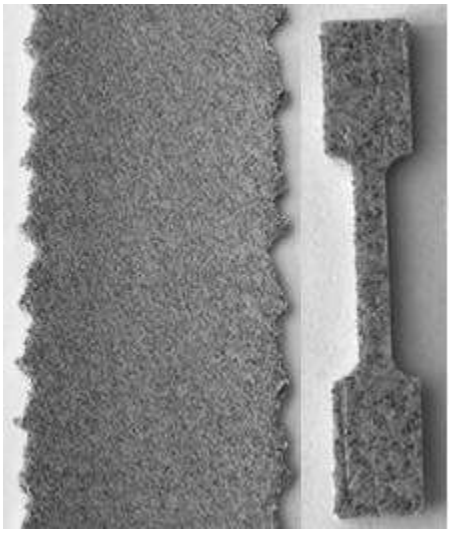

FIG 1. FOAMING SHEET AND THE SAMPLE FOR MECHANICAL (TENSILE) TEST

III. METHODS

3.1 Tensile test

The tensile test was performed by INSTRON 5566 device, according to ASTM D638-10 standard. The stress-strain behavior during the measurement was examined. The test's speed was 100 mm/min.

3.2 Hardness test

The hardness test was made by at Zwich/Roell Shore D equipment. Shore D punching tool was used for harder materials or composites. The test was performed according to standard ISO 868. The values (Table 3) were calculated as the average of 20 point on the specimen.

3.3 Thermal Conductivity test

The conductivity measurements were made by at C-Therm Conductivity Analyzer. The device is able to examine liquids, solids, and foam and etc. material properties. The technique is characterizing the thermal conductivity and effusion of the materials.

3.4 Scanning Electron Microscopy

The structure of the foaming sheets can be determined with Scanning Electron Microscope. The shape and the size can be determined with microscope. The test was measured by ZEISS equipment. The samples have to be made of conductive material; this is a thin conductive layer. The type of the layer was gold.

3.5 Dynamic Mechanical Analysis

The DMA analyze is a thermo-analytic method to determine elastic behavior. The load is applied in a periodically alternating in time manner, other than that everything is observed with the changing of temperature. During the analysis the applied temperature range, the glass transition temperature, rigidity, the efficiency of the softener and the structure of polymer mixtures can be determined also.

3.6 Differential Scanning Calorimetric

The DSC method monitors the heat transitions in the material which are mainly caused by chemical reactions. The DSC measures the electrical capacity needed to maintain the same temperature in the sample and the reference sample. During the measurement the crystallic transitions, the phase transitions and even the purity of the material can be defined.

IV. RESULTS

A number of tests were performed on specimens. These were: tensile test, hardness test, C-Therm, SEM, DMA and DSC analysis.

4.1 Tensile test

The Table 2 shows the results of average of 7 pcs sample.

TABLE 2

THE EFFECTS OF CORN COB FILLER ON THE TENSILE STRESS-STAIN VALUES

Material	Maximum Tensile Stress [MPa]	Maximum tensile stain [%]
Without corn cob	15.04±2.4	6.12±1.01
PVC-Corn cob composite	25.83±0.46	6.59±0.77

Generally, the results of measurement reflected the corn cob modifier effect. The result proves this modification; the mechanical strength increased. The stress-strain values show that the stress values increased, but the strain did not change to the properties of the original rigid PVC.

4.2 Hardness test

TABLE 3

HARDNESS TEST DATA

Material	Mean
Without corn cob	39.76±0.32
PVC-Corn cob composite	66.14±1

The hardness value tightly correlated with the result of SEM analysis. The values of hardness and density affected the foaming process.

4.3 Thermal Conductivity test

TABLE 4

THERMAL CONDUCTIVITY DATA OF THE COMPOSITE

Material	Conductivity [W/mK]
Without corn cob	0.090±0
PVC-Corn cob composite	0.090±0

The commercial PVC foams thermal conductivity value is in a range between to 0.03-0.07. The original rigid PVC foam and the composite conductivity values were the same from the Table 4. Based on the results, the values can be classified into the extruded sheet and the extruded foaming sheet.

4.4 SEM analysis

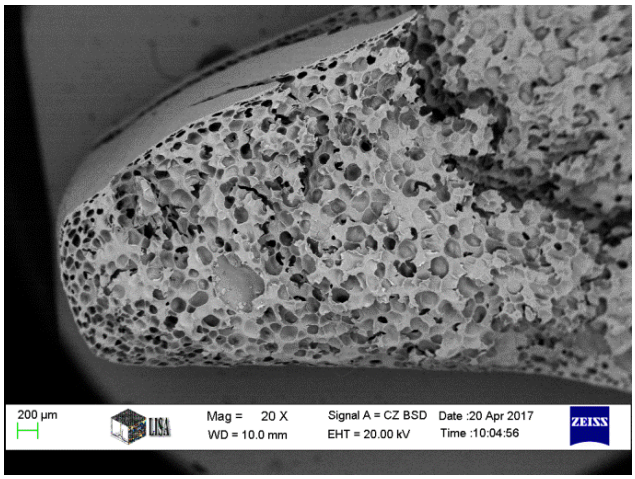

FIG 2. SCANNING ELECTRON MICROSCOPE FRACTURED STRUCTURE OF RIGID PVC FOAM

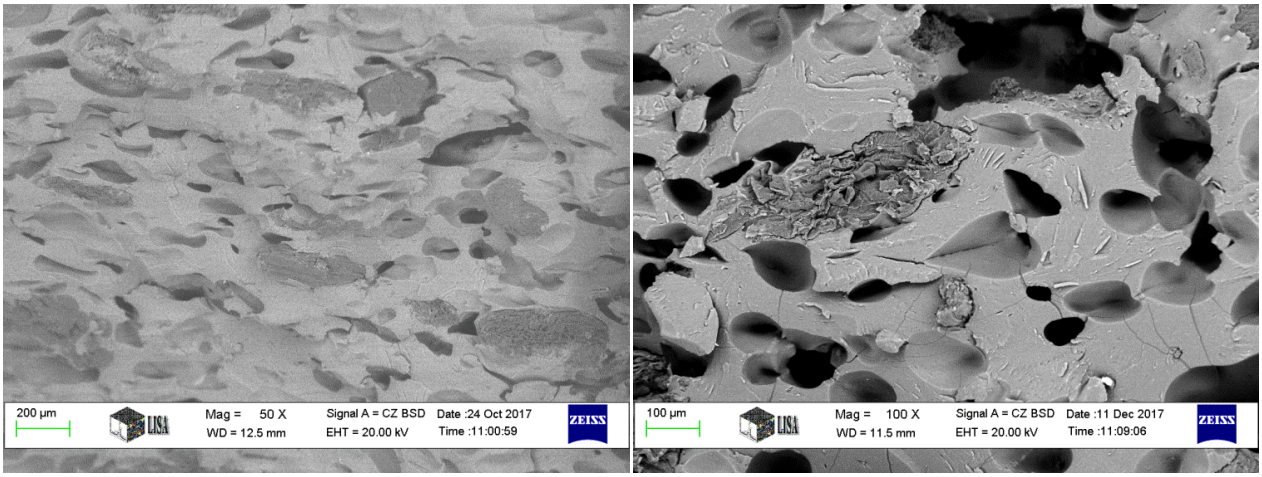

FIG 3. SCANNING ELECTRON MICROGRAPHS OF FRACTURED SURFACES OF PVC – CORN COB COMPOSITE; 50 x (left) and 100x (right)

The results of microscopy show the formation and structural deformations of the cells. The Fig 2. illustrated that the bowling agent works well; the morphology formed to open celled structured. The Fig 3. shows the fractured surfaces of the composites. We can see that the cells did not create due to the corn cob additives. Compact structure has formed.

4.5 DMA analysis

Fig 4. illustrated the glass transition temperature (Tg) and maximum tan δ. It was found that the glass transition temperature of PVC did not change because of the corn cob additives. The original PVCs glass transition was 83 °C.

From the result of DMA test the glass transition temperature of PVC is 90.48 °C. The glass transition temperature of original rigid PVC foam was 89.3 °C. Based on these result the corn cob did not change the characteristics of the main structure. It works as filler in the PVC system. It has no other effect in the internal structure properties.

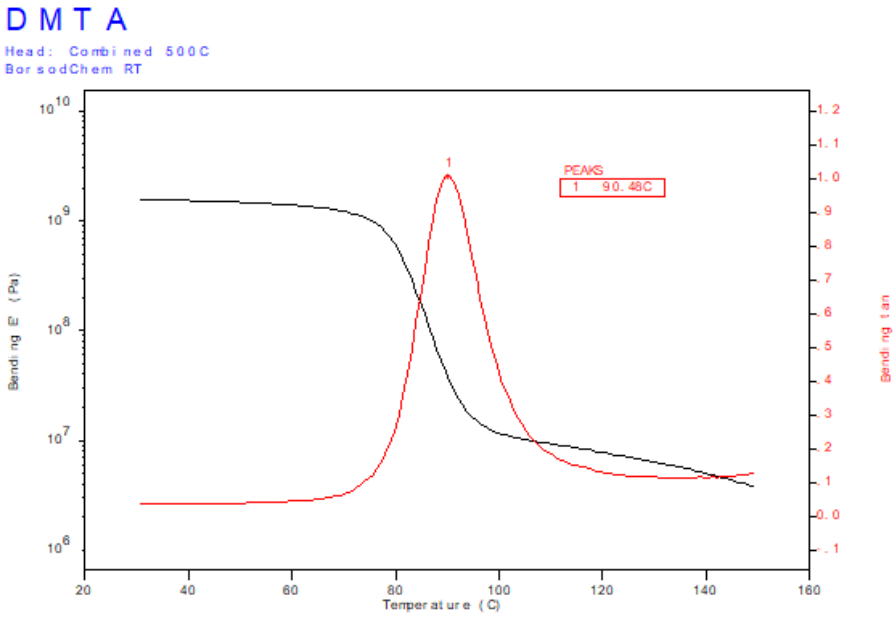

FIG 4. DMA RESULTS: PVC - CORN COB FORMULATION

4.6 DSC analysis

Based on the test results, we can conclude and predict the materials thermal processing history. The Fig 5. shows the actual production temperature (196 °C) and the level of processing. The processing temperature was increased from the die setting temperature. Apparently, the PVC super molecule was not completely processed. This 85% of processing was excellent regarding the materials properties.

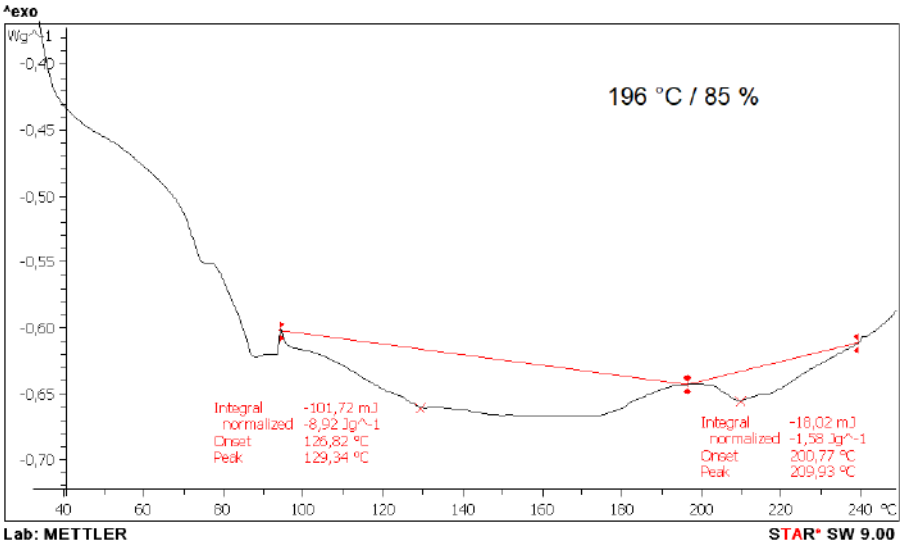

FIG 5. DSC RESULT: PVC - CORN COB COMPOSITE

V. CONCLUSION

The PVC-Corn cob composites were made successfully. The mechanical- and thermo analytical properties of the composites were improved with corn cob.

(1) The corn cob flour modified the PVCs main properties.
(2) The fillers were dispersed unequally in the rigid PVC.
(3) The reinforcement effects were appreciable; the tensile strength values were higher.
(4) The size and shape of the cells depend on the density and the filler's sizes.
(5) Corn cob additives work as an inactive filler, and does not changes the glass transition of composite.
(6) On the result of the DSC analysis the highest processing temperature of the composite can be observed. The processing of PVCs super molecular structure was carried out in 85%.

REFERENCES

[1] W. V. TITOW, PVC Solutions and their Applications. 1984.
[2] A. B. Akinyemi, J. O. Afolayan, and E. Ogunji Oluwatobi, "Some properties of composite corn cob and sawdust particle boards," Construction and Building Materials, 2016. vol. 127, pp. 436–441,
[3] S. T. Georgopoulos, P. A. Tarantili, E. Avgerinos, A. G. Andreopoulos, and E. G. Koukios, "Thermoplastic polymers reinforced with fibrous agricultural residues," Polymer Degradation and Stability, vol. 90, no. 2 SPEC. ISS., 2005. pp. 303–312,
[4] Y. Wan, H. Wu, L. Huang, J. Zhang, S. Tan, and X. Cai, "Preparation and characterization of corn cob/polypropylene composite reinforced by wood ash," Polymer Bulletin, 2017.
[5] G. Wypych, Degradation & Stabilization. 2015.

Rederivation and Investigation of $E=mc^2$ for higher energy Production

Dr Bijay Kumar Parida (MS, FRCSG.)

Associate Professor, Muthusamy Virtual University of Ophthalmology Post Graduation., Bhubaneswar, odisha, INDIA

Abstract— *$E=mc^2$ is derived from equation $E=Fd$, implying that photon behaves like a particle.*

Energy(E)=Force(F) into Displacement(d)

If a particle can reach higher speed, higher energy production is possible.

Keywords— energy, Einstein, velocity, particle.

I. INTRODUCTION

Photons have an interesting property is that they have momentum and yet have no mass. This was established in 1850 by James Clerk Maxwell Momentum is made up of 2 components, mass and velocity. Einstein's great insight was that the energy of a photon must be equivalent to a quantity of mass and hence could be related to the momentum.

In "Does the inertia of a body depend upon its energy-content?" Einstein used V to mean the speed of light in a vacuum and L to mean the energy lost by a body in the form of radiation. Consequently, the equation $E = mc^2$ was not originally written as a formula but as a sentence in German that meant if a body gives off the energy L in the form of radiation, its mass diminishes by L/V^2 .[1]

A remark placed above it informed that the equation was approximate because the conclusion was only justified if one neglected "magnitudes of fourth and higher orders" of a series expansion[2].

In 1960, Einstein's mass-energy relationship was written as $M_0 = E_0/c^2$ by Max Planck[3] and, subsequently, was given a quantum interpretation[4] by Johannes Stark, who assumed its validity and correctness (Gültigkeit).

However, Stark wrote the equation as $e_0=m_0 c^2$ which meant the energy bound in the mass of an electron at rest and still was not the present popular version of the equation.

In 1924, Louis de Broglie assumed the correctness of the relationship "énergie=masse c^2" on page 31 in his Research on the Theory of the Quanta (published in 1925) but he did not write $E = mc^2$. However, Einstein returned to the topic once again after the World War Two and this time he wrote $E = mc^2$ in the title of his article [5]intended as an explanation for a general reader by analogy[6].

Einstein derived existing $E=mc^2$ starting with result of relativistic variation of light energy but finally obtained $E=mc^2$ by applying classical conditions.

After Einstein, Max Planck also derived the same independently. In 1907 Planck made an in depth investigation of the energy confined within a body. The inertia of mass of body is altered by absorption or emission of heat energy. The increments of mass of body are equal to heat energy divided by square to speed of light.

Although Einstein started to derive $E=mc^2$ using relativistic variation of light energy yet he derived final results under classical condition. Einstein interpreted the results using Binomial Theorem which is applicable if v far less than c.

Isaac Newton,S. Tolver Preston Poincare De Pretto and F. Hasenohrt are the philosophers and physicists who have given idea of $E=mc^2$.

II. HYPOTHESIS

$E=mc^2$ can also be derived from $E=F.d$

Energy(E)=Force(F) into Displacement(d)

Force=Mass(m) into acceleration(a)

Acceleration=Rate of change of velocity(v), (assuming uniform acceleration)

Note:

*If particle can reach higher velocity, higher energy production is possible.

*Photon is a particle; however it behaves like a wave.

III. DISCUSSION

E=F.d

F=m.a

E=m.a.d

$a=v_2-v_1/t$

t=time required to change velocity

This is also the time required for displacement.

Now

$E=m.v_2-v_1/t$ .d

Velocity=displacement over time

v=d/t

Assuming a particle was static

$v_1=o$

So

$E=m.v_2/t$ d

$E=m.v_2$ .d/t

$E=m.d_2/t$ .d/t

d_2 is same as d as the velocity of particle becomes so fast that within a second the particle reaches d_1 from d.

So $E=m.d_2/t$ .d/t

$d_2=d$

So I shall name it only d

E=m.d/t .d/t

E=m.v.v

As (d/t=v)

What is highest possible velocity?

Till today =c=velocity of light=speed of light

E=m.c.c

E=mass into square of speed of light

$E=mc^2$

*There is a possibility of production of higher energy from same matter if speed of matter can exceed light. As our knowledge expands, higher than speed of light may be found. But this method of establishing $E=mc^2$, proposes that photon is a particle.

IV. CONCLUSION

$E=mc^2$ can also be derived from E=F.d

*If particle can reach higher velocity .higher energy production is possible.

*Photon is a particle; however it behaves like a wave**.**

DECLARATION FROM AUTHORS

I declare that the article I have sent to the journal is original & has not been published in any other journal. I transfer the right to publish in this journal, if accepted for publication.

REFERENCES

[1] See the sentence on the last page (p.641) of the original edition of Ist die Trägheit eines Körpers von seinem Energieinhalt abhängig? in Annalen der Physik, 1905, below the equation K0 - K1= L/V2 v2/2. See also the sentence under the last equation in the English translation, K0 - K1= 1/2 L/c2 v2, and the comment on the symbols used in About this editionthat follows the translation [1]

[2] See the sentence on the last page (p.641) of the original edition of Ist die Trägheit eines Körpers von seinem Energieinhalt abhängig? in Annalen der Physik, 1905, above the equation K0 - K1= L/V2 v2/2. See also the sentence above the last equation in the English translation, K0 - K1= 1/2 L/c2 v2, and the comment on the symbols used in About this editionthat follows the translation [2]

[3] Planck, M. (1907). Ber.d.Berl.Akad. 29: 542.

[4] Stark, J. (1907). "Elementarquantum der Energie, Modell der negativen und der positiven Elekrizitat". Physikalische Zeitschrift 24 (8): 881.

[5] A.Einstein 'E = mc2 ': the most urgent problem of our time Science illustrated, vol. 1 no. 1, April issue, pp. 16-17, 1946 (item 417 in the "Bibliography"

[6] M.C.Shields Bibliography of the Writings of Albert Einstein to May 1951 in Albert Einstein: Philosopher-Scientist by Paul Arthur Schilpp (Editor) Albert Einstein Philospher - Scientist.

Multiuser Resource Allocation Algorithms for Downlink OFDMA-based MIMO Network

Wei-Chiang Wu

Department of Electrical Engineering, Da-Yeh University Taiwan, R.O.C.

Abstract*—The problem of simultaneous multiuser resource (subcarriers-and-bits) allocation algorithm in OFDMA-based multiple input-multiple output (MIMO) system has recently attracted significant interest. In this paper, we employ adaptive modulation technique and advanced use of multiple antennas at both the transmitter and receiver to develop four resource allocation schemes. The first scheme assigns subcarrier to the user with best channel gain and employs spatial multiplexing (SM) on the MIMO system to further enhance the throughput. The space-division multiple-access (SDMA) scheme assigns single subcarrier simultaneously to the terminals with pairwise "nearly orthogonal" spatial signatures. In the third scheme, we propose to design the transmit beamformers based on the zero-forcing (ZF) criterion such that the multiuser interference (MUI) is completely removed. Specifically, we propose a low-complexity iterated terminals-selection algorithm in conjunction with the ZF criterion such that the selected ZF (SZF) scheme can be exploited to achieve throughput multiplication. Alternatively, we propose a least-squares (LS) based multiuser resource allocation algorithm to cope with the over-determined system such that all users are allowed to share single subcarrier.*

***Keywords*—SDMA, OFDMA, MIMO, Selected Zero-Forcing (SZF), Least-Squares (LS).**

I. INTRODUCTION

In 4G and future cellular networks, mushrooming users need to share the spectrum to achieve high-rate multimedia communication while ensure the fulfillment of quality-of-service (QoS) requirements. In the downlink (DL) of 4G LTE, orthogonal frequency division multiple access (OFDMA) technique is employed [1]. The advantages of OFDMA includes robust multipath suppression, ability to combat intersymbol interference (ISI), relative low complexity, and flexibility in accommodating many users with widely varying data rates [2]. The rationale for OFDMA is dynamically allocating subcarriers to the user with best channel state. However, the resource allocation algorithms are not specified in the LTE standard, and recently, quite a few scheduling and resource allocation algorithms have been proposed for OFDMA cellular system [3-7]. Resource allocation is essentially a constrained-optimization problem [Chap. 18 of [8]] that either maximizes the overall data rate or minimizes the total transmit power subject to specific constraints, e.g., the users' QoS requirements. The optimum resource allocation algorithm is itself a NP-complete problem whose solution can only be found with exhaustive search [7], which is infeasible for practical situation. In the work of [1], the sum rate of all users is maximized with the constraint of total transmit power and minimum data rate for each user. While the work of [3] aims to allocate the subcarriers and power such that the minimum user's data rate is maximized. Alternatively, proportional fairness scheduling [4] is designed to take advantage of multiuser diversity, while maintaining comparable long-term throughput for all users. In the work of [5], a Lagrangian-based algorithm is proposed to attain a dramatic gain in power efficiency. However, the load of computation is too high to put it into practical use.It is well-known that one of the largest advantages of LTE over incumbent standard is more advanced use of multiple antennas. And the massive multiple input-multiple output (MIMO) technique is apt to be included in future 5G network [9-12]. The key benefits of wireless communication provided by antenna array include:

1) **Spatial diversity:** It can effectively combat fading.
2) **Interference suppression:** The interference can be removed from the desired user as long as the array size exceeds the number of interferers.
3) **Spatial multiplexing:** It allows different signal sources to be sent simultaneously in the same bandwidth.

All the above techniques can effectively increase the capacity or throughput of a wireless communication system. The main focus of this paper is to jointly exploit the three benefits of multi-antenna technology to develop a simple yet efficient resource allocation algorithm in the downlink of an OFDMA-based cellular system.

This paper considers a multiuser MIMO system, in which each cell is consisted of a L-antenna base station (BTS) and K remote terminals (RT) each equipped with Q antennas. Downlink OFDMA system with the assumption that each RT estimates and feedback the instantaneous channel state information (CSI) to the BTS. We apply adaptive modulation according to the CSI to meet the minimum QoS requirement, in which the symbol error rate (SER) is the performance metric. We develop four resource allocation schemes, which allocate subcarriers and bits to each user via different antennas. Specifically, in order to maximize system throughput as well as spectral efficiency, we employ various array processing techniques. The algorithms proposed in this paper attempt to maximize system throughput subject to the constraints of total transmit power and minimum data rate for each user.

The first scheme jointly exploits spatial diversity and spatial multiplexing (SM) technique, in which the BTS designates subcarrier to the user with the highest channel gain between BTS and a specific RT. Since multiple substreams can be sent through the MIMO system, the data rate is expected to be increased. The SM scheme is inherently a single-user algorithm in which each subcarrier can only be assigned to single user at specific time. While in scheme 2, we assign subcarrier to the users with "nearly orthogonal" spatial signatures. We refer it as the space-division multiple-access (SDMA) scheme. Though throughput of the SDMA scheme is expected to be increased, nevertheless, an obvious flaw of this scheme is that spatial channels are rarely orthogonal in practice. In the third scheme, we propose to design prefilters at the BTS that meets the zero-forcing (ZF) criterion to remove the multiuser interference (MUI). Since MUI is removed and each subcarrier can be assigned simultaneously to all the user terminals, therefore throughput multiplication can be achieved. However, in the case of, complete MUI suppression is not possible; we propose two alternative multi-user resource allocation algorithms. The first algorithm selects out of spatial signatures that contribute to the system the maximum throughput. We refer it as the selected ZF (SZF) scheme. Moreover, we propose a low-complexity iterated algorithm to implement the SZF scheme. The second algorithm to overcome is based on the least-squares (LS) criterion. We refer it as the selected LS scheme. The LS scheme is feasible and efficient since each subcarrier can be shared simultaneously to all spatial signatures. Nevertheless, residual MUI is inevitable in the LS scheme.

The rest of this paper is organized as follows. In Section 2, we describe the system model and formulate the problem. Section 3 describes and analyzes the proposed multiuser subcarriers-and-bits allocation schemes. Section 4 focuses on the issue of multiuser resource allocation when the BTS array size is less than the sum of RTs' array size. In Section 5, we demonstrate the system performance and discuss the numerical results. Concluding remarks are finally made in section 6.

Notation: We use upper and lower case boldface letters to denote matrices and vectors, respectively. $[\ ]^T$,$[\ ]^H$ stand for matrix or vector transpose and complex transpose, respectively. We will use $E\{\ \}$ for expectation (ensemble average), $\|\ \|$ for vector norm, and $\equiv$ for "is defined as". $\|\mathbf{A}\|_F$ denotes the Frobenius norm of matrix $\mathbf{A}$. $\mathbf{I}_K$ denotes an identity matrix with size K. $\mathbf{e}_k$ denotes the kth column vector of an identity matrix. A complex normal variable with mean μ variance σ^2 reads as $\sim N(\mu,\sigma^2)$. $\delta(\cdot)$ is the dirac delta function. $\bar{x}$ denotes the complex conjugate of x. $\lfloor x \rfloor$ denotes the floor function, *i.e.*, the maximum integer value that is equal to or less than x. $[x]_- = \min\{1,x\}$. $\binom{n}{k}$ stands for the combination of k out of n. $tr(\mathbf{A})$ denotes the trace (sum of the diagonal elements) of square matrix $\mathbf{A}$.

II. SYSTEM MODEL AND PROBLEM FORMULATION

We consider an OFDMA-based cellular network, where in a specific cell, the BTS is equipped with L antennas and there are K RTs each with Q antennas. For each subcarrier, flat-fading channel model is assumed. Since all RTs share the same bandwidth, we attempt to develop an efficient resource allocation algorithm to allocate N subcarriers to the K users subject to pre-determined constraints.

Let $\left\{h_{k,l,q}^n\right\}_{\substack{l=1,\ldots,L\\ q=1,\ldots,Q\\ k=1,\ldots,K\\ n=1,\ldots,N}}$ be the instantaneous magnitude of the channel gain between the kth RT's qth antenna and the lth antenna of BTS on the nth subcarrier, which includesthe effect of path loss, shadowing and fading. For each subcarrier n, it can also be regarded as multiple MIMO system with channel matrix $\left\{\mathbf{H}_k^n\right\}_{\substack{k=1,\ldots,K\\ n=1,\ldots,N}}$, given by

$$\mathbf{H}_k^n \equiv \begin{bmatrix} h_{k,1,1}^n & h_{k,1,2}^n & \cdots & h_{k,1,Q}^n \\ h_{k,2,1}^n & h_{k,2,2}^n & \cdots & h_{k,2,Q}^n \\ \vdots & \vdots & \ddots & \vdots \\ h_{k,L,1}^n & h_{k,L,2}^n & \cdots & h_{k,L,Q}^n \end{bmatrix} = \begin{bmatrix} \mathbf{h}_{k,1}^n & \mathbf{h}_{k,2}^n & \cdots & \mathbf{h}_{k,Q}^n \end{bmatrix} \tag{1}$$

where $\left\{\mathbf{h}_{k,q}^n\right\}_{q=1,\ldots,Q}$ denotes the L-by-1 channel vector seen by the kth user's qth antenna.

$$\mathbf{h}_{k,q}^n \equiv \begin{bmatrix} h_{k,1,q}^n & h_{k,2,q}^n & \cdots & h_{k,L,q}^n \end{bmatrix}^T \tag{2}$$

Let us consider here a Time-Division Duplexing (TDD) scheme, in which reciprocity between uplink and downlink channels can be assumed. Consequently, according to the method proposed in [12], the BTS can estimate the CSI from the uplink pilot signals transmitted by each user. A schematic illustration of the system under consideration is depicted in Fig. 1. For simplicity, we invoke the following assumptions throughout this paper:

1) The BTS has perfect knowledge of the CSI, which are periodically reported by each user.
2) The channel matrices, $\left\{\mathbf{H}_k^n\right\}_{\substack{k=1,\ldots,K \\ n=1,\ldots,N}}$, stay constant during the resource allocation process.

The problem addressed in this paper is to exploit the available CSI to perform real-time subcarriers and bits allocation. The design goal of the resource allocation algorithm is to maximize the overall throughput (bits per unit time) subject to the following constraints:

1) The QoS for each RT should meet system requirement. In this paper, QoS is measured by SER.
2) The energy consumption at the BTS should be upper-bounded by E_{total}.
3) The data rate allocated for kth user should meet a minimum data rate requirement equal to R_k bits per OFDM symbol.

Please note that the resource allocation algorithms described in this paper is flexible with every attempt to maximize the throughput, thereby, the subcarriers allocated for each user are distributed rather than bunched.

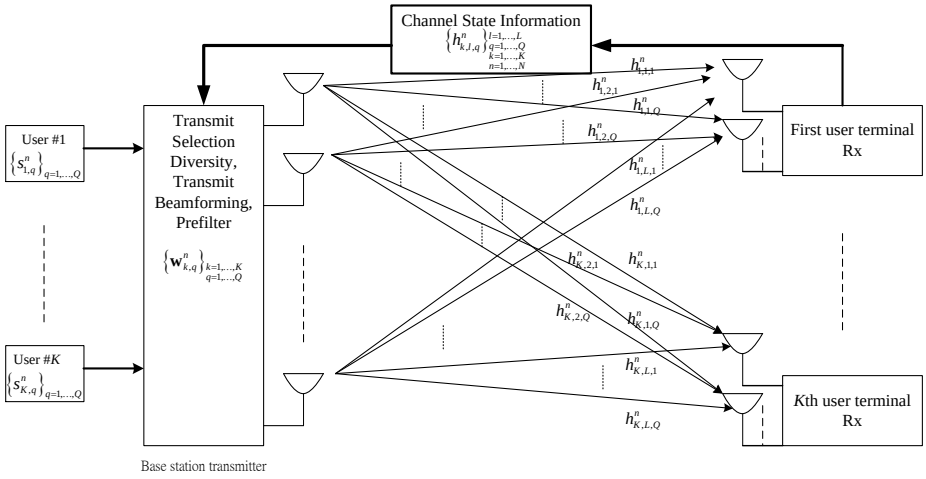

FIG. 1: BLOCK DIAGRAM OF THE MULTIUSER MIMO SYSTEM

III. JOINT SUBCARRIERS AND BITS ALLOCATION ALGORITHMS

In order to achieve the challenging spectral efficiency and user throughput targets, adaptive modulation and coding are also used and included in the specifications of LTE [1]. The rationale of adaptive modulation is to transmit as high a data rate as possible as long as the channel is good. On the other hand, data is transmitted at a lower rate when and where the channel is in poor condition. In this paper, we employ *M-ary* PSK (MPSK) for QoS measurement, though extension to other modulation techniques is without conceptual difficulty. The SER for MPSK modulation is upper bounded by [13]

$$P_{e,MPSK} < 2Q\left(\sqrt{\frac{2E}{N_0}}\sin\frac{\pi}{M}\right) \tag{3}$$

Where E denotes the received symbol energy. N_0 is the one-sided power spectral density of AWGN. The tail function is defined as $Q(x) \equiv \frac{1}{\sqrt{2\pi}} \int_x^\infty \exp\left(-\frac{t^2}{2}\right) dt$. Obviously, SER increases with respect to the number of bits per symbol, $m = \log_2 M$. To maximize the throughput while maintaining the QoS requirement, it is usually required that the SER must be lower than a pre-determined threshold, $P_{e,MPSK} \le \lambda$. Using (3) and after some manipulations, we have

$$M \le \frac{\pi}{\sin^{-1}\left(\left[\sqrt{\frac{N_0}{2E}} Q^{-1}\left(\frac{\lambda}{2}\right)\right]_-\right)} \tag{4}$$

Therefore, the allocated bits per OFDM symbol is upper bounded by

$$m = \left\lfloor \log_2 \left(\frac{\pi}{\sin^{-1}\left(\left[\sqrt{\frac{N_0}{2E}} Q^{-1}\left(\frac{\lambda}{2}\right)\right]_-\right)} \right) \right\rfloor \tag{5}$$

The algorithm for achieving optimum solution requires exhaustive search. The number of iterations needed in single antenna scenario (M=Q=1) is about $O\left(K^N\right)$ [7], which is infeasible even for moderate N and K. Therefore in this paper, we attempt to develop suboptimum solutions.

3.1 Single User Spatial Multiplexing (SM) Scheme

In the single user spatial multiplexing (SM) scheme, the BTS transmits multiple substreams simultaneously to a specific RT using the same subcarrier. For a specific n, the BTS first chooses among $\left\{\mathbf{H}_k^n\right\}_{k=1,..,K}$ with the largest Frobenius norm

$$k^* = \arg \max_{k \in \{1,..,K\}} \left\| \mathbf{H}_k^n \right\|_F \tag{6}$$

where $\left\| \mathbf{H}_k^n \right\|_F = \sqrt{\sum_{q=1}^{Q} \sum_{l=1}^{L} \left| h_{k,l,q}^n \right|^2}$. Let ρ_k^n be the subcarrier allocation index, that is, $\rho_k^n = 1$ when the nth subcarrier is assigned to the kth RT, $\rho_k^n = 0$, otherwise. That is

$$\text{If } \rho_k^n = 1 \Rightarrow \rho_{k'}^n = 0 \text{ for all } k' \ne k \tag{7}$$

In the SM scheme, the fact that each RT has Q receive antennas can be exploited in the spatial domain by transmitting up to Q independent symbol streams simultaneously for each user. In what follows, the outputs of the antenna array at the BTS can be described as

$$\mathbf{x}_k^n = \sum_{q=1}^{Q} \mathbf{w}_{k,q}^n s_{k,q}^n \tag{8}$$

where $\left\{s_{k,q}^n\right\}_{q=1,..,Q}$ is the symbol to be detected by the kth user's qth receive antenna. We let the transmitted symbol energy be normalized to be 1, *i.e.*, $E\left\{\left|s_{k,q}^n\right|^2\right\} = 1$, throughout the paper. $\left\{\mathbf{w}_{k,q}^n\right\}_{q=1,..,Q}$ is the L-by-1 transmit weight vector designated for $\left\{s_{k,q}^n\right\}_{q=1,..,Q}$, respectively. The received Q-by-1 vector signal at the kth RT yields

$$\mathbf{y}_k^n = \mathbf{H}_k^{nT} \mathbf{x}_k^n + \mathbf{n}_k^n \tag{9}$$

where $\mathbf{n}_k^n$ is the zero-mean Gaussian noise vector with covariance matrix $\frac{N_0}{2} \mathbf{I}_Q$. For each subcarrier, we aim at transmitting Q symbols simultaneously to the kth user. The design goal of $\left\{\mathbf{w}_{k,q}^n\right\}_{q=1,..,Q}$ is to avoid interference to other symbols. We assume L>Q, which is usually the case, and employ singular-value-decomposition (SVD) [chap. 7 of [8]] to decompose $\mathbf{H}_k^{nT}$ as

$$\mathbf{H}_k^{nT} = \mathbf{U}_k^n \boldsymbol{\Sigma}_k^n \mathbf{V}_k^{nH} \tag{10}$$

where $\mathbf{U}_k^n \in \mathbb{C}^{Q\times Q}, \mathbf{V}_k^n \in \mathbb{C}^{L\times L}$ are unitary matrices, and $\boldsymbol{\Sigma}_k^n \in \mathbb{C}^{Q\times L}$ is a zero matrix except for the square roots of *Q*nonzero eigenvalues of the matrix $\mathbf{H}_k^{nH}\mathbf{H}_k^n$ on thediagonals. We denote each diagonal element by $\left\{\sqrt{\sigma_{k,q}^n}\right\}_{q=1,\ldots,Q}$. Let $\mathbf{v}_{k,q}^n$ be the *q*th column vectors of $\mathbf{V}_k^n$, then bythe SVD theorem, the first *Q* columns of $\mathbf{V}_k^n$ are orthonormal basis of the column space of $\mathbf{H}_k^n$.

$$\text{span}\left\{\mathbf{v}_{k,1}^n,\cdots,\mathbf{v}_{k,Q}^n\right\} = \text{CSP}\left\{\mathbf{H}_k^n\right\} \tag{11}$$

Therefore, we choose the weightvectors $\left\{\mathbf{w}_{k,q}^n\right\}_{q=1,\ldots,Q}$ as

$$\mathbf{w}_{k,q}^n = \eta_{k,q}^n \mathbf{v}_{k,q}^n; q = 1,\ldots,Q \tag{12}$$

where $\eta_{k,q}^n$ denotes the energy normalization factor in order to meet the transmit energy constraint. In what follows, the received signal vector at the *k*th RT can be obtained as

$$\mathbf{H}_k^{nT}\mathbf{x}_k^n = \left(\mathbf{U}_k^n \boldsymbol{\Sigma}_k^n \mathbf{V}_k^{nH}\right)\mathbf{x}_k^n = \mathbf{U}_k^n \begin{bmatrix} \eta_{k,1}^n\sqrt{\sigma_{k,1}^n}s_{k,1}^n \\ \eta_{k,2}^n\sqrt{\sigma_{k,2}^n}s_{k,2}^n \\ \vdots \\ \eta_{k,Q}^n\sqrt{\sigma_{k,Q}^n}s_{k,Q}^n \end{bmatrix} \tag{13}$$

The optimum receiver is composed of a bank of matched-filters (correlators) with column vectors of $\mathbf{U}_k^n$ as template signals

$$\begin{aligned} \mathbf{U}_k^{nH}\mathbf{y}_k^n &= \mathbf{U}_k^{nH}\left(\mathbf{H}_k^{nT}\mathbf{x}_k^n + \mathbf{n}_k^n\right) \\ &= \mathbf{U}_k^{nH}\mathbf{U}_k^n \begin{bmatrix} \eta_{k,1}^n\sqrt{\sigma_{k,1}^n}s_{k,1}^n \\ \eta_{k,2}^n\sqrt{\sigma_{k,2}^n}s_{k,2}^n \\ \vdots \\ \eta_{k,Q}^n\sqrt{\sigma_{k,Q}^n}s_{k,Q}^n \end{bmatrix} + \mathbf{U}_k^{nH}\mathbf{n}_k^n \\ &= \begin{bmatrix} \eta_{k,1}^n\sqrt{\sigma_{k,1}^n}s_{k,1}^n \\ \eta_{k,2}^n\sqrt{\sigma_{k,2}^n}s_{k,2}^n \\ \vdots \\ \eta_{k,Q}^n\sqrt{\sigma_{k,Q}^n}s_{k,Q}^n \end{bmatrix} + \tilde{\mathbf{n}}_k^n \end{aligned} \tag{14}$$

It is easy to show that $\tilde{\mathbf{n}}_k^n \equiv \mathbf{U}_k^{nH}\mathbf{n}_k^n$ is still white with the same covariance matrix. It is evident from (14) that the *Q* symbols, $\left\{s_{k,q}^n\right\}_{q=1,\ldots,Q}$, can be simultaneously detected. The received symbol energy for the *k*th user's *q*th receiver at the *n*th subcarrier can be calculated by

$$E_{k,q}^n = E\left\{\left|\eta_{k,q}^n\sqrt{\sigma_{k,q}^n}s_{k,q}^n\right|^2\right\} = \sigma_{k,q}^n {\eta_{k,q}^n}^2 \tag{15}$$

Substituting (15) into (5), the bits that can be sent to the *k*th user's *q*th antenna can be obtained as

$$m_{k,q}^n = \left\lfloor \log_2\left(\frac{\pi}{\sin^{-1}\left(\left[\frac{1}{\eta_{k,q}^n\sqrt{\sigma_{k,q}^n}}\sqrt{\frac{N_0}{2}}Q^{-1}\left(\frac{\lambda}{2}\right)\right]_-\right)}\right)\right\rfloor \tag{16}$$

Based on (12), the energy consumption can be calculated as

$$E_{SM} = \sum_{k=1}^{K}\sum_{n=1}^{N}\sum_{q=1}^{Q}\rho_k^n E\left\{\left|s_{k,q}^n\right|^2\right\}\left\|\mathbf{w}_{k,q}^n\right\|^2 = \sum_{k=1}^{K}\sum_{n=1}^{N}\sum_{q=1}^{Q}\rho_k^n \eta_{k,q}^{n\ 2} \le E_{total} \tag{17}$$

To determine $\left\{\eta_{k,q}^n\right\}$ under the constraint $E_{SM} \le E_{total}$, we may choose $\left\{\eta_{k,q}^n\right\}$ as

$$\eta_{k,q}^n = \sqrt{\frac{E_{total}}{N}} \tag{18}$$

Substituting (18) into (16), the energy constraint and channel condition of the SM scheme are related by

$$m_{k,q}^n = \left\lfloor \log_2\left(\frac{\pi}{\sin^{-1}\left(\left[\frac{1}{\sqrt{\sigma_{k,q}^n}}\sqrt{\frac{NN_0}{2E_{total}}}Q^{-1}\left(\frac{\lambda}{2}\right)\right]_-\right)}\right)\right\rfloor \tag{19}$$

There then, the throughput of the *k*th user can be calculated by

$$T_k = \sum_{n=1}^{N}\sum_{q=1}^{Q}\rho_k^n m_{k,q}^n; \quad k = 1,\ldots,K \tag{20}$$

And the overall throughput is $T = \sum_{k=1}^{K} T_k$.

The joint subcarriers and bits allocation for the SM scheme is equivalent to finding $\left\{\rho_k^n\right\}_{\substack{k=1,\ldots,K \\ n=1,\ldots,N}}$ to satisfy the following constrained-optimization problem

$$\arg\max_{\rho_k^n} \sum_{k=1}^{K}\sum_{n=1}^{N}\sum_{q=1}^{Q}\rho_k^n m_{k,q}^n$$

Subject to

1) $T_k = \sum_{n=1}^{N}\sum_{q=1}^{Q}\rho_k^n m_{k,q}^n \ge R_k \quad ;\forall k = 1,\ldots,K$

2) $\sum_{k=1}^{K}\sum_{n=1}^{N}\rho_k^n = N$

3) if $\rho_k^n = 1 \Rightarrow \rho_{k'}^n = 0, \quad \forall k' \ne k$

We implement the SM scheme as follows:

Step 1: Starting from the first subcarrier, the BTS assigns the subcarrier to the user with the highest Frobenius norm of channel matrix, which corresponds to the maximum bits to be transmitted, among all users in that subchannel. Let *W* be the user set, $W = \{1,2,\ldots,K\}$, we have

$$k^* = \arg\max_{k\in W}\left\|\mathbf{H}_k^n\right\|_F$$

Since each subcarrier can only be assigned to single user, hence, as soon as subcarrier *n* has been assigned to user k^*, we set

$$\rho_{k^*}^n = 1, \rho_k^n = 0, \text{for all } k \ne k^*$$

Step 2: Perform SVD on $\mathbf{H}_{k^*}^{n\ T}$ to obtain $\left\{\mathbf{v}_{k^*,q}^n\right\}_{q=1,\ldots,Q}$

Step 3: Calculate $\left\{m_{k^*,q}^n\right\}_{q=1,\ldots,Q}$ using (19), and then calculate $T_{k^*} = \sum_{i=1}^{n}\sum_{q=1}^{Q}\rho_{k^*,q}^i m_{k^*,q}^i$

Step 4: Check whether user k^* meets the minimum bit rate constraint. If $T_{k^*} < R_{k^*}$, which means more subchannels should be assigned to user k^*, go back to step 1 and check for the next subcarrier. On the other hand, if $T_{k^*} \geq R_{k^*}$, we temporarily exclude user k^* and go back to step 1 to assign the subchannels to those users that have not attained the minimum bit rate constraint.

Step 5: As long as all the users meet the minimum bit rate constraint, remove all the exclusions, redo step 1 until all the subcarriers have been allocated.

3.2 SDMA Scheme

Different from the SM scheme, a subcarrier can be assigned simultaneously to multiple users in the SDMA scheme. In the proposed SDMA scheme, we systematically assigns "most orthogonal" user terminals to the same subchannel. It is plausible to measure the orthogonality of two spatial signatures at subcarrier *n* by the crosscorrelation magnitude, $\left|\mathbf{h}_{k,q}^{n\ H}\mathbf{h}_{k',q'}^{n}\right| \quad ;\forall(k,q)\neq(k',q')$.

Let W^n be the chosen set of spatial signatures for the *n*th subcarrier that are pairwise approximately orthogonal, which means

$$\left|\mathbf{h}_{k,q}^{n\ H}\mathbf{h}_{k',q'}^{n}\right| \approx 0 \quad ;\forall(k,q),(k',q')\in W^n \tag{21}$$

Since the users in W^n are allowed to transmit simultaneously on subcarrier *n* without causing interference to each other at the receiving end, the subcarrier allocation index for the *n*th subcarrier becomes

$$\rho_{k,q}^{n} = \begin{cases} 1; (k,q)\in W^n \\ 0; \text{otherwise} \end{cases} \tag{22}$$

Therefore, the transmitted signal at the BTS on subcarrier *n* can be described as

$$\mathbf{x}^n = \sum_{(k,q)\in W^n} \mathbf{w}_{k,q}^{n} s_{k,q}^{n} \tag{23}$$

Since the channel vectors are pairwise orthogonal, the weight vector for transmit beamforming can be designed as the complex conjugate of the spatial signature vector

$$\mathbf{w}_{k,q}^{n} = \eta_{k,q}^{n}\bar{\mathbf{h}}_{k,q}^{n}; (k,q)\in W^n \tag{24}$$

For a specific $(k,q)\in W^n$, the received signal at the *k*th user's *q*th antenna can be obtained as

$$\begin{aligned} y_{k,q}^{n} &= \mathbf{h}_{k,q}^{n\ T}\left(\sum_{(k',q')\in W_n} \mathbf{w}_{k',q'}^{n} s_{k',q'}^{n}\right) + n_{k,q}^{n} \\ &= \eta_{k,q}^{n} s_{k,q}^{n} \left\|\mathbf{h}_{k,q}^{n}\right\|^2 + \mathbf{h}_{k,q}^{n\ T}\left(\sum_{(k',q')\neq(k,q)} \eta_{k',q'}^{n} s_{k',q'}^{n}\bar{\mathbf{h}}_{k',q'}^{n}\right) + n_{k,q}^{n} \\ &\approx \eta_{k,q}^{n} s_{k,q}^{n} \left\|\mathbf{h}_{k,q}^{n}\right\|^2 + n_{k,q}^{n} \end{aligned} \tag{25}$$

Please note that in writing (25), we have neglected the residual MUI, based on the fact of (21). Since several users can simultaneously share single subchannel, the overall throughput is expected to be increased compared with the SM scheme.

The energy consumption of the SDMA scheme can be calculated as

$$\begin{aligned} E_{SDMA} &= \sum_{n=1}^{N}\sum_{(k,q)\in W^n} \rho_{k,q}^{n} E\left\{\left|s_{k,q}^{n}\right|^2\right\}\left\|\mathbf{w}_{k,q}^{n}\right\|^2 \\ &= \sum_{n=1}^{N}\sum_{(k,q)\in W^n} \rho_{k,q}^{n}\eta_{k,q}^{n\ 2}\left\|\mathbf{h}_{k,q}^{n}\right\|^2 \leq E_{total} \end{aligned} \tag{26}$$

Let $N' = \sum_{n=1}^{N}\sum_{(k,q)\in W^n} \rho_{k,q}^{n}$, be the sum of the number of elements of the subset $\{W^n\}_{n=1,\ldots,N}$. We may determine $\{\eta_{k,q}^{n}\}$ by

$$\eta_{k,q}^{n} = \frac{1}{\left\|\mathbf{h}_{k,q}^{n}\right\|}\sqrt{\frac{E_{total}}{N'}} \tag{27}$$

Substituting (27) into (5), we obtain the number of bits that can be sent to the *k*th RT's *q*th antenna at *n*th subcarrier provided that $(k,q) \in W^n$.

$$m_{k,q}^{n} = \left\lfloor \log_2\left(1 + \frac{\pi}{\sin^{-1}\left(\left[\frac{1}{\left\|\mathbf{h}_{k,q}^{n}\right\|}\sqrt{\frac{N'N_0}{2E_{total}}}Q^{-1}\left(\frac{\lambda}{2}\right)\right]_{-}\right)}\right)\right\rfloor \tag{28}$$

Henceforth, the throughput of each user yields

$$T_k = \sum_{n=1}^{N}\sum_{(k,q)\in W^n} \rho_{k,q}^{n} m_{k,q}^{n}; \quad k = 1,\ldots,K \tag{29}$$

The algorithm of the proposed SDMA scheme is proceeded in the following:

Step 1: ***Grouping***: Starting from the first subcarrier, the BTS first separates and groups all the spatial signatures $\left\{\mathbf{h}_{k,q}^{n}\right\}_{q=1,\ldots,Q}$ into a set of quasi-orthogonal subsets based on a predetermined criterion,

$$\left|\mathbf{h}_{k,q}^{n\ H}\mathbf{h}_{k',q'}^{n}\right| \le \alpha \quad ;\forall (k,q) \ne (k',q') \tag{30}$$

where α is a small positive value. We denote the quasi-orthogonal subsets for *n*th subcarrier as $\left\{W_i^n\right\}_{i=1,\ldots}$.

Step 2: ***Selecting***: Denoting the sum norm of each vector in W_i^n as $\left\|W_i^n\right\|$, the BTS assigns the *n*th subcarrier to all the users in W_i^n, which yields the highest sum norm

$$i^* = \arg\max_i \left\|W_i^n\right\| \tag{31}$$

And we immediately set the subcarrier allocation index for the *n*th subcarrier as

$$\rho_{k,q}^{n} = \begin{cases} 1; (k,q) \in W_{i^*}^{n} \\ 0; \text{otherwise} \end{cases}$$

Step 3: Step 1 and 2 are proceeded until all the subcarriers have been allocated, *i.e.*, $\left\{W_{i^*}^n\right\}_{n=1,\ldots,N}$, $\left\{\rho_{k,q}^n\right\}$ are created and $N' = \sum_{n=1}^{N}\sum_{(k,q)\in W_{i^*}^n} \rho_{k,q}^{n}$.

Step 4: Calculate $m_{k,q}^{n}$ using (28), and then calculate the throughput of each user by (29).

Step 5: ***Reallocating***: Starting from the first user, check whether the minimum bit rate constraint is attained. If $T_k \ge R_k$, check for the next user, otherwise, increase the threshold value from α to $\alpha + \Delta$, where Δ is a small positive value, redo step 2~5 until $T_k \ge R_k; k = 1,\ldots,K$.

If all users' bit rates exceed the minimum bit rate constraint, then the subcarrier and bits allocation process has been completed. The overall throughput can be obtained as

$$T = \sum_{k=1}^{K} T_k = \sum_{k=1}^{K}\sum_{n=1}^{N}\sum_{(k,q)\in W_{i^*}^n} \rho_{k,q}^{n} m_{k,q}^{n} \tag{32}$$

3.3 Zero-Forcing (ZF) Scheme

The zero-forcing (ZF) scheme is an extension of the SM scheme, in which each subcarrier may be shared by all the RTs. To attain this goal, the weight vector of ZF scheme is selected based on the zero-forcing criterion such that each user's transmission does not interfere with other users' data. Alternatively, a user's own data symbols are spatially multiplexed by the *Q* receiving antennas. To mitigate MUI, the weight vector should meet the following criterion

$$\mathbf{h}_{k',q'}^{n\ T}\mathbf{w}_{k,q}^{n}=\eta_{k,q}^{n}\delta\left(k-k',q-q'\right)=\begin{cases}\eta_{k,q}^{n};k=k',q=q'\\0;\text{otherwise}\end{cases} \tag{33}$$

Upon defining the *L*-by-*KQ* matrix, $\mathbf{H}^{n}\equiv\left[\mathbf{H}_{1}^{n}\ \ \mathbf{H}_{2}^{n}\ \ \cdots\ \ \mathbf{H}_{K}^{n}\right]$, (33) can be rewritten as a compact form

$$\mathbf{H}^{nT}\mathbf{w}_{k,q}^{n}=\eta_{k,q}^{n}\mathbf{e}_{(k-1)Q+q} \tag{34}$$

where $\mathbf{e}_{(k-1)Q+q}$ denotes the $\left((k-1)Q+q\right)$th column vector of $\mathbf{I}_{KQ}$. If the array size of BTS satisfies $L\geq KQ$, which is usually the case in massive MIMO [11,12] system, we have infinitely many solutions since (34) is an underdetermined system. Assuming that $\mathbf{H}^{n}$ is full column rank, then the minimum-norm solution of (34) can be obtained as

$$\mathbf{w}_{k,q}^{n}=\eta_{k,q}^{n}\mathbf{H}^{n}\left[\mathbf{H}^{nT}\mathbf{H}^{n}\right]^{-1}\mathbf{e}_{(k-1)Q+q} \tag{35}$$

The received signal at the *k*th RT's *q*th receiver yields

$$y_{k,q}^{n}=\mathbf{h}_{k,q}^{n\ T}\left(\sum_{l=1}^{K}\sum_{r=1}^{Q}s_{l,r}^{n}\mathbf{w}_{l,r}^{n}\right)+n_{k,q}^{n}=\eta_{k,q}^{n}s_{k,q}^{n}+n_{k,q}^{n} \tag{36}$$

As revealed by (36), though multiple users are simultaneously transmitted using the same subcarrier, only the desired signal retains. Consequently, the MUI is completely removed by transmit beamforming and each subcarrier can be assigned simultaneously to all the user terminals.

Since for arbitrary *n*, all user terminals are allowed to share a subchannel at the same time, hence, the subcarrier allocation index for the ZF scheme is

$$\rho_{k,q}^{n}=1;\forall k=1,\ldots,K,n=1,\ldots,N,q=1,\ldots,Q \tag{37}$$

The energy consumption of the ZF scheme can be calculated from (37) and (35) as

$$\begin{aligned}E_{ZF}&=\sum_{k=1}^{K}\sum_{n=1}^{N}\sum_{q=1}^{Q}\rho_{k,q}^{n}\left\|\mathbf{w}_{k,q}^{n}\right\|^{2}\\&=\sum_{k=1}^{K}\sum_{n=1}^{N}\sum_{q=1}^{Q}\eta_{k,q}^{n\ 2}\left\|\mathbf{H}^{n}\left[\mathbf{H}^{nT}\mathbf{H}^{n}\right]^{-1}\mathbf{e}_{(k-1)Q+q}\right\|^{2}\\&=\sum_{k=1}^{K}\sum_{n=1}^{N}\sum_{q=1}^{Q}\eta_{k,q}^{n\ 2}\left[\mathbf{H}^{nT}\mathbf{H}^{n}\right]^{-1}\left((k-1)Q+q,(k-1)Q+q\right)\end{aligned} \tag{38}$$

Since E_{ZF} should be upper-bounded by E_{total}, we may select $\left\{\eta_{k,q}^{n}\right\}$ as

$$\eta_{k,q}^{n}=\sqrt{\frac{E_{total}}{KNQ\left[\mathbf{H}^{nT}\mathbf{H}^{n}\right]^{-1}\left((k-1)Q+q,(k-1)Q+q\right)}} \tag{39}$$

Substituting the symbol energy $E_{k,q}^{n}=E\left\{\left|\eta_{k,q}^{n}s_{k,q}^{n}\right|^{2}\right\}=\eta_{k,q}^{n\ 2}$ and (39) into (5), we obtain the allowable bits that can be sent to user *k*'s *q*th antenna at subcarrier *n* as

$$m_{k,q}^{n}=\left\lfloor\log_{2}\left(\frac{\pi}{\sin^{-1}\left(\left[\sqrt{\frac{KNQN_{0}\left[\mathbf{H}^{nT}\mathbf{H}^{n}\right]^{-1}\left((k-1)Q+q,(k-1)Q+q\right)}{2E_{total}}}Q^{-1}\left(\frac{\lambda}{2}\right)\right]_{-}\right)}\right)\right\rfloor \tag{40}$$

Exploiting (40), the overall throughput of the ZF scheme can be calculated by

$$T_{ZF} = \sum_{k=1}^{K} T_k = \sum_{k=1}^{K} \sum_{n=1}^{N} \sum_{q=1}^{Q} m_{k,q}^{n} \tag{41}$$

However, in heavy-loaded or bursty traffic system, the assumption that $L \geq KQ$ no longer satisfies. Complete MUI suppression is not possible, we propose two algorithms to cope with this problem in the preceding section.

IV. MULTIUSER RESOURCE ALLOCATION IN THE CASE OF $L<KQ$

4.1 Selected ZF (SZF) Scheme

Consider the case $L < KQ$, it is not possible to use ZF scheme since (34) becomes an overdetermined system and the matrix $\mathbf{H}^{nT}\mathbf{H}^{n}$ in (35) is now singular. To make the ZF scheme feasible, one needs to select L out of the KQ column vectors of $\mathbf{H}^{n}$. We refer it as the selected ZF (SZF) scheme. For each subcarrier, the optimum SZF algorithm first requires to generate $\binom{KQ}{L}$ square matrices. Each possible matrix is substituted into (40) and (41) to evaluate the corresponding throughput, and the best (largest) one is chosen subject to the minimum rate constraint. However, since the optimum solution can only be found with exhaustive search, it is computationally prohibitive for most practical values of L and (or) KQ.

The objective of the proposed SZF algorithm is to allocate each subcarrier to L spatial signatures selected from $\mathbf{H}^{n}$ such that the throughput is maximized with reduced complexity. Such is accomplished as follows:

Step 1: Initialization

For each subcarrier (start from the first subcarrier, n=1), the BTS first assigns the subcarrier to the vector channel with the highest gain, which corresponds to the maximum bits to be transmitted, among all users and all antennas in that subchannel. Let W be the joint user antenna index set, $W = \{(k,q)\}_{\substack{k=1,2,\ldots,K \\ q=1,2,\ldots,Q}}$, we have

$$(k^{*}, q^{*}) = \arg \max_{(k,q)\in W} \left\| \mathbf{h}_{k,q}^{n} \right\| \tag{42}$$

Step 2: Set i=1,

$$W^{(1)} = W \setminus (k^{*}, q^{*})$$

Set $\mathbf{h}^{(1)} = \mathbf{h}_{k^{*},q^{*}}^{n}$ and construct $\mathbf{H}^{(1)} = \left[\mathbf{h}^{(1)}\right]$

Step 3: While $i < L$, set$i$=i+1

The BTS chooses each additional spatial signature based on the criterion that the throughput is maximized after the new spatial signature is added:

$$(k^{*}, q^{*}) = \arg \max_{(k,q)\in W^{(i)}} T\left(\left[\mathbf{H}^{(i)} \quad \mathbf{h}_{k,q}^{n}\right]\right) \tag{43}$$

where the objective function is as defined in (40), (41). As revealed by (43), we use total throughput for the considered subcarrier as the design metric, hence, the spatial signature which leads to maximum throughput is added. It is evident that maximizing $T\left(\left[\mathbf{H}^{(i)} \quad \mathbf{h}_{k,q}^{n}\right]\right)$ is equivalent to minimizing the trace (sum of the diagonal elements) of $\left(\left[\mathbf{H}^{(i)} \quad \mathbf{h}_{k,q}^{n}\right]^{T}\left[\mathbf{H}^{(i)} \quad \mathbf{h}_{k,q}^{n}\right]\right)^{-1}$. In what follows, we may use the following criterion instead of (43)

$$(k^{*}, q^{*}) = \arg \min_{(k,q)\in W^{(i)}} tr\left\{\left(\left[\mathbf{H}^{(i)} \quad \mathbf{h}_{k,q}^{n}\right]^{T}\left[\mathbf{H}^{(i)} \quad \mathbf{h}_{k,q}^{n}\right]\right)^{-1}\right\} \tag{44}$$

After the new spatial signature is assigned to the considered subcarrier, the BTS updates the record as

$$W^{(i+1)} = W^{(i)} \setminus (k^{*}, q^{*})$$

Set $\mathbf{h}^{(i+1)} = \mathbf{h}^{n}_{k^*,q^*}$ and construct $\mathbf{H}^{(i+1)} = \left[\mathbf{H}^{(i)} \quad \mathbf{h}^{(i+1)}\right]$

Step 4: Calculation

Step 2 is repeated until the *L*-by-*L* matrix, $\mathbf{H}^{(L)}$, is constructed, the BTS records the indices of the column (channel) vectors, $W^n \subset W$. Therefore, the bits that can be sent by the *l*th channel can then be calculated as

$$m^n_{k,q} = \left\lfloor \log_2 \left(\frac{\pi}{\sin^{-1}\left(\left[\sqrt{\frac{NLN_0 \left[\mathbf{H}^{(L)T}\mathbf{H}^{(L)}\right]^{-1}(l,l)}{2E_{total}}} Q^{-1}\left(\frac{\lambda}{2}\right) \right]_- \right)} \right) \right\rfloor \tag{45}$$

Henceforth, the throughput of each user yields

$$T^n_k = \sum_{i=1}^{n} \sum_{(k,q)\in W^n} m^i_{k,q}; \qquad k = 1,\ldots,K \tag{46}$$

Step 5: Based on the results obtained from (46), the BTS checks whether user k^* meets the minimum bit rate constraint. If $T^n_{k^*} < R_{k^*}$, which means more subchannels should be assigned to user k^*, go back to step 1 and check for the next subcarrier. On the other hand, if $T_{k^*} \geq R_{k^*}$, we temporarily exclude user k^*

$$W = W \setminus \left\{\left(k^*, q\right)\right\}_{q=1,\ldots,Q}$$

Set$n$=n+1, go back to step 1 to assign the subchannels to those users that have not attained the minimum bit rate constraint.

Step 6: As long as all the users meet the minimum bit rate constraint, remove all the exclusions, redo step 1 until all the subcarriers have been allocated.

Iterative method of evaluating (44)

In view of the SZF algorithm, a lot of matrix inverse are required to implement (44). The complexity hinders the applicability of this scheme. We aim at developing an iterated method to reduce the load of computations. To begin with, we define the (i+1)-by-(i+1) matrix, $\mathbf{A}^{(i+1)}$, as

$$\mathbf{A}^{(i+1)} \equiv \left[\mathbf{H}^{(i)} \quad \mathbf{h}^{(i+1)}\right]^T \left[\mathbf{H}^{(i)} \quad \mathbf{h}^{(i+1)}\right] = \begin{bmatrix} \mathbf{H}^{(i)T}\mathbf{H}^{(i)} & \mathbf{H}^{(i)T}\mathbf{h}^{(i+1)} \\ \mathbf{h}^{(i+1)T}\mathbf{H}^{(i)} & \mathbf{h}^{(i+1)T}\mathbf{h}^{(i+1)} \end{bmatrix} \tag{47}$$

Upon defining $\mathbf{a}^{(i+1)} = \mathbf{H}^{(i)T}\mathbf{h}^{(i+1)}$, (47) can be rewritten into the recursive form

$$\mathbf{A}^{(i+1)} = \begin{bmatrix} \mathbf{A}^{(i)} & \mathbf{a}^{(i+1)} \\ \mathbf{a}^{(i+1)T} & \left\|\mathbf{h}^{(i+1)}\right\|^2 \end{bmatrix} \tag{48}$$

Exploiting the matrix inversion lemma [Chap. 4 of [8]], and the method proposed in [15], we have

$$\left(\mathbf{A}^{(i+1)}\right)^{-1} = \begin{bmatrix} \left(\mathbf{A}^{(i)}\right)^{-1} & \mathbf{0}_i \\ \mathbf{0}_i^T & 0 \end{bmatrix} + \frac{1}{\left(\left\|\mathbf{h}^{(i+1)}\right\|^2 - \mathbf{a}^{(i+1)T}\mathbf{b}^{(i+1)}\right)} \begin{bmatrix} \mathbf{b}^{(i+1)}\mathbf{b}^{(i+1)T} & -\mathbf{b}^{(i+1)} \\ -\mathbf{b}^{(i+1)T} & 1 \end{bmatrix} \tag{49}$$

where $\mathbf{b}^{(i+1)} \equiv \left(\mathbf{A}^{(i)}\right)^{-1}\mathbf{a}^{(i+1)}$, $\mathbf{0}_i$ is a zero vector with size *i*. As we can observe from (49), each time when we attempt to calculate $\left(\mathbf{A}^{(i+1)}\right)^{-1}$ in (44), $\left(\mathbf{A}^{(i)}\right)^{-1}$ is already available. The complexity can be extensively reduced.

4.2 Least-Squares (LS) algorithm

Assuming that $\mathbf{H}^n$ is full (row) rank, the least-squares (LS) solution [8] of an overdetermined system of (34) becomes

$$\mathbf{w}_{k,q}^{n}=\eta_{k,q}^{n}\left[\mathbf{H}^{n}\mathbf{H}^{nT}\right]^{-1}\mathbf{H}^{n}\mathbf{e}_{(k-1)Q+q} \tag{50}$$

It follows that the energy consumption of the LS scheme can be calculated from (50) as

$$\begin{aligned}E_{LS}&=\sum_{k=1}^{K}\sum_{n=1}^{N}\sum_{q=1}^{Q}\rho_{k,q}^{n}\left\|\mathbf{w}_{k,q}^{n}\right\|^{2}\\&=\sum_{k=1}^{K}\sum_{n=1}^{N}\sum_{q=1}^{Q}\eta_{k,q}^{n\ 2}\left\|\left[\mathbf{H}^{n}\mathbf{H}^{nT}\right]^{-1}\mathbf{H}^{n}\mathbf{e}_{(k-1)Q+q}\right\|^{2}\\&=\sum_{k=1}^{K}\sum_{n=1}^{N}\sum_{q=1}^{Q}\eta_{k,q}^{n\ 2}\mathbf{M}^{n}\left((k-1)Q+q,(k-1)Q+q\right)\end{aligned} \tag{51}$$

where $\mathbf{M}^{n}\equiv\mathbf{H}^{nT}\left[\mathbf{H}^{n}\mathbf{H}^{nT}\right]^{-2}\mathbf{H}^{n}$. Since E_{LS} should be upper-bounded by E_{total}, we may select $\left\{\eta_{k,q}^{n}\right\}$ as

$$\eta_{k,q}^{n}=\sqrt{\frac{E_{total}}{KNQ\mathbf{M}^{n}\left((k-1)Q+q,(k-1)Q+q\right)}} \tag{52}$$

The received signal at the *k*th RT's *q*th receiver is

$$\begin{aligned}y_{k,q}^{n}&=\mathbf{h}_{k,q}^{n\ T}\left(\sum_{l=1}^{K}\sum_{r=1}^{Q}s_{l,r}^{n}\mathbf{w}_{l,r}^{n}\right)+n_{k,q}^{n}\\&=\eta_{k,q}^{n}s_{k,q}^{n}+\sum_{l=1}^{K}\sum_{\substack{r=1\\(l,r)\neq(k,q)}}^{Q}s_{l,r}^{n}i_{l,r}^{n}+n_{k,q}^{n}\end{aligned} \tag{53}$$

where $i_{l,r}^{n}\equiv\mathbf{h}_{k,q}^{n\ T}\mathbf{w}_{l,r}^{n}$ is the residual MUI. The signal-to-interference-plus-noise ratio (SINR) can be obtained from (53) as

$$\gamma_{k,q}^{n}=\frac{\eta_{k,q}^{n\ 2}}{\sum_{l=1}^{K}\sum_{\substack{r=1\\(l,r)\neq(k,q)}}^{Q}\left|i_{l,r}^{n}\right|^{2}+\frac{N_{0}}{2}}=\frac{\frac{E_{total}}{KNQ\mathbf{M}^{n}\left((k-1)Q+q,(k-1)Q+q\right)}}{\sum_{l=1}^{K}\sum_{\substack{r=1\\(l,r)\neq(k,q)}}^{Q}\left|i_{l,r}^{n}\right|^{2}+\frac{N_{0}}{2}} \tag{54}$$

The allowable bits that can be sent to user *k*'s *q*th antenna at subcarrier *n* can be obtained as

$$m_{k,q}^{n}=\left\lfloor\log_{2}\left(\frac{\pi}{\sin^{-1}\left(\left[\frac{1}{\sqrt{\gamma_{k,q}^{n}}}Q^{-1}\left(\frac{\lambda}{2}\right)\right]_{-}\right)}\right)\right\rfloor \tag{55}$$

Exploiting (55), the overall throughput of the LS scheme can be calculated by

$$T_{LS}=\sum_{k=1}^{K}T_{k}=\sum_{k=1}^{K}\sum_{n=1}^{N}\sum_{q=1}^{Q}m_{k,q}^{n} \tag{56}$$

In summary, the main difference between SZF and LS schemes resides in how they deal with MUI. SZF relies on complete MUI suppression, thus a maximum of *L* spatial signatures are chosen to carry information bits. While in LS scheme, all the *KQ* spatial signatures convey information bits, nevertheless, the inevitable residual MUI may degrade SER as well as the bits that can be sent through each channel.

V. PERFORMANCE EVALUATION

We set the target QoS (SER upper bound) to be $\lambda=10^{-4}$ throughout all the simulation examples. For each subcarrier, we generate the channel vector $\mathbf{h}_{k,q}^{n}=\sqrt{\alpha_{k,q}^{n}}\mathbf{g}_{k,q}^{n}$, in which $\mathbf{g}_{k,q}^{n}$ denotes small-scale fading and $\alpha_{k,q}^{n}$ denotes large-scale fading coefficient (lognormal distribution and geometric decay). We assume $\mathbf{g}_{k,q}^{n}\sim\square N\left(\mathbf{0},\mathbf{I}_{L}\right)$ and are statistically independent across users. The result in each simulation example is obtained from the average of 100 independent trials. Unless otherwise

mentioned, we set the total energy consumption constraint at the BTS is set such that the energy to noise ratio for each user is $\frac{E_{total}}{NN_0} = 10dB$. The predetermined threshold, α, and step size, Δ, for the SDMA scheme is set to be 1 and 0.5, respectively. To treat users fairly, we set equal rate constraint on each user, *i.e.*, $R_1 = R_2 = \cdots = R_K = R$ bits per OFDM symbol. A plausible criterion to measure the performance of the subcarriers and bits allocation algorithms is the bandwidth (spectral) efficiency, which is defined as the ratio of the data rate in bits per second to the effectively utilized bandwidth. In this paper, we define the bandwidth efficiency as the overall throughput normalized by the total number of subcarriers

$$c \equiv \frac{T}{N} = \frac{\sum_{k=1}^{K}\sum_{n=1}^{N}\sum_{q=1}^{Q}\rho_{k,q}^{n} m_{k,q}^{n}}{N} \tag{57}$$

In the first simulation example, we aim at comparing the performance of the proposed SZF with the optimum SZF schemes, where the number of subcarriers, the number of RTs and the array size at each RT are N=64, K=10 and Q=2, respectively. Fig. 2 presents the bandwidth efficiency with respect to the number of BTS antennas (varying from L=4 to L=16), where the SDMA and SM schemes are also provided for comparison. As depicted in Fig. 2, the bandwidth efficiency of the SZF scheme increases in accordance with larger L, whereas, the SDMA and SM schemes are insensitive to L. It results from that the SM scheme is essentially based on single-user algorithm. Somewhat surprisingly, the SM scheme outperforms SDMA scheme. It may due to the fact that the number of "nearly orthogonal" channel vectors is rare in case that L is small. We have also verified from Fig. 2 that the proposed iterated SZF scheme is close to optimum SZF scheme, nevertheless, the complexity of the proposed algorithm is extensively reduced.

Fig. 3 presents the bandwidth efficiency with respect to the number of user terminals (ranging from K=3 to K=45), where N=300, and the array size at the BTS and each RT are L=60 and Q=3, respectively. As shown in the figure, the bandwidth efficiency is in ascending order from SM scheme to SDMA scheme, then LS scheme, and SZF scheme is the best. Please note that as K<20, (*i.e.*, KQ<L), LS as well as SZF schemes coincide with the regular ZF, which is applied in underdetermined system. We can also observe that the performance of the SZF scheme increases rapidly in accordance with K while LS scheme slightly degrades for larger K. This arises from the fact that both algorithms allow multiple user terminals to share a subchannel at the same time. Thereby, larger K extensively increases the throughput for SZF scheme, whereas the residual MUI resulted from larger K degrades the performance of the LS scheme. Fig. 4 compares the bandwidth efficiency with respect to the number of BTS antennas, where N=256, K=20, and Q=5. As revealed by Fig. 4, the SM and SDMA schemes are insensitive to the variation of L, nevertheless, performance discrepancy between the multiuser algorithms (SZF and LS) and other schemes is obvious for larger L. This may due to the facts that larger L corresponds to larger degrees-of-freedom to suppress MUI. Specifically, Fig. 4 reveals that LS outperforms SZF scheme when L is small. This is due to the fact that a maximum of L spatial signatures are chosen to carry information bits in SZF, whereas LS allows all the KQ channels to send information bits. Fig. 5 presents the bandwidth efficiency with respect to $\frac{E_{total}}{NN_0}$ (ranging from 6 to 15 dB), where N=256, K=20, Q=5 and L=60, respectively.As revealed by the figure, only SZF scheme has obvious improvement by increasing the dedicated power at each subchannel. The aim of the final simulation example is to evaluate performance improvement invoked by the spatial diversity at the RT. We present the bandwidth efficiency with respect to the number of RT's antennas (ranging from Q=1 to Q=19) in Fig. 6, where N=400, K=20, and L=200, respectively.As verified by the numerical results, the bandwidth efficiency of the SM and SZF schemes has obvious improvement by inducing larger antenna array at the RT.Please note that as$Q$<10, LS as well as SZF schemes coincide with the regular ZF.The LS scheme, though simple in structure, suffers from MUI for larger Q. Specifically, throughput for the SZF scheme decreases as $Q \approx 10$. This may result from ill-condition for matrix $\mathbf{H}_k^n$ as KQ approaches L.As a whole, the proposed SZF scheme outperforms the other three schemes to a large extent under different scenarios.

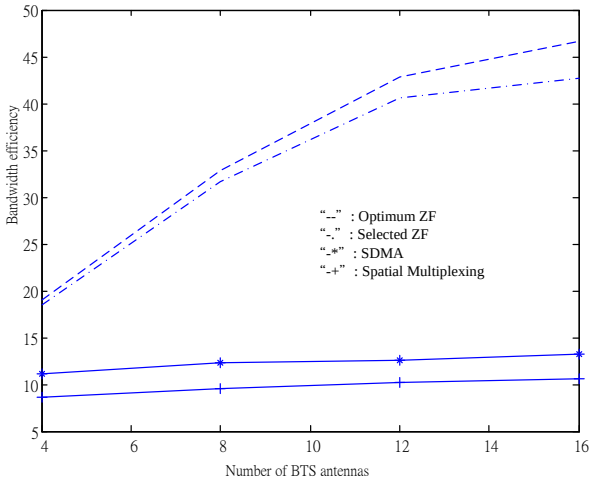

FIG. 2: Bandwidth efficiency with respect to the number of BTS antennas.

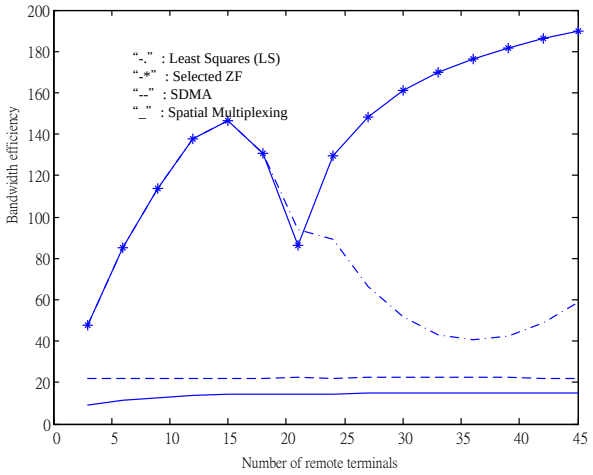

FIG. 3: Bandwidth efficiency with respect to the number of RTs, *N*=300, *L*=60 and *Q*=3.

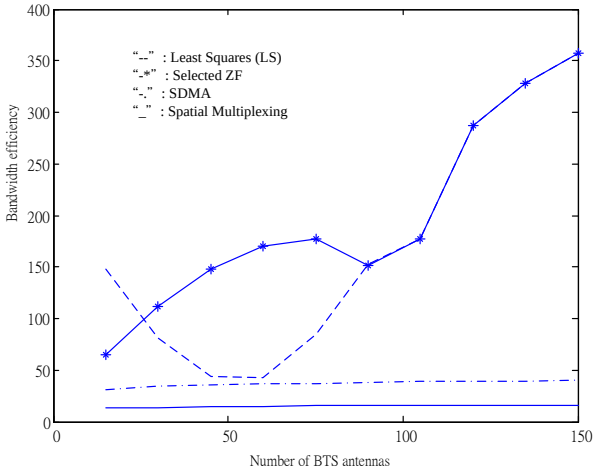

FIG. 4: Bandwidth efficiency with respect to the number of BTS antennas, *N*=256,*K*=20, *Q*=5.

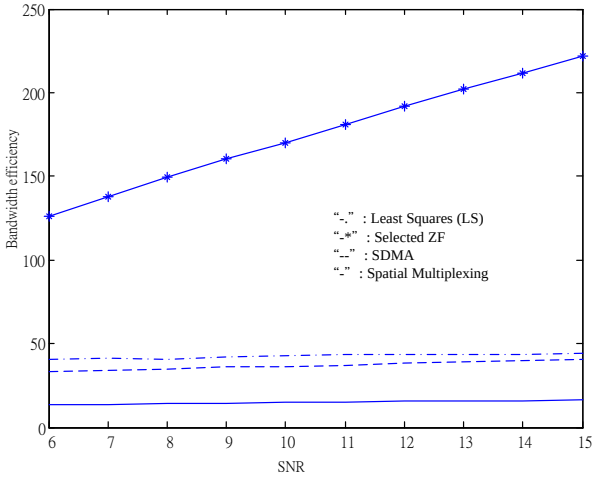

FIG. 5: Bandwidth efficiency with respect to $\frac{E_{total}}{NN_0}$, where *N*=256, *K*=20, *Q*=5 and *L*=60.

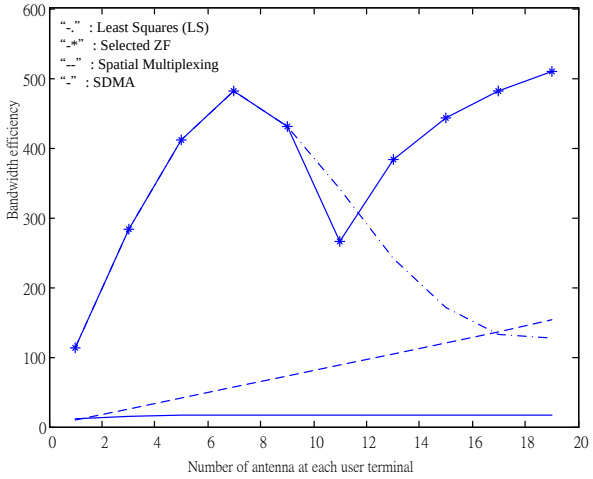

FIG. 6: Bandwidth efficiency with respect to the number of RT's antennas, where *N*=400, *K*=20 and *L*=200.

VI. CONCLUSION

In this paper, we have proposed four resource allocation algorithms in OFDMA based multiuser MIMO system, namely, SM, SDMA, SZF and LS schemes. All the proposed algorithms are channel aware in the sense that they adapt to the channel conditions. Specifically, the SDMA and SZF algorithms judiciously select co-channel users based on their spatial signatures

to enable significant improvement in the system throughput. Analytical and simulation results demonstrated that employing the antenna array at the BTS and RT has extensively increased the spectral efficiency. Furthermore, since the proposed algorithms are simple yet reliable, it is plausible to apply it for resource allocation in practical multiuser OFDMA-based LTE system, where multiple antenna transmission and reception are available.

REFERENCES

[1] A. Ghosh, J. Zhang, J. G. Andrews and R. Muhamed, Fundamentals of LTE, Prentice Hall, Inc. 2011.

[2] S.S. Prasad, C.K. Shukla and R.F. Chisab, "Performance analysis of OFDMA in LTE", 2012 third International Conference on Computing Communication and Networking Technologies (ICCCNT), 26-28 July 2012.

[3] M. Al-Imari, P. Xiao, M. Ali Imran and R. Tafazolli, "Low complexity subcarrier and power allocation algorithm for uplink OFDMA systems", EURASIP Journal on Wireless Communications and Networking 2013 doi:10.1186/1687-1499-2013-98.

[4] P. Svedman, S. K. Wilson, L. J. Cimini, and B. Ottersten, "Opportunistic beamforming and scheduling for OFDMA systems" IEEE Trans. on Communications, 55(5):941-952, May 2007.

[5] C. Y. Wong, R. S. Cheng, K. B. Letaief, and R. D. Murch, "Multiuser OFDM with adaptive subcarrier, bit, and power allocation", IEEE Journal on Selected Areas in Communications, vol. 17, pp. 1747–1758, Oct. 1999.

[6] Y. J. Zhang, and K. B. Letaief, "Multiuser Adaptive Subcarrier-and-Bit Allocation With Adaptive Cell Selection for OFDM Systems", IEEE Trans. Wireless Communications, vol. 3, no. 5, pp. 1566~1575, Sep. 2004.

[7] W. C. Wu and C. Y. Hsu, "A Low Complexity Algorithm for Subcarrier-and-Bit Allocation in OFDMA-based LTE Systems", to be published in Journal of Electronic Science and Technology.

[8] T. K. Moon and W. C. Stirling, Mathematical Methods and Algorithms, Upper Saddle River, NJ, Prentice Hall 2000.

[9] M. Matthaiou, C. Zhong, M. R. Mckay and T. Ratnarajoh, "Sum rate analysis of ZF receivers in distributed MIMO systems", IEEE Journal on Selected Areas in Communications, vol. 31, no. 2, pp. 180~191, Feb. 2013.

[10] C. Studer, and E. G. Larsson, "PAR aware large-scale multi-user MIMO-OFDM downlink", IEEE Journal on Selected Areas in Communications, vol. 31, no. 2, pp. 303~313, Feb. 2013.

[11] L. Lu, Geoffrey Y. Li, A. Lee Swindlehurst, A. Ashikhmin and R. Zhang, "An overview of massive MIMO: benefits and challenges", IEEE Journal on Selected Areas in Communications, vol. 8, no. 5, pp. 742~758, Oct. 2014.

[12] F. Fernandes, A. Ashikhmin and T. L. Marzetta, "Inter-cell interference in noncooperative TDD large scale antenna systems", IEEE Journal on Selected Areas in Communications, vol. 31, no. 2, pp. 1~10, Feb. 2013.

[13] S. Haykin, Communication Systems, Chap. 6, 4th editions, John Wiley & Sons, Inc. 2001.

[14] W. C. Wu, "Robust Pre-filtering Based Space Division Multiple Access over Multi-path Channels", Transaction on Emerging Telecommunications Technologies, vol. 26, no. 3, pp. 403~413, Mar. 2015.

[15] G. Dimic and N. D. Sidiropoulos, "Low-complexity downlink beamforming for maximum sum capacity", 2004 IEEE International Conference on Acoustics, Speech, and Signal Processing (ICASSP 2004), vol. 4, pp. IV. 701~704, 2004.

Online Shopping With Spoofing Detection Using Web and Mobile Application

M.Poovizhi[1], K.Karthika[2], S.Nandhini[3], Dr.P.Gomathi[4]

[1,2,3]Computer Science and Engineering, N.S.N College of Engineering and Technology, Tamil Nadu, India
[4]Electrical and Electronics Engineering, N.S.N College of Engineering and Technology, Tamil Nadu, India

Abstract— *E-commerce is that the shopping for marketing of products and services, or the sending of funds or knowledge, over a web and straightforward access to immense stores of reference material, email, and new avenues for advertising and data distribution, to call some. Like most technological advances, there conjointly another side: criminal hackers. Governments, companies, and personal voters round the world area unit anxious to be an area of this revolution, however, they are afraid that some hacker can burgle their net server and replace their brand with erotica, scan their e-mail, steals their MasterCard range from an on-line searching web site, or implant computer code that may on the QT transmit their organization secrets to the open net. Online shopping is used to getting order from the user through internet and mobile so, this is also called as mobile commerce. The goods are delivered to the customer with secured manner. The status about the product during delivery is to be monitored. A Secured Socket Layer (SSL) certificate is that the common place technique that wanted to defend net communications and it defend sensitive data because it travels across the net preventing any potential security attacks or threats on the approach. Essentially SSL could be a technology that encrypts and decrypts messages sent between the browser and server. Once the message is received by the server, SSL decrypts it, and verifies that it came from the right sender.*

Keywords— HMM, K-MEANS, SSL.

I. INTRODUCTION

Networks square measure all over thus hardly doing one thing with information that does not involve a network. Rather like the human networks, all square measure components of laptop networks to share data and resources. In business, the reliance on networks is even further pervasive than in homes or facilities. Networks facilitate folks and businesses alike save money; however, in addition facilitate manufacture gain .while not a doubt, networking at intervals the house can catch on over succeeding few years as a results of it is in business. Soon, nearly all people in even moderately developed nations can have networked parts throughout their homes. Here it begins by relating networks to think and ideas are already familiar. In fact, it is so useful to be told the ropes of networking through active guided that what is planned. If play the role of associate staff throughout a fictional company, and to be told on the duty. The extra will become the person; the extra will study the necessity for operation of laptop networks. Altogether likelihood taking this class to be told regarding laptop networks, and also the manner necessary networks are a unit for businesses that require to survive, may very be associate employee operational for such a corporation and trying to help it out of that issue, or may acknowledge of people or companies that square measure throughout this type of struggles. Lauren has recently been utilized as a result of the laptop manager for sink or swim pools. Lauren could also be a licensed network administrator.

II. LITERATURE SURVEY

[1]The importance of automatic data processing system security of banks is exaggerated. Conducting risk assessment of automatic data processing system security of banks will increase safety management and guarantee traditional operation. It explains risk assessment indexes for automatic data processing system security of banks through literature review and survey. Secondly, it uses AHP to substantiate the load of indicators and establishes five security levels. In line with the judgment of specialists, it finally establishes the chance assessment model for automatic data processing system security of banks.

[2]A formalized methodology to particularly quantify the protection level in real time from the attitude of state transition chance through estimating the stable chance of staying within the security state in heterogeneous continuous time Markov process. The paradigm permits users to customize the protection mechanisms for adapting to the often varied context. The numerical calculations and empirical analysis to comprehensively investigate the response of the planned security quantification framework to the assorted mixtures of the involved parameters, e.g., SNR, velocity, and the traffic flow. The results show that the planned framework

is capable of capturing the period security level adaptively to the vehicle context and provides a dependable call basis for security protection.

[3]Traffic volumes in mobile networks are rising and end-user wants to chop-chop ever-changing. Mobile network operators would like a lot of flexibility, lower network operative prices, quicker service rollout cycles, and new revenue sources. The new technologies are at risk within the context of the new telecommunication paradigm. We have a tendency to gift a multi-tier component-based security design to handle these challenges and secure 5G software system defined mobile network by handling security at totally different levels to safeguard the network and its users.

[4] Security issues became obstacles within the exercise of wireless device networks, and intrusion detection is that the second line of defence. During the work, associate intrusion detection supported dynamic state context and hierarchical trust in WSN is planned, that is versatile and appropriate for perpetually ever-changing Wireless Sensor Network (WSN)characterized by changes within the sensory activity surroundings, transitions states of nodes and variations in the trust priceimplies that the trust of Sensor Node (SN) is evaluated by Cluster Head (CH), and therefore the thrust of CH is evaluated by neighbour CH and Base Station (BS).

[5]Effect of antivirals within the electronic network prevents a space the spreading behaviour of malicious objects and therefore the role of Quarantine treatment in a very electronic network will increase the recovery rate of the infected computers. The steadiness of the model and therefore the basic replica variety of the model are additionally derived. Moreover, the impact of antivirus and quarantine within the system is analysed.

[6] In the last decade, the progress of net technologies has junction rectifier to a significant increase in security and privacy problems for users. Within the network security, law-breaking technologies have brought several delicacies by suggesting that of the internet: electronic commerce, easy accessibility to immense stores of reference material, cooperative computing, email, and new avenues for advertising and knowledge distribution, to call many.

III. EXISTING SYSTEM

In day to day life tend to use virtual card for on-line dealing or physical card for associate offline dealing. The prevailing system would not integrate with the PayPal and also the payout. Engaging pictures area unit most generally used for the client to shop for the merchandise through the app, however, within the existing the pictures solely have a typical structure therefore we tend to cannot update a desired structure of the image. Commonplace kind means that we are able to solely use victimization the actual image, therefore it does not have associate higher image. An important one is that in associate existing system security is not higher. It is simple to access the browser or user data, profile, buying things and their checking account. It causes the browser during a risky manner throughout the buying products through a web. To hold out dishonourable transactions during this quite purchase, associate assailant has got to steal the MasterCard. If the cardholder does not notice the loss of card, it will result in a considerable loss to the Master Card Company.

On-line payment mode, attackers want solely very little data for doing dishonourable dealing. During the purchase technique, in the main transactions are going to be done through the web or phone. To commit fraud in these forms of purchases, a fraudster merely has to recognize the cardboard details. Most of the time, the real cardholder is not aware that somebody else has seen or purloined his card data. Thanks to that the image are not in associate commonplace kind and fewer security the buying of products among the user area unit reduced. It is troublesome to analysis of the one who is hacking the user profile throughout the ordering of the things or throughout the dealing of the user through the web buying.

Disadvantages

a. In on-line payment mode, attackers want solely very little info for doing dishonest dealings.

b. The pictures do not seem to be in associate degree commonplace kind as a result of it doesn't use the PayPal and Paytm system

c. It does not have a more robust security throughout the dealings of the number throughout getting and a customer profile.

IV. PROPOSED SYSTEM

A Hidden Markov Model may be a finite set of states; every state is connected with a likelihood distribution. Transitions between these states are a unit ruled by a collection of chances referred to as transition chances. During an explicit state a potential outcome or observation is generated that is associated image of observation of likelihood distribution. It is solely

the end result, not the state that is visible to associate external observer and so state area unit "hidden" to the outside; therefore the name Hidden Markov Model. Hence, Hidden Markov Model may be an excellent answer for addressing the detection of fraud dealings through MasterCard.

The Hidden Markov Model is used to reduce the false positive transitions and it also used to detect the anomaly. The anomaly is nothing but different from the normal behaviour by victimization the K-means bunch formula which might outlay the profile of the user into low, medium, high cluster and consequently generates observation symbols. That area unit any divided into HMM for coaching also as detection purpose. K-means bunch will divide the dealings quantity into completely different clusters. The main advantage is that it will use PayPal and Paytm therefore it will get a gorgeous and completely different structure of pictures and it is used to store the large amount of data.

4.1 Hidden Markov Model

Hidden Andre Markov Model is that the one amongst the formula utilized in this idea. The practicality of the Hidden Markov Model may be a finite set of states; every state is joined with a likelihood distribution. Transitions between these states are a unit ruled by a group of possibilities referred to as transition possibilities.

The Hidden Markov Model only shows their status not the process so it is called as a Hidden Markov Model. In an exceedingly explicit state an attainable outcome or observation is often generated that is associated image of observation of likelihood distribution. It is solely the result, not the state that is visible to associate external observer and thus states area unit "hidden" to the outside; Hence, Hidden Andre Markov Model may be an excellent answer for addressing the detection of fraud dealing through Master Card. Another essential preferred standpoint of the HMM-based approach is a partnership outrageous lessoning inside the scope of False Positives exchanges perceived as noxious by an extortion location framework regardless of the way that they're to a great degree genuine.

In this prediction method, HMM considers chiefly 3 value price ranges like. Low, Medium and, High. First, it will be needed to search out the dealing quantity belongs to a selected class either it will be in low, medium, or high ranges. At first the HMM is trained with the conventional behavior of a card holder then defrayment patterns of user are often determined with the assistance of K-means clump formula. If associate incoming dealing isn't accepted by the HMM with adequate likelihood, then it is often detected as fraud for any confirmation security question module are activated that contains some personal queries that area unit solely celebrated to approved client and if the dealing is dishonest, then verification code is inquiring for any confirmation.

The hidden Andre Markov model works on Markov chain property within which likelihood of every consequent state depends on the previous state that consists of observation possibilities, transition possibilities and initial possibilities. The hidden Andre Markov model are often thought about a generalization of a mixture model wherever the hidden variables or latent variables, that management the mixture element to be designated for every observation, area unit connected through a Markov method instead of freelance of every different.

4.2 K-Means Clustering Algorithm

K-Means bunch algorithmic rule are often used for the aim of cacophony from the user profile time. Meaning in however durable that the user is defrayal his time throughout the buying of things. By victimization K-MEANS bunch algorithmic rule that divides the defrayal profile of a user into low, medium and high cluster and consequently generates observation symbols that are any given to HMM for coaching in addition, as detection purpose K-means bunch algorithmic rule first divides the dealings quantity into totally different clusters. It will split the dealings quantity into associate degree totally different clusters. Totally different clusters means the number are often split into occasional, medium and high clusters. It will produce a collection of patterns supported the bunch or cacophony of a customer profile and therefore the dealings quantity. When bunches the user profile or bunch the dealt method. This information is given to the Hidden mathematician Model for coaching in addition as detection purpose. The most method of the Hidden Markov Model is to match the user profile or characterize the behaviour of the client. If any changes in pattern, it will cite as a snoofing and send it to the admin mail id, where, '||Xi - VJ||' is that the geometer distance between xi and VJ. 'Chi' is that the variety of knowledge points in it clusters. 'C' is that the variety of cluster centers.

Let X = be the set of knowledge points and V = be the set of centers.

1) Willy-nilly choose 'c' cluster centers.
2) Calculate the space between every information and cluster centers.

3) Assign the informational purpose of the cluster center whose distance from the cluster center is minimum of all the cluster centers.
4) Work out the new cluster center using: Where, 'chi' represents the amount of knowledge points in its cluster.
5) Work out the space between every information and new obtained cluster centers.
6) If no information was reassigned then stop, otherwise repeat from step 3.

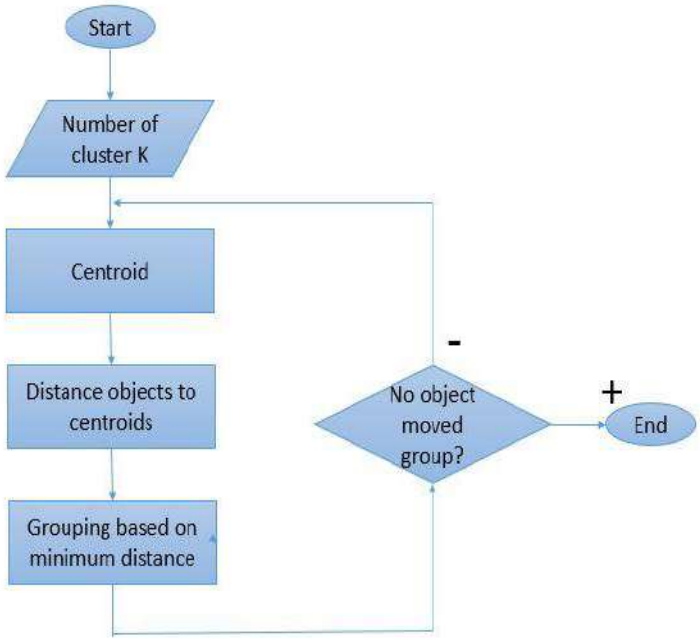

FIG: 1. K-MEANS CLUSTERING

V. IMPLEMENTATION

The planned system provides the secured application throughout the acquisition of the products through an online. It will offer a user's needed vogue which may be a beautiful to the user when put next to the prevailing system pictures. As a result of the existing system will contain solely a custom style of pictures. The planned system will be achieved this type of pictures by employing a PayPal and Paytm. There are five modules. The modules are listed below:

a. Product
b. Cart
c. Category
d. Checkout
e. Share

The product is that the one in each of the modules within the application. The getting things are chosen via the merchandise module. It will useful to look at all the product that may be uploaded into the associate degree application. It will categorize the every product with its rate, stock and its options or important. By victimization the merchandise module the whole product is viewed in a very completely different page with continuous manner. It's not classified all the merchandise; however, it will show all the merchandise with full details of the appliance throughout the acquisition of the merchandise.

The cart is that the one in the entire module within which buying things may be disbursed. Once the merchandise may be chosen within the product list, it will like a shot has added into a cart for distinctive the client that that things may be ordered by the user. The identification may be used for the client throughout future use. The module can even be useful to spot the user buying item through that the snoofing person may be known.

That category is the one among the modules during this application. It is equally same because the merchandise module. However the distinction between the merchandise and also the class module is that the class module may be classed all the merchandise in keeping with their shots. It may be classed all the kinds as electronical things, dresses, sports things, etc. Through the class module the user will simply determine regarding the actual list.

Checkout is that the one in each of the modules during the application. It may be useful for the user to ascertain out the complete data regarding the appliance, however, it may be delivered and what product that may be delivered. It also can give associate degree data regarding the appliance is that what banks that may coordinate with this bank attributable to on-line group action may be done throughout the acquisition of the merchandise during the application.

The share is that the one of the module in this application. The module may be helpful to share the data or a specific product to different the opposite user via other applications. It may be useful to share the data concerning this application to a different client. By victimization the share module, the applying may be rated by the client throughout the acquisition of the merchandise in on-line.

VI. EXPERIMENTAL RESULTS

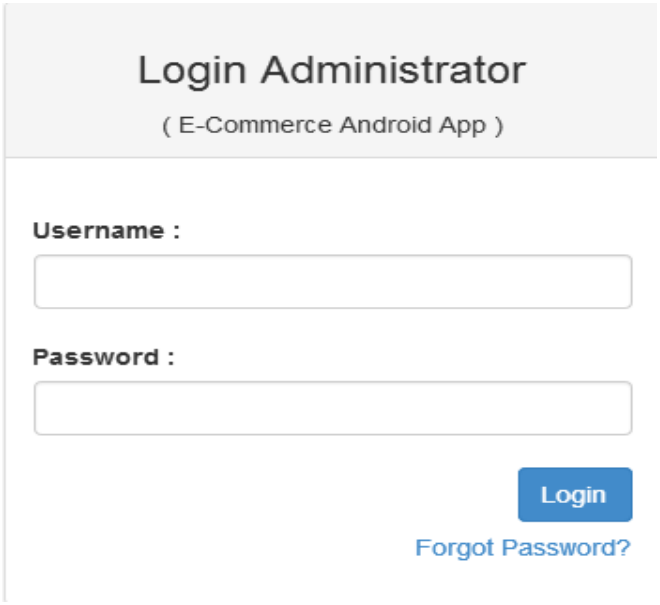

FIG: 2 ADMIN LOGIN PAGE

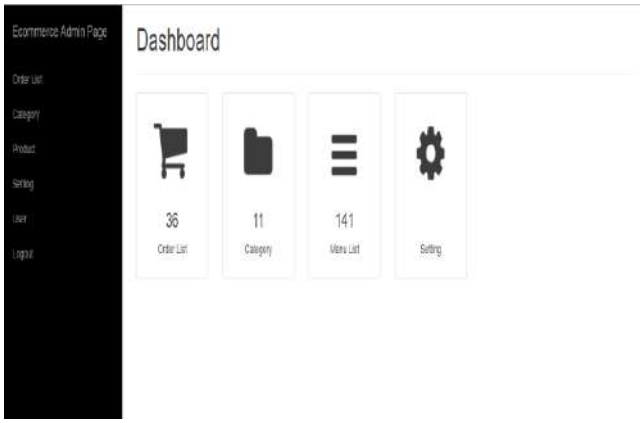

FIG: 3 DASHBOARD PAGE

VII. CONCLUSION

The system that is associate application of HMM in Anomaly Detection. The various steps in the MasterCard dealings process are portrayed because the underlying theoretical

account of associate HMM. The ranges of dealings quantity are used because the observation symbols, whereas the categories of item are thought about to be state of the HMM. Additionally, projected system suggests a technique for locating the outlay profile of cardholders, yet as application of the data decides the worth of observation symbols associated an initial estimate of the model parameters. The system is additionally ascendible for handling giant volumes of transactions. The hidden Markov model is essentially a model consisting of a sequence of states that works on the Markov chain property. Name Hidden here indicates that the observer does not recognize within which state, it is however, having a probabilistic insight on wherever it ought to be. Input to HMM be observation sequence and output is that the likelihood of a sequence. A hidden Markov model will be thinking of a generalization of a mixture model wherever the hidden variables that management the mixture element to be selected for every observation, area unit connected through a Markov process instead of freelance of every alternative.

REFERENCES

[1] X.Y.Tian,Y.H.Liu,J.Wang,W.Deng,"Attribute based computational security for context-awareness in vehicular ad-hoc networks "International journal of network security,Vol.4,no.1,pp.5268-5279,augest 2017.

[2] Tan Juan "Attribute-based encryption for Risk Assessment of Computer Network Security in Banks," International Journal of Security and its Application, Vol.10, No.4 pp.1–10, October 2017.

[3] MadhusankaLiyanage, IjazAhmed1, Jude okwuibe"Attribute-basedEnhancing Security of Software Defined Mobile Networks," International Journal of Security and its Application,Vol.5,No.4 08 May 2017

[4] Zhihua Zhang, Hongliang Zhu, ShoushanLuo, Yang Xin and Xiaoming Liu"Attribute-based Intrusion Detection Based on State Context and Hierarchical Trust in Wireless Sensor Networks," Vol.5, No.6,pp.12088-12102, 20 June 2017

[5] Prasant Kumar Nayak, Debdas Mishra "Attribute-based Attack of malicious objects in computer network under antivirus and quarantine defence" International Journal of Applied Engineering Research, Vol 11, No.9,pp.6250-6253, 9 November 2016.

[6] SonaJathe ,Dipti , Charjan, Pallavi, Patil "Computer Network Security and Attacks on Wireless Sensor Network,Hacking issues" International Journal of Applied Engineering Research, Vol 3, No.3,pp.6250-6253, 06 June 2016.

[7] GbadamosiLuqmanand AkanbiLukman " Modelling and Simulation of Load Balancing in Computer Network" International Journal of Applied Engineering Research, Vol 5, No.1,pp111-117, 17 March 2016.

[8] Sung Jiajia "Computer Network Performance Optimization Approaches based on Distributed System" International Journal of Applied Engineering Research, Vol 2, No.11,pp553-678, 20 August 2015.

[9] Zhendong Yin, Mingyang Wu, Zhutian Yang, Nan Zhao, Yunfei Chen "A Joint Multiuser Detection Scheme for UWB Sensor Networks Using Waveform Division Multiple Access" International Journal of Applied Engineering Research, Vol 2, No.11,pp2169-3536, 2015.

[10] Jun Wu, Kaoru Ota, Mianxiong Dong, andChunxiao Li "A Hierarchical Security Framework for Defending Against Sophisticated Attacks on Wireless Sensor Networks in Smart Cities", IEEE Transaction on Informatics, Volume 10, Issue 6, 2015.

Antimicrobial effect of bacteriocin from *Lactobacillus fermentum* isolated from goat milk on perishable foods. San Luis. Argentina

Nuria M Mitjans[1], Mariela J Coria[2], Javier O Alfonso[3], Patricia V Stagnitta[4]

Biological Chemistry Area.[1], Biochemistry and Biological Sciences Department[2], Faculty of Chemistry[3], Biochemistry and Pharmacy.[4], San Luis National University. San Luis, Argentina.

Abstract— *Strain selected for this study was isolated and named as sl36, from samples of goat milk collected from stainless steel drums in a dairy farm (San Luis, Argentina). The LAB strain was biochemically typified as Lactobacillus fermentum and designated as L. fermentum sl36. This identification was confirmed by 16S rRNA full sequences. The selected strain showed antimicrobial activity against food-borne pathogens, Listeria monocytogenes, Listeria innocua, Staphylococcus aureus, Enterococcus faecalis, Pseudomonas aeruginosa and Escherichia coli. The inhibitory activity was lost after treatment with trypsin, which indicates that this activity is due to a protein nature substance compatible with bacteriocins produced by Gram positive bacteria.The inhibitory substance was stable at different pH and temperatures. Perishable food samples (semi-hard cheese, cream, cooked pork shoulder) were treated with cell free supernatant from studied strain and then with indicator S. aureus and E. faecalis bacteria suspensions. Lactobacillus fermentum sl36 caused the inhibition of the growth of E. faecalis and S. aureus in the treated foods. Our work shows that it is possible to increase the safety of food perishable directly using the bacteriocins produced by the LAB strains, difference from the more frequent practice of using the bacteria themselves as probiotics.*

Keywords— Antimicrobial activity, goat milk, Lactic Acid Bacteria, Lactobacillus fermentum, perishable foods.

I. INTRODUCTION

There is an increasing demand on preservatives from natural sources due to potential toxicity of food chemical preservatives. In the last years, numerous studies have been focused on the reduction of the use of chemical preservatives; additionally, new preservation techniques by physical methods or by using natural antimicrobials have been developed. [1]

Lactic acid bacteria (LAB) have been used for centuries in food processing and are very important for their contribution to the value of products. Due to several metabolic properties, LAB play an important role in the food industry, for their contribution to flavour, smell, texture, sensory characteristics, therapeutic properties and nutritional value of food products. The use of LAB and its metabolites in food preservation is accepted as natural by consumers [2] and integrate an important group of generally recognized as safe (GRAS) for the American Food and Drug Administration (FDA). [3]

These microorganisms are found in very diverse environments, including resident microbiote of humans, as well as in cereals, fruits and vegetables, milk and meat, playing an essential role in the fermentation of these substrates and for the manufacture of many fermented foods and beverages[4].

The protective role of LAB lies in their capability to decrease pH and synthesis of bacteriostatic and bactericidal substances. These substances include hydrogen peroxide, lactic acid, carbon dioxide and bacteriocins which are defined as peptides produced by bacteria that inhibit or kill other related and unrelated microorganisms. In these years, a lot of studies have focused on the inhibition, by using bacteriocins, of food spoilage and of human pathogens associated with vegetable foods and beverages, and bacteriocin application has appeared as an interesting alternative to chemical compounds and antibiotics. [5], [6]

The bacteriocins produced by LAB exhibit properties that make them suitable for food preservation: recognized as GRAS, nontoxic and have no activity against eukaryotic cells, inactivated by digestive proteases, having little influence on the gut microbiota, are stable in wide ranges of pH and temperature, have a relatively broad antimicrobial spectrum against many food-borne pathogenic and spoilage bacteria, generally have a bactericidal mechanism and no cross resistance with antibiotics; and their genetic determinants are usually plasmid encoded, facilitating genetic manipulation, including the transfer of the gene clusters involved in their production to other food grade bacteria.[7]

Bacteriocins have emerged as an alternative antimicrobial treatment; consequently it is important to continue investigating about bacteriocin-producer strains and their spectrum of antimicrobial activity.

Contamination of raw milk and cheese during ripening process has been reported with *Listeria monocytogenes, Escherichia coli* and members of the family Enterobacteriaceae causing alterations in taste and flavors and affecting human health. [8], [9]

L. monocytogenes, the bacterial agent of listeriosis, is of particular concern to the food industry since it is a difficult foodborne pathogen to control due to its ubiquitous distribution, tolerance to high levels of salt, and its ability to grow at a relatively low pH and at low refrigeration temperatures. Other pathogens as *Staphylococcus aureus* can also cause food-borne diseases. [10]

In recent years, the genus *Enterococcus* has acquired great importance because of its high incidence in nosocomial diseases and the resistance to antimicrobials. In addition, they are considered indicators of food contamination and faecal contamination of the waters, due to their wide distribution and to their high resistance to adverse conditions. [11]

Many studies are aimed to selection and development of protective bacteriocinogenic cultures for food applications. Although a large body of data concerning bacteriocin-producing LAB has been reported, strains prevalent in San Luis region has not been studied much, as well as which of them are producers of bacteriocins that might be used in food preservation. [12]

The purposes of this study were to evaluate the antimicrobial activity of a LAB strain isolated in this region from raw goat milk, to characterize the inhibitory substance, and also to study its effect on the conservation of perishable foods. The antimicrobial activity was tested against foodborne pathogens such as *Listeria monocytogenes*, *Listeria innocua*, *Staphylococcus aureus, Pseudomonas aeruginosa*, *Escherichia coli* and *Enterococcus faecalis.*

II. MATERIALS AND METHODS

2.1 Bacterial strain and growth conditions

Strain selected for this study was isolated and named as sl36, from samples of goat milk collected from stainless steel drums in a dairy farm (San Luis, Argentina). 10-fold dilutions of samples were made in 0.1 % peptone water and plated onto Man, Rogosa and Sharpe agar medium (MRS) and incubated at 37° C for 48 h in microaerophilic conditions.

2.2 Identification and characterization of LAB strain

The isolated strain was characterized as LAB by Gram stain, catalase and oxidase tests, and was biochemically typified by identification system API 50 CHL (BioMerieux) The identification of the microorganism was performed by using the software Apilab plus (Biomerieux).Confirmation of identification was obtained by amplifying the genomic DNA based on 16S rRNA full sequences (Macrogen, Inc, Seoul).

2.3 Obtaining cell-free supernatant

sl36 strain was propagated, in microaerophilic conditions, twice in MRS broth at 37°C for 24h and then propagated in MRS broth at 37ºC for 16h, incubation time in which a maximum of antimicrobial activity is detected (results not shown).After that, cell free supernatant (CFS) was obtained by centrifugation (8000 g, 20 min, and 4 °C) and filtered through a 0.2 µm pore-size cellulose acetate membrane. For some tests CFS was neutralized (NCFS) by adjusting pH to 7.0 with 4N NaOH.

2.4 Sensitive strains

The indicators organisms selected to be used in antimicrobial test were *Listeria monocytogenes CLIP 74902*, *Listeria innocua CLIP 74915*, *Staphylococcus aureus* (Microbiology Laboratory collection, San Luis National University), *Enterococcus faecalis ATCC 29212*, *Pseudomonas aeruginosa ATCC 27853*, *Escherichia coli* (Microbiology Laboratory collection, San Luis National University) which were grown in Trypticase Soy agar (TSA) at 37°C for 24 h.

2.5 Antimicrobial Activity

The antimicrobial activity was determined by liquid medium method described by Cabo M.L. et al [13]. To 1 ml of sensitive strains suspension (6×10^8 UFC.ml^{-1}) was added 0.5 ml of CFS and 0.5 ml of medium Trypticase Soy Broth (TSB). The mix was incubated for 6 h a 37°C. Absorbance measurements were made at 700 nm. The inhibition percentage (%I) was calculated according to the formula $I= 1-A_s/A_c$, considering A_s and A_c as sample absorbance and control absorbance

respectively. In control assay, the CFS was replaced by MRS broth. Each trial was done in triplicate and the average value was reported.

2.6 Characterization of the inhibitory substance

2.6.1 Determination of peptide nature of the inhibitory substance

The peptide nature of the antimicrobial agent in CFS was verified by treatment CFS aliquots with the following enzymes: Trypsin (Fluka, optimal conditions: pH 8, temperature 37°C, final concentration: 5 $mg.ml^{-1}$), proteinase K (Productos Bio-Lógicos, optimal conditions, pH 7,0, temperature 37ºC, final concentration: 0,1 $mg\ ml^{-1}$) and Pepsin (optimal conditions: pH 2, temperature 37°C, Fluka,final concentration:1 $mg\ ml^{-1}$). The experiments were conducted at optimal conditions for each enzyme and were incubated for 2 h at 37ºC. [14] Supernatants treated with proteases were adjusted to pH 6.8 with 4 N NaOH and then the antimicrobial activity against *E. faecalis* was determined by liquid medium method.

2.6.2 Effect of pH on antimicrobial activity

The effect of pH variation on bacteriocin stability was measured by rising from 2.0 to 10.0, varying every 2 pH units with 1 N HCl or 4 N NaOH. The samples were incubated for 2 h at 37ºC. After incubation, pH of each aliquot was adjusted to 6.8 and assays of antimicrobial activity against *E.faecalis* were performed.

2.6.3 Effect of temperature on antimicrobial activity

Aliquots of CFS neutralized were preserved for one week at 4°C and at -20°C and then were treated at 50ºC, 100ºC and 121ºC for 15 min. Residual antimicrobial activity was determined by the liquid medium method using *E. faecalis* as sensitive strain.

2.7 Application of antimicrobial peptides produced by BAL as preservatives of perishable foods

Perishable food samples (semi-hard cheese, cream, cooked pork shoulder) were treated with CFS from studied strain and then with indicator *S. aureus* and *E. faecalis* bacteria suspensions.

2.7.1 Treatment of semi-hard cheese.

Cheese aliquots of 1g were treated with CFS or with MRS broth (controls). Samples were incubated at 4°C for 6h. At a later stage, the aliquots were submerged in tubes containing 10^8 $CFU.ml^{-1}$ of each indicator and maintained at 4°C for 30 min. After that, samples were placed in sterile Petri dishes and incubated at 37 °C for 24 h, at the end of the incubation period were placed in tubes with 10 ml of sterile distilled water and mixed for 2 min, 1 ml of 10-fold serial dilution was poured on Petri dishes using 1.5% TSA medium. The plates were incubated at 37°C for 24h. *S. aureus* and *E. faecalis* counts in samples were determined according to National Standard Test Methods for Food Microbiology [15].

2.7.2 Treatment of cream

Aliquots of 8 ml of milk cream were treated with 1 ml of CFS or 1 ml MRS broth (controls) and 1 ml of indicator strain suspension (10^8 $CFU.ml^{-1}$). Aliquots were incubated at 37 °C for 12 h, 1 ml of 10-fold serial dilution was poured on a Petri dish using 1.5% TSA medium. The plates were incubated at 37°C for 24h. *S. aureus* and *E. faecalis* counts in samples were determined according to National Standard Test Methods for Food Microbiology.[15]

2.7.3 Treatment of cooked pork shoulder.

Sample aliquots of 1 g were treated with CFS or with MRS broth (controls). Samples were maintained at 4°C for 6 hours. Then, the aliquots were submerged in tubes containing 10^8 $CFU.ml^{-1}$ of each indicator and maintained at 4°C for 30 min. The samples were then placed in sterile Petri dishes and incubated at 37°C for 24 h. At the end of the incubation period were placed in tubes with 10 ml of sterile distilled water and mixed for 2 min, 1 ml of 10-fold serial dilution was poured on Petri dishes using 1.5% TSA medium. The plates were incubated at 37°C for 24h. *S. aureus* and *E. faecalis* counts in samples were determined according to National Standard Test Methods for Food Microbiology [15].

2.8 Statistical analysis

Statistical analyses were carried out with InfoStat software using Friedmann nonparametric variance testA $p<0.05$ was considered to be significant.

III. RESULTS AND DISCUSSION

3.1 Identification and characterization of LAB strain

The isolated strain was characterized as LAB,bacilli Gram positive, catalase and oxidase tests negative.

The LAB strain was biochemically typified as *Lactobacillus fermentum* and designated as *L. fermentum sl36*. This identification was confirmed by 16S rRNA full sequences. (Fig.1)

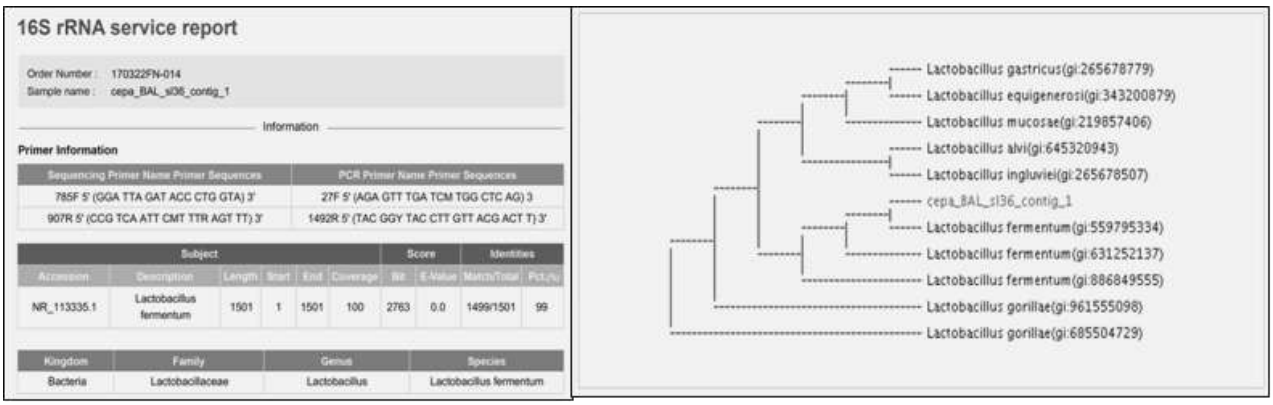

FIGURE 1: IDENTIFICATION BY AMPLIFYING THE GENOMIC DNA BASED ON 16S rRNA FULL SEQUENCES

3.2 Antimicrobial activity

Spectrum of inhibitory activity as inhibition average percentage (%I) against the microorganisms selected as sensitive strains is shown in Table 1.

TABLE 1
INHIBITORY ACTIVITY SPECTRUM FROM *L fermentum sl36*.

Sensitive Strains	Inhibition Percentage	
	CFS	NCFS
P. aeruginosa ATCC 27853	96.50%	27.0%
E. coli	94.00%	34.0%
S. aureus	96.75%	37.0%
E. faecalis ATCC 29212	94.40%	41.0%
L. monocytogenesCLIP 74902	97.75%	38.0%
L. innocuaCLIP 74915	96.75%	43.0%

CFS antimicrobial activity was higher than 90% against all the microorganisms tested and no significant differences were found ($p = 0.8587$) when comparing the inhibition against all the indicators used. The antimicrobial activity of NCFS showed percentages of inhibition between 27% and 43%. By analysis of CFS versus NCFS, a significant difference was found ($p = 0.0008$). The inhibition percentage decreases considerably when NCFS is analyzed, which shows that part of the inhibitory effect is due to the production of acids by *L. fermentum sl36*.The results agree with those obtained by Kang et al (2017) [16], Andreeva et al, (2016) [17] and Gong et al (2014) [18], where the production of lactic acid is presented as one of the mechanisms antimicrobials of lactobacilli. It is important to note that CFS and NCFS inhibited the growth of *E. coli* and *P. aeruginosa* that are Gram-negative strains.

3.3 Characterization of the inhibitory substance

3.3.1 Determination of peptide nature of the inhibitory substance.

The inhibitory activity of NCFS was lost after treatment with trypsin. This indicates that the antimicrobial activity is due to a peptide nature substance compatible with bacteriocins produced by Gram positive bacteria.

3.3.2 Effect of pH on antimicrobial activity

The pH stability of the active compound present in NCFS was studied in the range of pH 2.0–10.0. It was observed that the inhibitory substance was active at pH values from 2.0 to 6.0 but reduced at pH 8.0 and 10.0. *L. fermentum sl36* produces antimicrobial compounds that remain stable over a wide pH range, losing part of their inhibitory capacity at alkaline pH values.

TABLE 2
EFFECT OF PH TREATMENT ON CFS PRODUCED BY *L fermentum sl36*

NCFS treatment pH values	pH: 2,0	pH:4,0	pH:6,0	pH:8,0	pH:10
Average Inhibition Percentage	94.0 %	93.7 %	94.6 %	41.9 %	33.0 %

3.3.3 Effect of temperature on antimicrobial activity

Antibacterial activity was not altered by the storage for one week at 4ºC and at -20ºC. Identically the inhibitory activity was not modified by heat treatment as shown in Table 3.

TABLE 3
EFFECT OF HEAT TREATMENT ON CFS PRODUCED BY *L fermentum sl36*

HEAT TREATMENT	CFS preserved at 4°C	CFS preserved at -20 ° C
CFS Without Heat Treatment	94.00%	86.20 %
NCFS Without Heat Treatment	40.85 %	41.00 %
50ºC 15’	40.75 %	42.20 %
100ºC 15’	40.40 %	42.6 %
121ºC 15’	40.20 %	40.70 %

3.4 Application of antimicrobial peptides produced by BAL as preservatives of perishable foods

The inhibitory substance present in the CFS of the culture of *Lactobacillus fermentum sl36* caused the inhibition of the growth of *E. faecalis* and *S. aureus* in the treated foods, when compared with the growth of the indicator strains in the controls (aliquots of samples treated with MRS broth), since the average values of the counts expressed as $CFU.ml^{-1}$ in the

controls were significantly higher than the counts in the aliquots of foods treated with CFS. The CFS inhibits the development of the two indicators with similar efficacy. The figure 2 show that *L. fermentum sl36* has a lower inhibitory effect against *E. faecalis* and *S. aureus* when cream was treated. It is possible to establish, when analyzing the development of the indicators in each food separately, that there is a significant difference (<0.0001) between the counts of the controls and those treated with CFS (Friedman test).

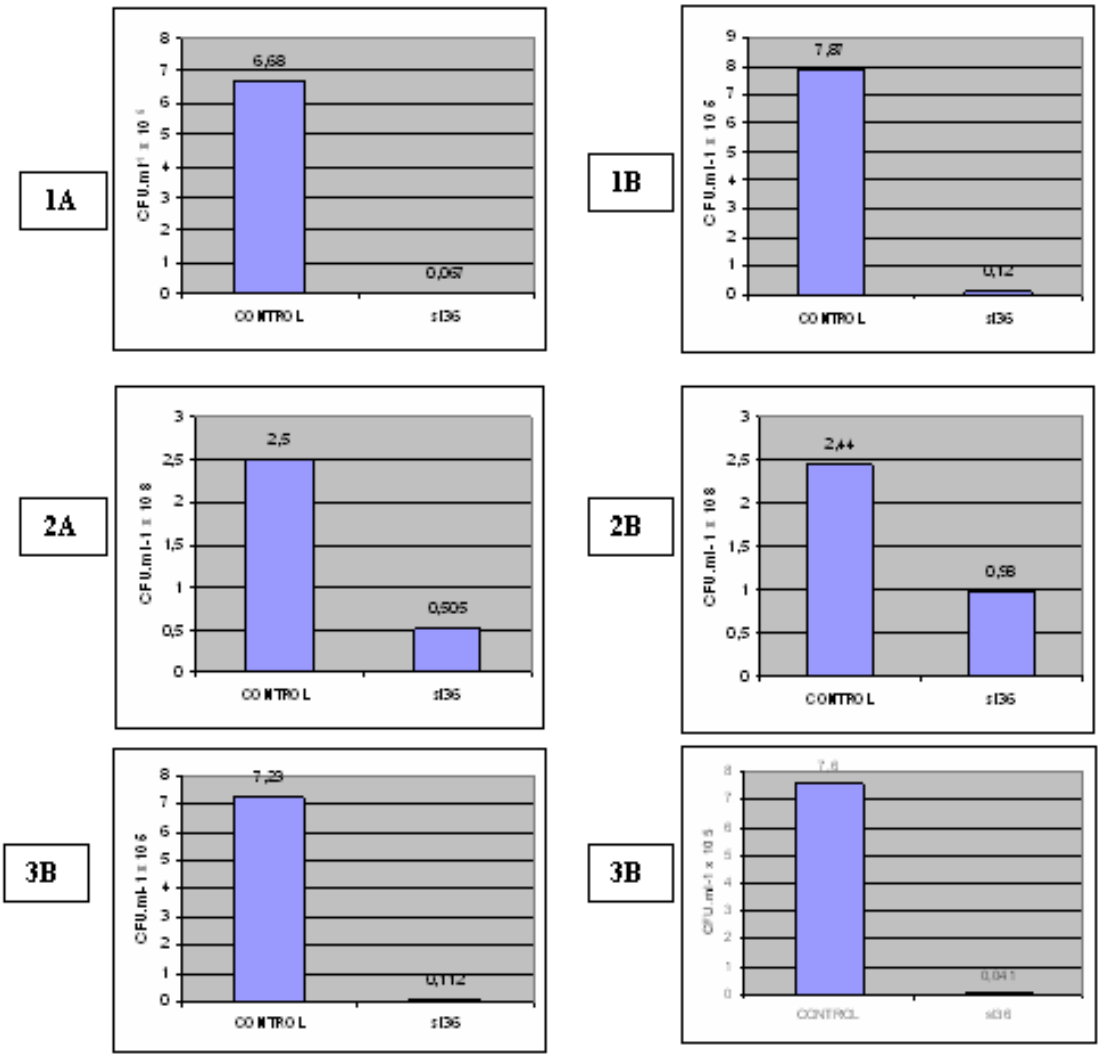

FIGURE 2: Counts of *E. faecalis* and *S. aureus* in perishable foods treated with CFS of *Lactobacillus fermentum sl36*. 1A.semi-hard cheese inoculated with *E. faecalis*. 1B.semi-hard cheese inoculated with *S. aureus*. 2A cream inoculated with *E. faecalis*. 2B cream inoculated with *S. aureus*. 3A.cooked pork shoulder inoculated with *E. faecalis*. 3B cooked pork shoulder inoculated with *S. aureus*

Antimicrobial activity of *Lactobacillus spp* strains isolated of food has been studied for many investigators. Azizi et al (2017) [19] showed that *Lactobacillus spp.* strains isolated from Iranian raw milk Motal cheese inhibited growth of *Staphylococcus aureus* from ATCC, *Escherichia coli* and *Listeria innocua* strains. In accordance of this, Macaluso et al (2016) [20 found lactobacilli strains isolated from Sicilian cheese with antimicrobial activity for *Listeria monocytogenes*, nevertheless the same strains did not inhibit the *Staphylococcus aureus*, *Escherichia coli* and *Salmonella enteritidis* growth.

The use of bacteriocins in the food industry is proposed by many investigators. The control of the development of pathogen microorganisms in cheese using bacteriocin-producing LAB strains has been effective for the treatment of dairy products [21]. Castellano et al (2018) [22] described bacteriocins produced by *Lactobacillus curvatus* and *Lactobacillus sakei* strains able to prevent the growth of *L. monocytogenes* in frankfurters stored at 10 °C during 36 days. In the same way, Mills et al (2017) [23] generated a suite of single- and double-bacteriocin-producing starter cultures capable of produce two classes of bacteriocins, and demonstrated an increment in the control of the *Listeria innocua* growth in laboratory-scale cheeses. On the

other hand, Scatassa et al (2017) [24] demonstrated that bacteriocin-like inhibitory substances produced by lactic acid bacteria prevented the growth of *L. monocytogenes* in tradicional Sicilian Cheeses, nevertheless this effect was not observed neither in raw nor in pasteurized milk. In our research, growth inhibition of *S. aureus* and *E. faecalis* in cheese and cream was studied by applying the supernatants of cultures containing the antimicrobials, which avoids possible alterations in the food that could cause the use of LAB on foods. With regard to meat products treatment, the results of Beristain Bauza (2012) [25] and Camargo Peralta et al (2009) [26] coincide with our results what refers to the evident inhibition of *S. aureus* and other pathogens.

The antimicrobial properties of bacteriocin isolated in our research, in combination with their sensitivity to the digestive proteases as trypsin, as well as their stability at different temperatures and over a wide range of pH values, converts them into prospective agents destined to be applied to the bio-conservation of food.

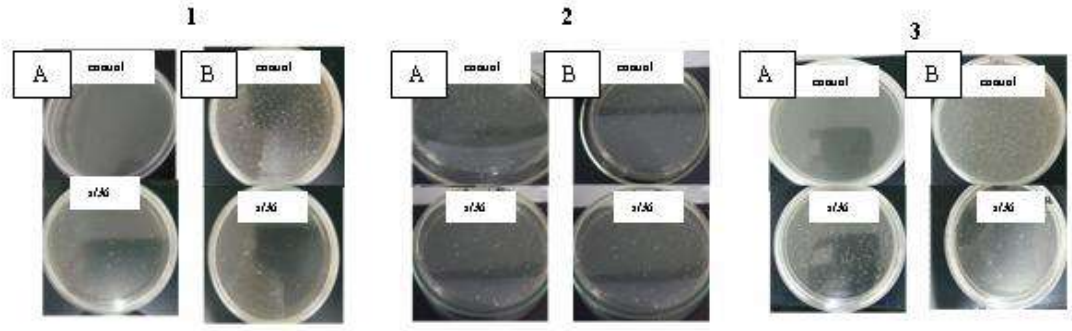

FIGURE 3. PERISHABLES FOOD TREATED WITH CFS OF *LACTOBACILUS FERMENTUM* (s136).

1. **Semi-hard cheese, 1A. inoculated with *E. faecalis*, 1B inoculated with *S. aureus.***
2. **Cream, 2A inoculated with *E. faecalis*. 2B inoculated with *S.aureus*.**
3. **Coocked park shoulder, 3A inoculated with *E. faecalis*. 3B inoculated with *S.aureus*.**

IV. CONCLUSION

The strain of *Lactobacillus fermentum sl36* isolated in this region from raw goat milk showed antimicrobial activity that remain stable at different pH values and at different heat treatment. Our work demonstrates that it is possible to increase the safety of perishable foods by utilization of bacteriocins produced by LAB strains, unlike the using the bacteria as probiotics which is most frequent practice. The development of biotechnological alternatives that use bacteriocins, such as smart packaging and aerosols for application on surfaces, would improve the conditions of storage and preservation of food by controlling microorganisms. The discovery of new bacteriocins represents an opportunity in the production of substances with preservative qualities.

ACKNOWLEDGEMENTS

We are grateful toNatalia Gaido Risso and Gerardo Randazzo for technical help. This study was supported by San Luis National University.

REFERENCES

[1] P Castellano, C Belfiore, S Fadda, G Vignolo. "A review of bacteriocinogenic lactic acid bacteria used as bioprotective cultures in fresh meat produced in Argentina". Meat Science, vol. 79, pp. 483–499, 2008.

[2] A Parra Huertas. Review: Bacterias Lácticas: Papel funcional en los alimentos. Revista de Ciencias Agropecuarias, vol 8 (1), pp. 93-105, 2010.

[3] Y Huang, Y Luo, Z Zhai, H Zhang, C Yang, H Tian, Z Li, J Feng, H Liu, Y Hao. "Characterization and application of an anti-Listeria bacteriocin produced by *Pediococcus pentosaceus* 05-10 isolated from Sichuan Pickle, a traditionally fermented vegetable product from China" Food Control vol.20), pp 1030–1035, 2009.

[4] M P Doyle, L R Steenson, J Meng. "Bacteria in food and beverage production". The prokaryotes, pp 797-811, 2013.

[5] E M Balciunas, F A Castillo Martinez, S D Todorov, B D Gombossy de Melo Franco, A Converti, R Pinheiro de Souza Oliveira. " Novel biotechnological applications of bacteriocins: A review". Food Control, vol 32 (1), pp 134-142,2013.

[6] V Ahmad, MS Khan, QM Jamal, MA Alzohairy, MA Karaawi, MU Siddiqui (2017). "Antimicrobial potential of bacteriocins: in therapy, agriculture and food preservation" International Journal of Antimicrobial Agents, vol 49, pp 1–11,2017

[7] A Gálvez, H Abriouel, R.L Lopez, N Ben Omar. "Bacteriocin-based strategies for food preservation". International Journal of Food Microbiology vol 120 (1-2), pp 51–70, 2007.

[8] J Mc Lauchlin, R T Mitchell, W J Smerdon, K Jewell. (2004). "*Listeria monocytogenes* and listeriosis: a review of hazard characterisation for use in microbiological risk assessment of foods". International Journal of Food Microbiology, vol 92(1), pp15-33, 2004.

[9] A Caridi. "Selection of *Escherichia coli*-inhibiting strains of *Lactobacillus paracasei subsp. paracasei"*. Journal of Industrial Microbiology and Biotechnology, vol. 29, pp 303-308, 2002.

[10] L H Deegan, P D Cotter, C Hill, P Ross. (2006) Bacteriocins: Biological tools for bio-preservation and shelf-life extension. International Dairy Journal 16 (9), pp 1058–1071, September 2006.

[11] M Díaz Pérez, C Rodríguez Martínez, R Zhurbenko. Artículo de Revisión: "Aspectos fundamentales sobre el género *Enterococcus* como patógeno de elevada importancia en la actualidad". Revista Cubana de Higiene y Epidemiología, vol. 48 (2), pp 147-161, 2010.

[12] N M Mitjans, M J Coria, A C. Anzulovich, N Gaido Risso, J M. Castro, I G. Rezza, P V Stagnitta. "Antimicrobial activity of *Lactococcus* and *Lactobacillus* species isolated from raw goat milk. San Luis Argentina"International Journal of Engineering Research and Science, vol 2 (8), pp 141-147, 2016.

[13] M L Cabo, M A Murado, M P González, L Pastoriza. Review Article: "A method for bacteriocin quantification". Journal of Applied Microbiology, vol. 87, pp 907-914, 1999.

[14] M Atanassova, Y Choiset, M Dalgalarrondo, J.-M Chobert, X Dousset, I Ivanova, T Haertle. "Isolation and partial biochemical characterization of a proteinaceous anti-bacteria and anti-yeast compound produced by *Lactobacillus paracasei subsp.paracasei* strain M3". International Journal of Food Microbiology, vol 87 (1-29), pp 63-73, 2003.

[15] **Microbiology Laboratory Guidebook.**Food Safety and Inspection Service, United States Department of Agriculture, Washington, DC (2015). Chapter 3.6: Aerobic Plate Count (APC).

https://www.fsis.usda.gov/wps/portal/fsis/topics/science/laboratories-and-procedures/guidebooks-and-methods/microbiology-laboratory-guidebook/microbiology-laboratory-guidebook.

[16] M. S Kang, H S Lim, J S Oh, Y. J Lim, K Wuertz-Kozak, J M Harro, M E Shirtliff, Y Achermann. "Antimicrobial Activity of *Lactobacillus salivarius* and *Lactobacillus fermentum* against *Staphylococcus aureus".* Pathogens And Disease, vol 75(2), ftx009, pp 1-10, 2017.

[17] P Andreeva, A Shterev, S Danova. "Antimicrobial activity of vaginal *Lactobacilli* against *Gardnerella Vaginalis* and Pathogens". International Journal Of Advanced Research in Biological Sciences, vol 3(5), pp 200-207, 2016.

[18] Z Gong, Y Luna, P Yu, H Fan. "*Lactobacilli* inactivate *Chlamydia Trachomatis* through Lactic Acid but not H_2O_2". PLoS One, 9(9), e107758, 2014.

[19] F Azizi, M B Habibi Najafi, M R Edalatian Dovom. "The biodiversity of Lactobacillus spp. from Iranian raw milk Motal cheese and antibacterial evaluation based on bacteriocin-encoding genes". AMB Express, vol 7, pp 176-186, 2017.

[20] G Macaluso,G Fiorenza, R Gaglio, I Mancuso, M L Scatassa."*In Vitro* Evaluation of Bacteriocin-Like Inhibitory Substances Produced by Lactic Acid Bacteria Isolated During Traditional Sicilian Cheese Making". Italian Journal of Food Safety, vol 5 (1), pp 5503.

[21] D Beshkova, G Frengova. "Bacteriocins from lactic acid bacteria: Microorganisms of potential biotechnological importance for the dairy industry" Engineering in Life Sciences, vol. 12 (4), pp 419-432, 2012.

[22] P Castellano, N Peña, M P Ibarreche, F Carduza, T Soteras, G Vignolo. "Antilisterial efficacy of Lactobacillus bacteriocins and organic acids on frankfurters. Impact on sensory characteristics". Journal of Food Science and Technology, vol 55, pp 689-697, 2018..

[23] S Mills, C Griffin, P M O'Connor, L M Serrano, W C Meijer, C Hill, R P Ross. "A Multibacteriocin Cheese Starter System, Comprising Nisin and Lacticin 3147 in Lactococcus lactis, in Combination with Plantaricin from Lactobacillus plantarum".Applied and Environmental Microbiology, vol 83 (14), ppe00799-17.

[24] M L Scatassa, R Gaglio, C Cardamone, G Macaluso, L Arcuri, M Todaro, I Mancuso."Anti-Listeria Activity of Lactic Acid Bacteria in Two Traditional Sicilian Cheeses".Italian journal of food safety, vol 6 (1):6191.

[25] S C Beristain-Bauza, E Palou, A López-Malo. "Bacteriocinas: antimicrobianos naturales y su aplicación en los alimentos". Temas selectos de ingeniería de alimentos, vol. 6 (2), pp 64-78, 2012.

[26] I Camargo Peralta; S Gómez Bertel; V Salazar Montoya, (2009). "Impacto de las bacteriocinas, importancia como preservantes en la industria de alimentos" Teoría y praxis investigativa, vol 4 (2), pp27-32, 2009.

Microbial Fructosyltransferase: Production by Submerged Fermentation and Evaluation of pH and Temperature Effects on Transfructosylation and Hydrolytic Enzymatic Activities

Perna, RF[1], Cunha, JS[2], Gonçalves, MCP[3], Basso, RC[4], Silva, ES[5], Maiorano, AE[6]

[1,2,3,4]Bioprocess Laboratory, Institute of Science and Technology, Federal University of Alfenas, José Aurélio Vilela Road 11999, Km 533, CEP 37715-400, Poços de Caldas, MG, Brazil.
[5,6]Biotechnology Laboratory, Institute for Technology Research of São Paulo, Professor Almeida Prado Avenue 532, CEP 05508-901, Butantã, São Paulo, SP, Brazil.

Abstract**—***Fructosyltransferases (FTase, E.C. 2.4.1.9) are enzymes that catalyze transfructosylation reactions obtaining, as final product, fructose oligomers. In terms of industrial production, the use of microbial enzymes is interesting, especially those produced by Aspergillus sp. The aim of the work was to study the production of FTase by submerged fermentation and evaluation of pH and temperature effects on fructosyltransferase activity. The enzyme was produced by Aspergillus oryzae IPT 301 in a 10-liter bioreactor with growth medium containing sucrose as main carbon source. The assay was performed at 800 rpm, 30 °C, 0.75 vvm and pH 4.5. Transfructosylation (At) and hydrolytic (Ah) activities were determined in the temperature range from 35 to 65 °C and pH range from 3.5 to 6.0. It was observed that mycelial is increases with temperature, holding the maximum value at 50 – 65 ºC, while the optimum pH value were 5.0. The optimum temperature for extracellular At ranged from 55 to 65 °C and the optimum pH ranged from 5.0 to 6.0. Furthermore, the optimum temperature for mycelial Ah was 65 °C and optimum pH 4.5 - 5.0. For extracellular Ah, the optimum temperature and optimum pH were 55 to 65 °C and 3.5 to 6.0, respectively.*

Keywords**—*****Aspergillus oryzae, Bioreactor, Fructooligosaccharides, Fructosyltransferase.***

I. INTRODUCTION

Fructooligosaccharides (FOS) are oligosaccharides of fructose containing a single glucose moiety [1,2]. They are mainly composed of 1-kestose (GF2), nystose (GF3), and 1-β-fructofuranosyl nystose (GF4), in which fructosyl units (F) are bound at the β (2→1) position of the sucrose molecule (GF) [2,3,4,5]. FOS with low polymeric degree has better therapeutic properties than those with a high polymeric degree [6]. These fructose oligomers are classified as prebiotics and have numerous beneficial properties for human health [1,2,7]. They are non-cariogenic sweeteners of low caloric value, safe for diabetes, as they are not hydrolyzed by the gastro-intestinal enzymes, selectively promoting the growth of Bifidobacterium in the colon [8,9,10] thus helping to eliminate microorganisms which are pathogenic to human health and preventing colonic carcinogenesis [11,12], and increase the adsorption of calcium and magnesium [13]. In addition, FOS favor the reduction of plasma levels of cholesterol, triglycerides and phospholipids [14,15,16]. They are about 0.4 and 0.6 times as sweet as sucrose and have been widely utilized in food and pharmaceutical industries as a functional sweetener [2,6,17].

Although FOS can be produced by the action of enzymes present in some plants, the commercially available FOS are produced mainly by enzymatic synthesis from sucrose by microbial enzymes called β-fructofuranosidases (FFases, E.C.3.2.1.26) and fructosyltransferases (FTases, E.C.2.4.1.9) [18,5] which have been found in several fungal strains, such as *Penicillium* sp. [19,20,21,22], *Aureobasidium* sp. [23,24,25], *Fusarium* sp. [26,27,28,29] and mainly *Aspergillus sp*. [3,6,9,17,18,30,31,32,33,34,35,36]. FOS-producing enzymes from microorganisms are excreted either outside the cell as extracellular enzymes or retained within the cell as intracellular enzymes [9,35,37]. FFase enzymes catalyse hydrolytic and transfructosylating reactions, but their ability for transfer is only with high sucrose amounts. On the other hand, FTases possess transfructosylating activity, acting on the β(2→1) link of sucrose and transfer a fructose molecule to an acceptor such as another sucrose molecule, leading to the generation of FOS with a different chain length and release of glucose in the reaction as a by-product [22,36,38]. FTases shows a little affinity towards water as an acceptor, which means that the hydrolases activity of enzyme is relatively low [38].

Even though other manuscripts have presented data on FOS and FTases production, there is a scarcity of works on the production of these components by submerged fermentation in a pilot reactor, as well as regarding the screening of optimal pH and temperature for extracellular and mycelial FTase activities produced by *Aspergillus oryzae*. Thus, the aim of the

present paper was the production of fructosyltransferase by *Aspergillus oryzae* IPT 301 performed by submerged fermentation using batch reactor with growth medium containing sucrose as main carbon source. The paper also reports the influence of pH and temperature on mycelial and extracellular activities of the enzyme by these fungi. The microorganism was used at first for amylase [39] and pectinase [40] production. After these initial applications, the fungus was tested for fructosyltransferase production at the Institute for Technology Research of São Paulo (IPT/SP, Brazil), obtaining positive results.

II. MATERIAL AND METHODS

2.1 Microorganism and Cultivation Conditions

The fungal strain *Aspergillus oryzae* IPT 301 from the Institute for Technology Researchof São Paulo (IPT/SP - Brazil) culture collection was used for fructosyltransferase production. This fungal strain was used since it has previously shown the best results of enzyme production [9]. For inoculum preparation, the fungal strain was grown on malt extract agar plates for 7 days at 30 ^{0}C; the conidia were suspended in saline solution (NaCl 0.95%, w/v and Tween-80 0.1 %, v/v) and diluted to obtain a spore suspension containing around 108 spores.mL^{-1}. Experiments were performed in a bioreactor containing 10 L of culture medium, with the following composition (g.L^{-1}): sucrose 320.500; yeast extract 2.107; urea 7.130; $MgSO_4.7H_2O$ 0.500; K_2HPO_4 5.000; $MnCl_2.4H_2O$ 0.030; $FeSO_4.7H_2O$ 0.010. 5 mL of polypropylene glycol were used as antifoam. The bioreactor was inoculated with 100 mL of spore suspension and fermentation was performed at 30 ^{0}C and 800 rpm for 63 h. Culture medium pH was adjusted to 4.5 before sterilization and maintained during fermentation using $H_2SO_4$2 mol.L^{-1}and NaOH 4 mol.L^{-1}. The aeration system was 0.75 vvm (volume of air per volume of medium per minute) with air flow rate of 6.0 L.min^{-1}. Samples for analysis were collected and filtered using filter paper (Whatman No 1). In the filtered broth, the residual sugar (sucrose, glucose, fructose and fructooligosaccharides), pH and extracellular enzyme activity were measured. Cell mass concentration and mycelial enzymatic activity were determined using the biomass produced. Fermentation experiments were performed in duplicate.

2.2 Cell mass Concentration

Cell mass concentration was determined by dry cell weight per volume (g.L^{-1}). The cell mass obtained by vacuum filtration of the fermentation broth was washed with distilled water and dried at 105 ºC for 4 h.

2.3 Enzymatic activity

The extracellular and mycelial enzymatic activities were determined as follows: 0.1 mL of suitably diluted supernatant or 0.05 g of cells was mixed with 3.7 mL of 636 g.L^{-1} sucrose and 1.2 mL of 0.2 mol. L^{-1} tris-acetate buffer pH 5.0. The enzymatic reaction was conducted in a rotary shaker at 55 ^{0}C and 190 rpm for 60 min and stopped by heating the mixture in boiling water for 10 min [6,9,41]. The units of fructosyltransferase (At) and hydrolytic (Ah) activities were defined as the amount of enzyme that produces a 1 µmol of FOS or releases a 1 µmol of fructose, respectively, per minute under the chosen experimental conditions.

2.4 Sugars and FOS concentration

Sugar and FOS concentration in the samples were analyzed using high performance liquid chromatography (HPLC) with a Rezex RCM-Monosaccharides Ca^{2+} (8%) (300 x; 7.8 mm, Phenomenex®) Ion-Exclusion column, and a system composed of a 510 pump, a differential refraction index detector and a data processor with register, all from Waters®, USA. The samples were eluted with Milli-Q water at the flow rate 0.6 mL.min^{-1}, maintaining column temperature at 85 ^{0}C.

2.5 Temperature and pH effects on enzymatic activity

After 63 h of fermentation, samples of the culture medium were collected from the bioreactor and vacuum-filtered. Biomass (mycelium) containing mycelial FTase and permeate (filtered broth) containing extracellular FTase were used for enzymatic characterization assays at different pH values (3.5, 4.0, 4.5, 5.0, 5.5 and 6.0) at 55 °C and distinct temperatures (35, 40, 45, 50, 55, 60 and 65 °C) at pH 5.0. All experiments were performed using a reaction mixture composed of 3.7 mL of 636 g.L^{-1} sucrose, 1.2 mL of 0.2 mol.L^{-1} tris-acetate buffer and 0.1 mL of appropriately diluted enzyme solution (extracellular activity) or 0.05 g of cells (mycelial activity). Enzymatic reaction was performed for 60 min at pH and temperatures tested in a rotary shaker at 190 rpm and stopped by heating the mixture in boiling water for 10 min. All experiments were performed in triplicate.

III. RESULTS AND DISCUSSION

3.1 Production of FTase by submerged fermentation

Fig. 1 shows a decrease of approximately 50% in sucrose concentration and 112 $g.L^{-1}$ FOS production in 17 h of process. In this period, glucose and fructose were produced in small amounts. Although an initial hydrolytic activity is observed, resulting in glucose and fructose production, the high content of FOS indicates favorable pH, temperature and agitation for the production of this sugar by submerged fermentation.

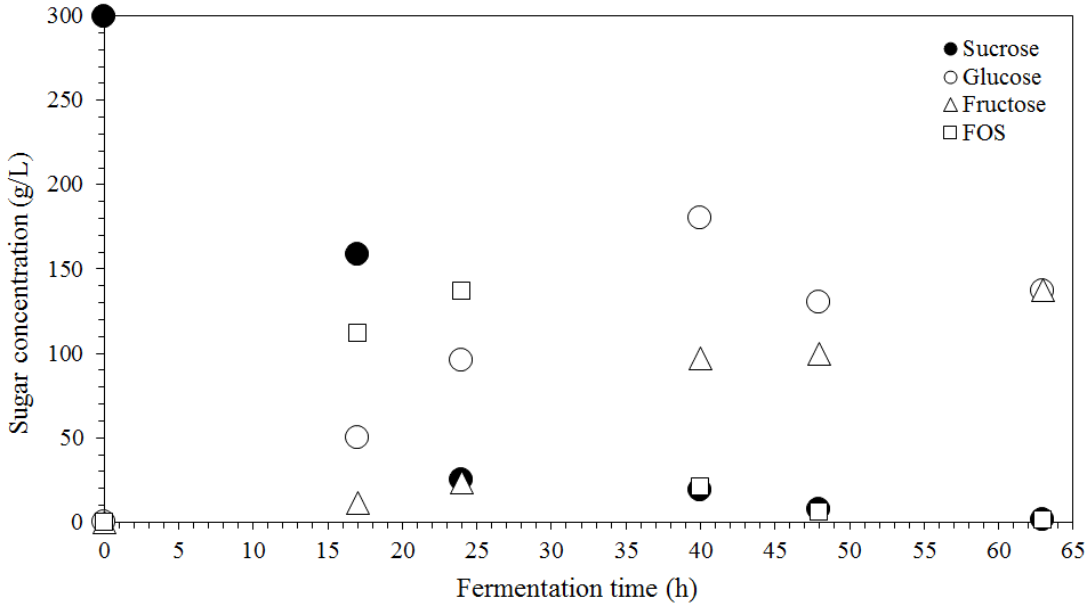

FIGURE 1: Sugar concentration (sucrose, glucose, fructose and FOS) quantified during fermentation time in 10-liter batch reactor using Aspergillus oryzae IPT-301. Fermentation was performed at 30 ^{0}C and 800 rpm agitation for 63 h, culture medium pH 4.5 and 0.75 vvm aeration with air flow rate of 6.0 $L.min^{-1}$.

The maximum FOS concentration was obtained at about 24 h of fermentation, when its content was 137 $g.L^{-1}$ and the yield was 45.8%. For the same period, the content of sucrose decreased from 300 $g.L^{-1}$ to 25 $g.L^{-1}$, and with the content of fructose reaching 25 $g.L^{-1}$. Glucose concentration also doubled, rising from 50 $g.L^{-1}$(17 h of fermentation) to 100 $g.L^{-1}$(24 h). Elapsed 40 h of process and comparing with the results after 24 h, glucose and fructose contents increased, respectively, about 87.5% and 415%. Simultaneously, FOS content decreased to 21 $g.L^{-1}$and sucrose concentration decreased about 75%. This fermentative behavior indicates FOS consumption by the fungal metabolism, once sucrose content is considerably low, and a concomitant increase in hydrolytic activity. The fermentation was conducted in an acid culture medium maintained at pH 4.5 throughout the enzyme production process.

For 48 h and 63 h of process, it was observed that the amounts of sucrose and FOS were almost depleted from the culture medium. It is believed that the molecules of these oligomers were hydrolyzed by the action of hydrolytic enzymes produced during fermentation. It is presumed that the high hydrolytic activity of the medium favored a considerable rise in the concentration of glucose and fructose monomers in the final fermentation steps.

[2] and [9] reported a partial hydrolysis and consumption of the initial sucrose content in the culture medium for growth and maintenance of the cellular metabolism, whereas the remaining sucrose is subjected to the action of the enzymeβ-fructofuranosidase produced by the growing microorganisms, generating FOS, glucose and fructose. Considering only the extracellular enzymes, FTase activity increased as a function of fermentation time, from 6 $U.mL^{-1}$in 17 h to a maximum of 36 $U.mL^{-1}$in 40 h, as showed in Fig. 2. After this period, the activity of this enzyme was almost constant, indicating a slight trend for decrease to 29 $U.mL^{-1}$, keeping approximately this same value until 63 h of fermentation. These results indicate an increase in FTase activity, concomitant to a decrease in sucrose content until 24 h, and a decrease in FOS content as a function of the higher hydrolytic activity after this time. This behavior is probably related to a predominant transfructosylation activity in the first stages of the process, and a sequential hydrolytic activity, resulting in the breakdown of FOS molecules.

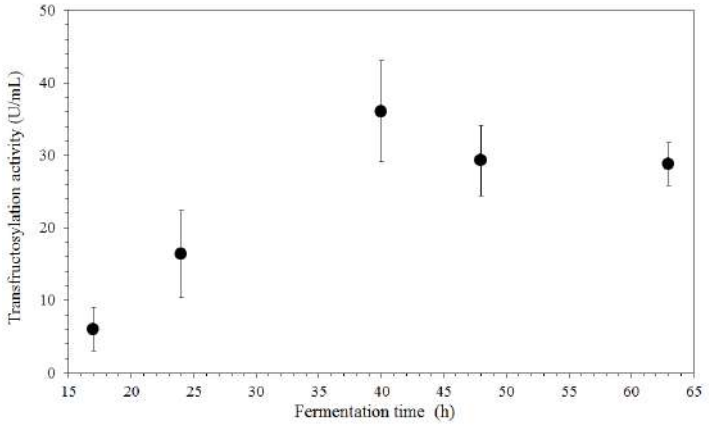

FIGURE 2: Extracellular transfructosylation activity obtained during the fermentation time in 10-liter batch reactor using *Aspergillus oryzae* IPT-301. Fermentation was performed at 30 ^{0}C and 800 rpm agitation for 63 h, culture medium pH 4.5 and 0.75 vvm aeration with air flow rate of 6.0 L.min^{-1}.

Only a few reports exist regarding the production of FTase and FOS in bioreactors. [42] reported the maximum production of FTase, 11 U.mL^{-1}, for 12 h of fermentation at 37 °C using *Bacillus macerans* as a production source of the enzyme. Sucrose (15 g.L^{-1}) was used as carbon source. Additionally, aeration (1.0 vvm), agitation (400 rpm) and pH 5.5 of the culture medium were controlled in the bioreactor. [41] reported on FTases produced with low transfructosylation activity (0.053 U.mL^{-1}) from *Penicillium citrinum* using 200 g.L^{-1} of sucrose in the culture medium, with pH 6.0. Fermentation was performed for 36 h at 28 °C and the bioreactor was maintained at 1.5 vvm aeration and agitation at 500 rpm. [43] reported a maximum FOS yield of 62.8% in a continuous process, with the biomass harvested after 48 h of *Aspergillus sp*. N74 growth using a mechanically-agitated airlift reactor. In this fermentation, an initial sucrose concentration of 70% (w/v) was employed, twice that used in the present work, at 60 °C. In spite of the higher FOS yield obtained by these authors, the maximum transfructosylation activity obtained was about 18.5 U.mL^{-1} lower than that obtained in the present work. Therefore, the extracellular FTases reported by the authors were observed to show a lower transfructosylation activity when compared to the present study. The results suggest that *Aspergillus oryzae* IPT-301 can be viewed as a potential microorganism for the production of FTases using bioreactors, according to the experimental conditions presented in this work.

Fig. 3 presents a maximum mycelial FTase activity of 2900 U.g^{-1}dry cell in the initial stages of the process for 17 h of fermentation. From this time, mycelial enzyme activity ranged between 2000 U.g^{-1}and 2600 U.g^{-1}dry cell, until 63 h of fermentation. The highest mycelial FTase activity at the beginning of the fermentation is coincident with the minimum extracellular activity time, possibly indicating a requirement of this type of enzyme, adhered to the mycelium, for the initial biomass development. Presumably, elapsed 24 h of fermentation, after the initial biomass development, the fungus starts to produce concomitantly extracellular FTase in large scale. From this fermentation period, mycelial and extracellular enzymes show relatively high activities, aiming to support the cell metabolism when sucrose, the primary carbon source, content is low.

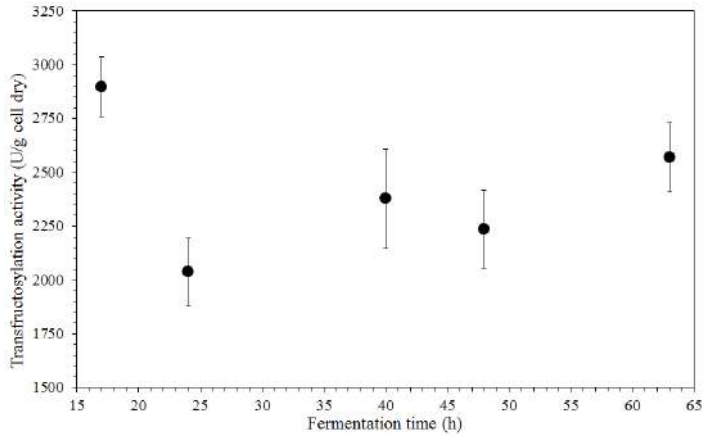

FIGURE 3: Mycelium transfructosylation activity obtained during the fermentation time in 10-liter batch reactor using *Aspergillus oryzae* IPT-301. Fermentation was performed at 30 ^{0}C and 800 rpm agitation for 63 h, culture medium pH 4.5 and 0.75 vvm aeration with air flow rate of 6.0 L min^{-1}.

3.2 Evaluation of pH and temperature effects on FTase activities

Transfructosylation and hydrolytic activities were higher, and constant, at temperatures from 55 °C to 65 °C, as was observed from screening of the extracellular FTase activity as a function of temperature, presented in Fig. 4. In this temperature range, transfructosylation activity was about 155 $U.mL^{-1}$ and at 55 °C the maximum (At/Ah) ratio was observed, about 21. This temperature range is different from that used for microbial cultivation, indicating the advantages of using the isolated FTase, and not the fungus, for FOS production. Some studies, such as [44], stated that the optimum temperature for FTase transfructosylation activity was obtained between 50 and 60 °C.

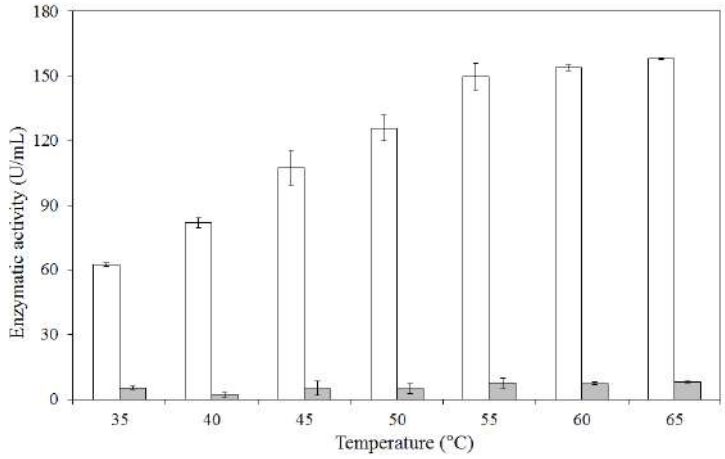

FIGURE 4: Effects of temperature on extracellular transfructosylation activity (unfilled bars) and extracellular hydrolytic activity (gray bars). Experimental conditions: activities were performed in rotary shaker at 190 rpm agitation for 60 min using 0.2 $mol.L^{-1}$tris-acetate buffer (pH 5.0) and 636 $g.L^{-1}$ sucrose as substrate.

The ratio between transfructosylation and hydrolytic activities (At/Ah) can be considered as the most important criteria when evaluating FOS production from different microbial enzyme [9,45]. When high ratio values (At/Ah) are obtained, FTase exhibits greater transfructosylation activity in the reaction medium. Therefore, high transfructosylation activity allows a high conversion of sucrose to FOS while a high (At/Ah) is required to avoid FOS molecule hydrolysis [9,45,46]. In addition, for the industrial FTase application, high ratio (At/Ah) values are preferred associated with the potential production of the enzyme to achieve efficient FOS synthesis [9,47,48,49].

As shown in Fig. 5, FTase transfructosylation activity for mycelial enzymes was higher, and very similar at the temperature range from 50 °C to 65 °C, presenting values of about 2700 $U.g^{-1}$ dry cell. The hydrolytic activity increased as a function of temperature from 70 $U.g^{-1}$ dry cell, at 35 °C to 350 U.g-^{1} dry cell at 65 °C and the maximum (At/Ah) was about 17 at 55 °C.

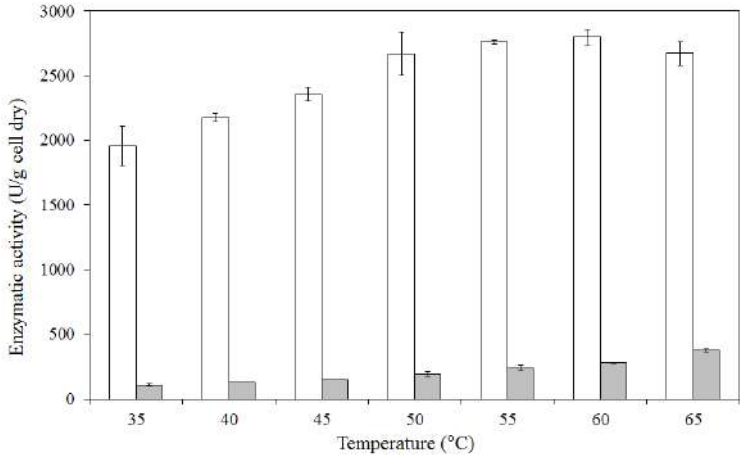

FIGURE 5: Effects of temperature on mycelium transfructosylation activity (unfilled bars) and mycelium hydrolytic activity (gray bars). Experimental conditions: activities were performed in rotary shaker at 190 rpm agitation for 60 min using 0.2 $mol.L^{-1}$tris-acetate buffer (pH 5.0) and 636 $g.L^{-1}$ sucrose as substrate.

In Fig. 6, a great influence of pH values on extracellular FTase transfructosylation activity and hydrolytic activity is observed, showing, respectively, maximum values of 146 $U.mL^{-1}$ at pH 6.0 and 35 $U.mL^{-1}$ at pH 3.5. The pH range from 4.5 to 5.5 showed the best ratios (At/Ah), having a maximum of 38 at pH 5.0. On the other hand, Fig. 7 shows an almost constant mycelial FTase hydrolytic activity as a function of pH, and a maximum mycelial FTase transfructosylation activity of 3265 $U.g^{-1}$ dry cell at pH 5.0, resulting in (At/Ah) of about 13. Some studies stated the optimum pH for these enzyme activities from 4.5 to 6.5 [50].

The difference between activity behavior of mycelial and extracellular FTase may occur because mycelial enzymes are affected by the cell. Enzymes inside the cells require that substrates and products cross the membrane; additionally, the cellular environment affects enzymatic activities. In addition, enzymes on the cell surface are stabilized by the cell membrane and are less accessible to degradation and adsorption of materials from the reaction medium [51].

IV. CONCLUSION

FOS production using *Aspergillus oryzae* IPT 301 by submerged fermentation results in a 45.8% yield after 24 h of fermentation, and maximum extracellular FTase activity of 36 $U.mL^{-1}$ at 40 h. The temperature used in fermentation (30 °C) is very different from the one 55 °C resulting in the maximum transfructosylation activity and (At/Ah) ratio. The optimum temperature and pH for transfructosylation activity, ideal for FOS production, are different for the extracellular and mycelial enzymes. Using a proper pH value and temperature, it is possible to maximize the transfructosylation activity and minimize the hydrolytic activity for FOS production using the FTase from the microorganism studied.

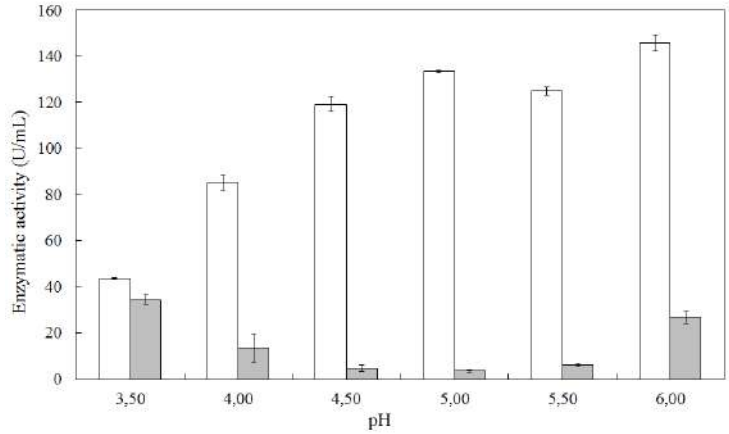

FIGURE 6: Effects of pH on extracellular transfructosylation activity (unfilled bars) and extracellular hydrolytic activity (gray bars). Experimental conditions: activities were performed in rotary shaker at 55 ˚C, 190 rpm agitation for 60 min using 0.2 $mol.L^{-1}$tris-acetate buffer and 636 $g.L^{-1}$ sucrose as substrate.

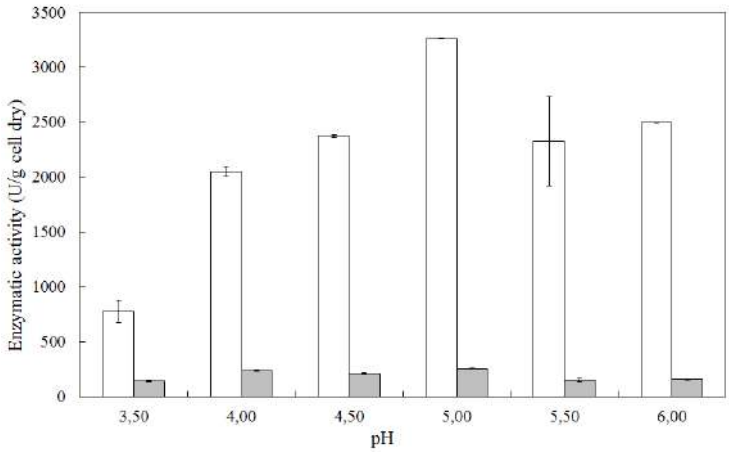

FIGURE 7: Effects of pH on mycelium transfructosylation activity (unfilled bars) and mycelium hydrolytic activity (gray bars). Experimental conditions: activities were performed in rotary shaker at 55 ˚C, 190 rpm agitation for 60 min using 0.2 $mol.L^{-1}$tris-acetate buffer and 636 $g.L^{-1}$ sucrose as substrate.

ACKNOWLEDGMENT

The authors gratefully acknowledge The State of Minas Gerais Research Foundation (FAPEMIG, Process APQ-02131-14) for providing financial support.

REFERENCES

[1] M. Hirayama, K. Nishizawa, H. Hidaka, "Production and Characteristics of Fructo-oligosaccharides", in: A. Fuchs (Eds.), Inulin and Inulin-containing Crops, Elsevier Science, Wageningen, 1993.

[2] J.W. Yun, "Fructooligosaccharides – Occurrence, preparation, and application", Enzyme and Microbial Technology, vol. 19, pp. 107, 1996.

[3] W.C. Chen, C.H. Liu, "Production of β-fructofuranosidase by *Aspergillus japonicas*", Enzyme and Microbial Technology, vol. 18, pp. 153, 1996.

[4] S.C. Chen, D.C. Sheu, K.J. Duan, "Production of fructooligosaccharides using β-fructofuranosidase immobilized onto chitosan-coated magnetic nanoparticles", Journal of the Taiwan Institute of Chemical Engineers, vol. 45, pp. 1105, 2014.

[5] N. Romano, M. Santos, P. Mobili, R. Vega, A. Gómez-Zavaglia, "Effect of sucrose concentration on the composition of enzymatically synthesized short-chain fructo-oligosaccharides as determined by FTIR and multivariate analysis", Food Chemistry, vol. 202, pp. 467, 2016.

[6] O. Sánchez, F. Guio, D. Garcia, E. Silva,L. Caicedo, "Fructooligosaccharides production by *Aspergillus sp*. N74 in a mechanically agitated airlift reactor", Food and Bioproducts Processing, vol. 86, pp. 109, 2008.

[7] M. Antosová, V. Illeová, M. Vandáková, A. Druzkovská, M. Polakovic, "Chromatographic separation and kinetic properties of fructosyltransferase from Aureobasidium pullulans", J. Biotechnol., vol. 135, pp. 58-63, 2008.

[8] N.C.C. Moore, L.P. Yang, H. Storm, M. Oliva-Hemker, J.M. Saavedra, "Effects of fructo-oligosaccharide-supplemented infant cereal: a double-blind, randomized trial", British Journal of Nutrition, vol. 90, pp. 581, 2003.

[9] R. Cuervo, C.A. Ottoni, E.S. Silva, R.M.M. Matsubara, J.M. Carter, L.R. Magossi, M.A.A. Wada, M.F.A. Rodrigues, B. Guilarte, A.E. Maiorano, "Screening of β-fructofuranosidase-producing microorganisms and effect of pH and temperature on enzymatic rate", Applied Microbiology and Biotechnology, vol. 75, pp. 87, 2007.

[10] A.L. Dominguez, L.R. Rodrigues, N.M. Lima, J.A. Teixeira, "An overview of the recents developments on fructooligosaccharide production and applications", Food and Bioprocess Technology, vol. 07, pp. 324, 2014.

[11] G.R. Gibson, M.B. Roberfroid, "Dietary modulation of the human colonic microbiota: introduction the concept of prebiotics", The Journal of Nutrition, vol. 125, pp. 1401, 1995.

[12] M.A. Ganaie, A. Lateef, U.S. Gupta, "Enzymatic trends of fructooligosaccharides production by microorganisms", Applied Biochemistry and Biotechnology, vol. 172, pp. 2143, 2014.

[13] C.J.A. Díaz, A.M. Gutierrez, I. Bahamon, A. Rodríguez, M.A. Rodríguez, O.F. Sánchez, "Computational analysis of the fructosyltransferase enzyme in plants, fungi and bacteria", Gene, vol. 484, pp. 26, 2011.

[14] T. Tokunaga, T. Oku, N. Hosoya, "Influence of chronic intake of new sweetener fructooligosaccharide (Neosugar) on growth and gastrointestinal function of the rat", Journal of Nutritional Science and Vitaminology, vol. 32, pp. 111, 1986.

[15] M. Roberfroid, N. Delzenne, "Dietary fructans", Annual Review of Nutrition, vol. 18, pp. 117, 1998.

[16] M.B. Roberfroid, "Inulin-type fructans: functional food ingredients", The Journal of Nutrition, vol. 137, pp. 2493, 2007.

[17] X.A. Zeng, K. Zhou, D.M. Liu, C.S. Brennan, M. Brennan, J.S. Zhou, S.J. Yu, "Preparation of fructooligosaccharides using *Aspergillus niger* 6640 whole-cell as catalyst for bio-transformation", Food Science and Technology, vol. 65, pp. 1072, 2016.

[18] C.S. Chien, W.C. Lee, T.J. Lin, "Immobilization of *Aspergillus japonicus* by entrapping cells in gluten for production of fructooligosaccharides", Enzyme and Microbial Technology, vol. 29, pp. 252, 2001.

[19] F.J. Bealing, J.S.D. Bacon, "The action of mold enzymes on sucrose", Biochem. J.,vol. 53, pp. 277-285, 1953.

[20] S. Usami, T. Ishii, K. Kirimura, K. Uehara, J. Chen, "Production of β-fructofuranosidase showing fructose-transferring activity by Pinicillium frequentans (P. glabrum)", Journal of Fermentation and Bioengineering, vol. 72, pp. 303, 1991.

[21] J.S. Lim, M.C. Park, J.H. Lee, S.W. Park, S.W. Kim, "Optimization of culture medium and conditions for Neo-fructooligosaccharides production by Penicillium citrinum", European Food Research and Technology, vol. 221, pp. 639, 2005.

[22] M.A. Ganaie, U.S. Gupta, N. Kango, "Screening of biocatalysts for transformation of sucrose to fructooligosaccharides", Journal of Molecular Catalysis B: Enzymatic, vol. 97, pp. 12, 2013.

[23] J.W. Yun, D.H. Kim, S.K. Song, "Enhanced production of fructosyltransferase and glucosyltransferase by substrate-feeding cultures of Aureobasidium pullulans", Journal of Fermentation and Bioengineering, vol. 84, pp. 261, 1997.

[24] A. Lateef, J.K. Oloke, S.G. Prapulla, "The effect of ultrasonication on the release of fructosyltransferase from Aureobasidium pullulans CFR 77", Enzyme and Microbial Technology, vol. 40, pp. 1067, 2007.

[25] A. Dominguez, C. Nobre, L.R. Rodrigues, A.M. Peres, D. Torres, I. Rocha, "New improved method for fructooligosaccharides production by Aureobasidium pullulans", Carbohydrate Polymers, vol. 89, pp. 1174, 2012.

[26] Y. Maruyama, K. Onodera, "Production and some properties of invertase isozyme of Fusarium oxysporum", The Journal of General Applied Microbiology, vol. 25, pp. 361, 1979.

[27] A.K. Gupta, I.S. Bhatia, "Glucofructosan biosynthesis in Fusarium oxysporum regulation and substrate specificity of fructosyltransferase and invertase", Phytochemistry, vol. 21, pp. 1249, 1982.

[28] V. Patel, G. Saunders, C. Bucke, "Production of fructooligosaccharides by Fusarium oxysporum", Biotechnology Letters, vol. 16, pp. 1139, 1994.

[29] V. Patel, G. Saunders, C. Bucke, "N-Deglycosylation of fructosyltransferase and invertase from Fusarium oxysporum decreases stability but has little effect on kinetics and synthetic specificity", Biotechnology Letters, vol. 19, pp. 75, 1997.

[30] J.H. Pazur, "Transfructosidation reactions of an enzyme of *Aspergillus oryzae*", The Journal of Biological Chemistry, vol. 199, pp. 217, 1952.

[31] L. L'Hocine, Z. Wang, B. Jiang, S. Xu, "Purification and partial characterization of fructosyltransferase and invertase from *Aspergillus niger* AS0023", Journal of Biotechnology, vol. 81, pp. 73, 2000.

[32] P.T. Sangeetha, M.N. Ramesh, S.G. Prapulla, "Production of fructosyltransferase by *Aspergillus oryzae* CFR 202 in solid-state fermentation using agricultural by-products", Applied Microbiology and Biotechnology, vol. 65, pp. 530, 2004.

[33] L.M. Wang, H.M. Zhou, "Isolation and identification of a novel *A. japonicus* JN19 producing β-fructofuranosidase and characterization of the enzyme", Journal of Food Biochemistry, vol. 30, pp. 641, 2006.

[34] S.I. Mussatto, J.A. Teixeira, "Increase in the fructooligosaccharides yield and productivity by solid-state fermentation with *Aspergillus japonicus* using agro-industrial residues as support and nutrient source", Biochemical Engineering Journal, vol. 53, pp. 154, 2010.

[35] C.A. Ottoni, R. Cuervo, R.M. Piccoli, R. Moreira, B.G. Maresma, E.S. Silva, M.F.A. Rodrigues, A.E. Maiorano, "Media optimization for β-fructofuranosidase production by *Aspergillus oryzae*", Brazilian Journal of Chemical Engineering, vol. 29, pp. 49, 2012.

[36] D.B.M. Márquez, J.C. Contreras, R. Rodríguez, S.I. Mussatto, J.A. Teixeira, C.N. Aguilar, "Enhancement of fructosyltransferase and fructooligosaccharides production by A. oryzae DIA-MF in solid-state fermentation using aguamiel as culture medium", Bioresource Technology, vol. 213, pp. 276, 2016.

[37] M.A. Ganaie, U.S. Gupta, "Recycling of cell culture and efficient release of intracellular fructosyltransferase by ultrasonication for the production of fructooligosaccharides", Carbohydrate Polymers, vol. 110, pp. 253, 2014.

[38] M. Antosová, M. Polakovic, "Fructosyltransferases: The enzymes catalyzing production of fructooligosaccharides", Chemical Papers, vol. 55, pp. 350, 2001.

[39] A.E. Maiorano, "Influência da concentração de inóculo e da temperature na produção de enzimas aminolíticas por cultivo de *Aspergillus oryzae* em meio semi-sólido", MSc. Thesis, University of São Paulo, 1982.

[40] A.E. Maiorano, "Produção de pectinase por fermentação em estado sólido", PhD. Thesis, University of São Paulo, 1990.

[41] J.S. Lim, J.H. Lee, J.H. Kim, S.W. Park, S.W. Kim, "Effects of morphology and rheology on neo-fructosyltransferase production by Penicillium citrinum", Biotechnology and Bioprocess Engineering, vol. 11, pp. 100, 2006.

[42] J.P. Park, T.K. Oh, J.W. Yun, "Purification and characterization of a novel transfructosylating enzyme from Bacillus macerans EG-6", Process Biochemistry, vol. 37, pp. 471, 2001.

[43] L. Caicedo, E. Silva, O. Sánchez, "Semibatch continuous fructooligosaccharides production by *Aspergillus sp.* N74 in a mechanically agitated airlift reactor", Journal of Chemical Technology and Biotechnology, vol. 84, pp. 650, 2009.

[44] A. Madlová, M. Antosová, M. Polakovic, V. Báles, "Thermal stability of fructosyltransferase from Aureobasidium pullulans", Chemical Papers, vol. 54, pp. 339, 2000.

[45] H. Hidaka, M. Hirayama, N. Sumi, "A fructooligosaccharide-producing enzyme from *Aspergillus niger* ATCC 20611", Agricultural and Biological Chemistry, vol. 52, pp. 1181, 1988.

[46] H. Hidaka, "Fructooligosaccharides", in: The Amylase Research Society of Japan (Ed.), Handbook of Amylases and Related Enzymes, Pergamon Press, Tokyo, 1988.

[47] M.H. Kim, M.J. In, H.J. Cha, Y.J. Yoo, "An empirical rate equation for the fructooligosaccharide-producing reaction catalyzed by β-fructofuranosidase", Journal of Fermentation and Bioengineering, vol. 82, pp. 458, 1996.

[48] R. Cuervo, B. Guilarte, A. Juárez, J. Martínez, "Production of fructooligosaccharides by β-fructofuranosidase from *Aspergillus sp.* 27H", Journal of Chemical Technology and Biotechnology, vol. 79, pp. 268, 2004.

[49] E.A. Oliveira, 'Immobilization of extracellular enzyme fructosyltransferase from Rhodotorula sp. and application in fructooligosaccharides production", MSc. Thesis, University of Campinas, 2007.

[50] A.E. Maiorano, R.M. Piccoli, E.S. Silva, M.F.A. Rodrigues, "Microbial production of fructosyltransferase for synthesis of pre-biotics", Biotechnology Letters, vol. 30, pp. 1867, 2008.

[51] J. Schuurmann, P. Quehl, G. Festel, J. Jose, "Bacterial whole-cell biocatalysts by surface display of enzymes: toward industrial application", Applied Microbiology and Biotechnology, vol. 98, pp. 8031, 2014.

Effect of particle size distribution on mixing and segregation in a gas-solid fluidized bed with binary system

Taek Woon Hong[1], Dong Hyun Lee[2*]

Department of Chemical Engineering, SungkyunKwan University, 2066, Seobu-ro Jangan-gu Suwon-si Gyeonggi-do, 16419 Republic of Korea

Abstract*—The mixing and segregation characteristics were investigated in gas-solid fluidized beds with binary solid mixture. Bed materials were constituted with binary solids, having different size and density. To investigate the effect of particle size distribution on the mixing characteristics, two other binary solid mixtures were used, which have similar mean particle size and particle density, but their particle size distribution was different to each other. Bed column has ID=0.14 m and H=2.14m. Bed aspect ratio was 3.0. Bed materials were two sets: one of bed materials was the mixture of ilmenite (d_p=153 μm, ρ_s=3,860 kg/m^3) and coke (d_p =582 μm, ρ_s =1,762 kg/m^3), which has wide size distribution. The other bed materials was the mixture of ceramic beads (d_p =122 μm, ρ_s =3,800 kg/m^3) and plastic beads (d_p =813 μm, ρ_s =1,500 kg/m^3), which has narrow size distribution. Bed composition of ilmenite-coke mixture was determined to 0.7:0.3 by mass ratio. And, bed composition of ceramic beads-plastic beads was 0.75:0.25 by mass ratio. Axial bed pressure drop was measured according to gas velocity. Bed composition was measured according to axial bed height by sampling. Bed pressure drop of ilmenite-coke mixture was maximized above U_o=0.15 m/s, and fully fluidization was occurred. However, criterion of mixing to segregation was not found in the axial bed composition according to gas velocity. In the case of ceramicbeads-plastic beads mixture, bed pressure drop was maximized at U_o=0.05 m/s, and the criterion of mixing to segregation was found at the same gas velocity.*

Keywords*—gas-solid fluidized bed, segregation, mixing index, takeover velocity.

I. INTRODUCTION

The contents of each section may be provided to understand easily about the paper. Particle mixing and segregation characteristics are important in industrial fluidized beds, where particles of wide size distribution or particles of different density are usually handled. Therefore, to analyze gas-solid fluidized beds with binary solids, the degree of these properties should be evaluated. Past studies on particles in a gas fluidized bed have concentrated primarily on the mixing aspect of the phenomenon, notably those by Rowe and Nienow [1] using two separate layers of flotsam and jetsam as a starting mixture. The flotsam is the lighter or smaller particles; which tend to float at the top of the bed, while the jetsam is those heavier or larger particles, which tend to settle to the bottom part of the fluidized bed. These words were coined originally by Rowe et al. [2] and now have become widely accepted terminology. There are two primary objectives for investigating the particle segregation characteristic in gas fluidized beds. In one respect, the fluidized beds are studied to determine the operating conditions required to promote bed mixing and minimize particle segregation. The other objective is to study the optimum conditions under which clean separation can be accomplished between different materials in the bed [3].Takeover velocity is the superficial gas velocity which the gas-solid fluidized bed with binary solids is transformed from segregated to a solid mixing region. Therefore, mixing or segregation in binary solid beds is classified if takeover velocity could be estimated. However, in case of binary solids mixture dealing with wide size distribution has different range that certain or every particle can be fluidized. The mixing phenomena are beneficial for the process which perfect mixing has to be required. In contrast, it could be harsh to separate each particle for separation process. In this study, fluidized beds with binary solids mixture which

are different size and density were investigated. Mixing and segregation characteristics were investigated from experimental results, and takeover velocity was estimated. Also, alternative types of binary particles which its size distribution is narrow compared to ilmenite/coke set were chosen and analyzed.

II. THEORY

There is the empirical correlation for the takeover velocity in gas-solid fluidized beds with binary system [4]:

$$\frac{U_{TO}}{U_{mfS}} = \left(\frac{U_{mfB}}{U_{mfS}}\right)^{1.2} + 0.9\left(\frac{\rho_H}{\rho_L} - 1\right)^{1.1}\left(\frac{d_H}{d_L}\right)^{0.7} - 2.2\sqrt{\bar{x}}\left(1 - e^{-\frac{H}{D}}\right)^{1.4} \quad (1)$$

where U_{mfB} and U_{mfS} are the bigger and smaller minimum fluidization velocities, respectively; ρ_H and ρ_L are the particle densities of the denser and less dense particle, respectively; d_H and d_L are the particle size of the denser and less dense particle, respectively; $\bar{x}$ is the mass fraction of the denser particles in the whole bed; H and D are the height and diameter of the bed; U_{TO} is the takeover velocity at which mixing takes over from segregation. In general, $U_{TO} > U_{cf}$. Mixing index with calculated U_{TO} suggested by Rowe and Nienow [5] is as follows:

$$M_I = \frac{x}{\bar{x}} = (1 + e^{-Z})^{-1} \quad (2)$$

Where,

$$Z = \frac{U - U_{TO}}{U - U_{mf,S}} e^{U/U_{TO}} \quad (3)$$

mixing index is maximum at U_{TO}, and MI=0.5. Brereton and Grace [6] defined the solid mixing index as the following Eqs. (4)-(8): segregation index:

$$\gamma = \frac{\sigma}{\sigma_{fs}} \quad (4)$$

where,

$$\sigma = \sqrt{\frac{1}{N}\sum x_i - \bar{x}} \quad (5)$$

$$\bar{x} = \frac{1}{N}\sum x_i \quad (6)$$

$$\sigma_{fs}\sqrt{\bar{x}(1 - \bar{x})} \quad (7)$$

$$M_I = 1 - \gamma \quad (8)$$

III. EXPERIMENTAL

Fig.1 shows schematic diagram of experimental setup. The dimension of column was 0.14 m of inner diameter and 2.4 m of height with cylindrical acrylic column. The distributor to make uniform gas distribution was used bubble cap distributor. The orifice diameter is 1.4 mm with 76 holes. Pressure taps were installed horizontally at 0.05 m intervals to a height of 0.55 m, and then at 0.1 m intervals to 2.35 m, starting at 0.05 m above the gas distributor. The pressure drop across the bed was measured by a differential pressure transducer, connected to pressure taps, located axially. Transmitter signals were processed by a personal computer at a sampling time of 10 ms for 5000 data. To verify the entire composition of the bed, sampling ports were installed 0.1 m intervals to 0.45 m from 0.05 m above the gas distributor. Each sampling tube is 8 mm of inner diameter and 0.25 m long. All experiments were treated at steady state.

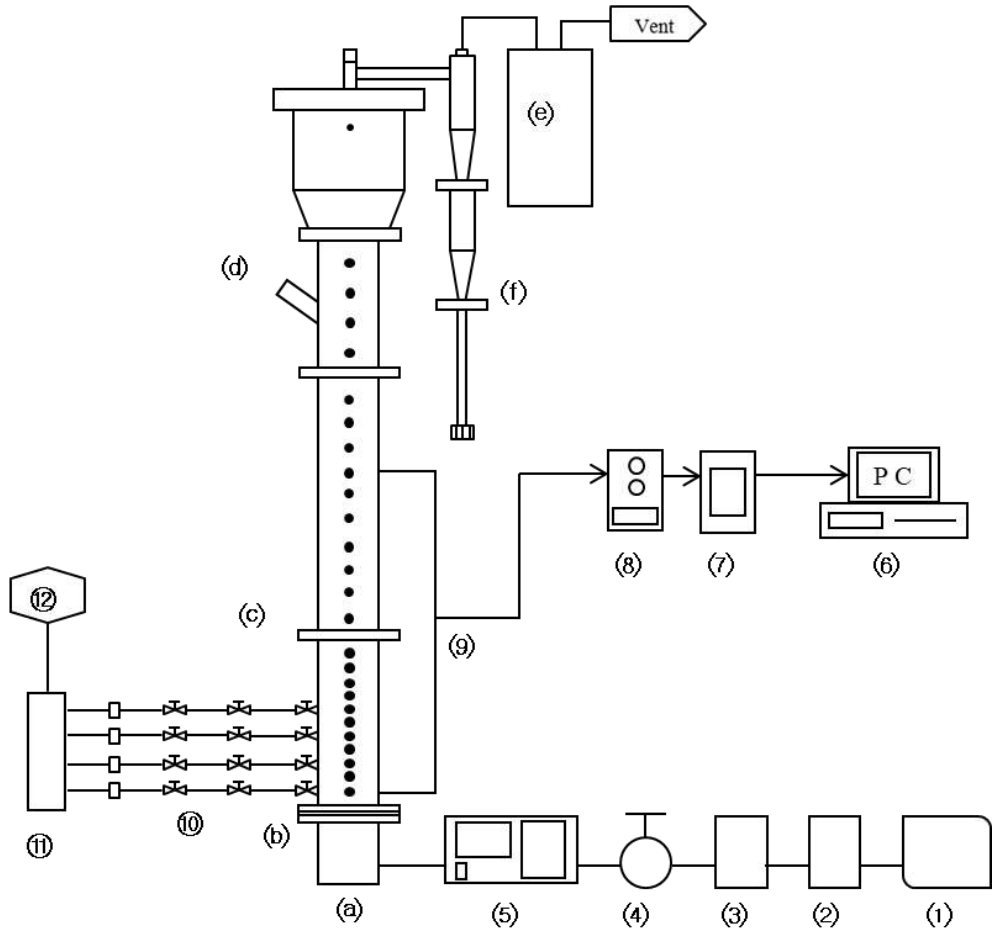

FIG. 1. Schematic diagram of experimental apparatus: (1) Compressor; (2) Air dryer; (3) Air filter; (4) Regulator; (5) MFC; (6) Computer; (7) A/D converter; (8) Pressure transducer; (9) Pressure line; (10) Sampling line; (11) Vacuum chamber; (12) Vacuum pump; (a) Plenum chamber; (b) Distributor; (c) Main column; (d) Particle inlet; (e) Bag filter; (f) Cyclone.

Fig. 2 shows particle size distributions of two binary mixtures used in experiments. The bed materials in this study are Ilmenite/coke and Ceramic beads/ Plastic beads with volumetric ratio of 0.5:0.5. All bed components are Geldart B particles. Physical properties ofthese solids were indicated in table 1. The Ilmenite/Coke set has wide size distribution and the set of Ceramic beads/Plastic beads has relative narrow size distribution.

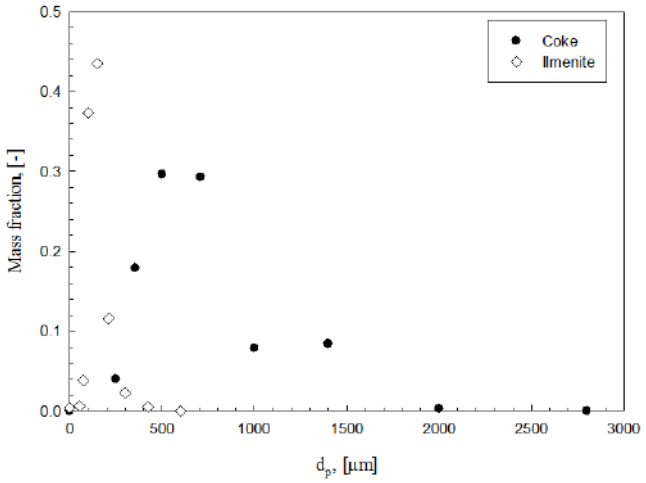

FIG.2(a). Particle size distribution of ilmenite-coke mixture

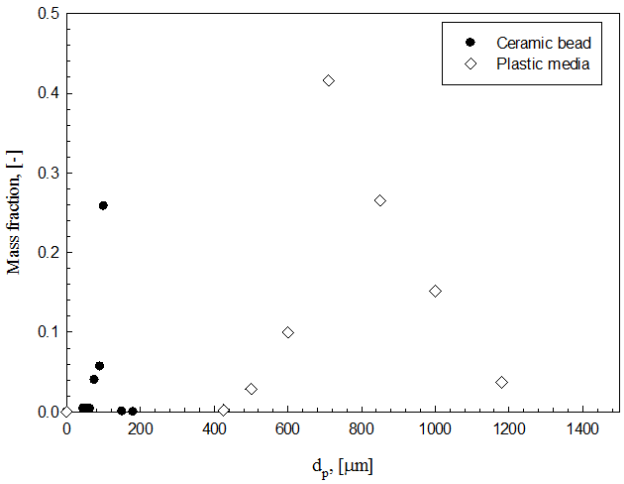

FIG. 2(b). Particle size distribution of ceramic beads-plastic beads mixture

TABLE 1
MATERIAL PROPERTIES OF PARTICLES USED IN EXPERIMENTS.

	Ilmenite	Coke	Ceramic bead	Plastic beads
d_p (μm)	153	582	122	813
ρ_s (kg/m^3)	3,860	1,762	3,800	1,500
U_{mf} (m/s)	0.026	0.3	0.019	0.28

Analysis of axial bed composition is essential to investigate mixing or segregation characteristics in the beds. First, particle mixture in the beds was sampled from sampling port installed on the side of columns. Second, coke in the mixture was combusted. Finally, weight differential was measured, and composition of binary mixture was determined. Fig. 3 shows the result of thermogravimetric analysis of binary mixtures. The weight of ilmenite was rarely changed according to temperature. Coke was perfectly combusted at 760oC. Therefore, binary mixture of ilmenite and coke was combusted at 800° C, and total operating time was 2 hours.

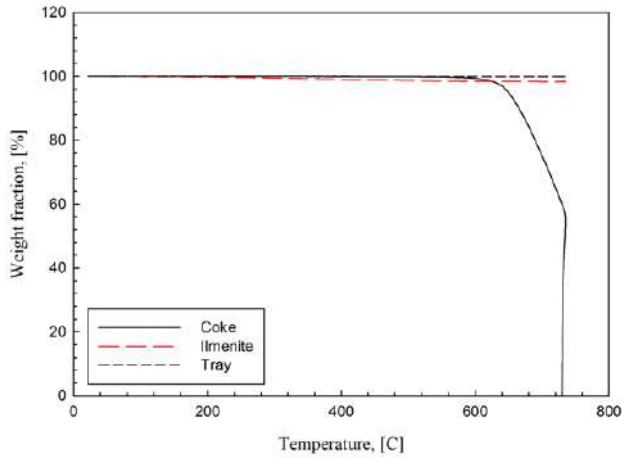

FIG.3. THERMOGRAVIMETRIC ANALYSIS OF ILMENITE-COKE MIXTURE

IV. RESULTS AND DISCUSSION

Fig. 4 shows the axial pressure drop of binary mixture of ilmenite and coke (mass ratio 7:3) in each operating superficial gas velocities. The gradient of bed pressure drop in the bottom of beds below h=0.2 m was rarely differed according to superficial gas velocity. However, in the top of beds above h=0.2 m, the gradient of pressure drop was decreased according to superficial gas velocity, because the height of bed surface was increased with increasing of superficial gas velocity.

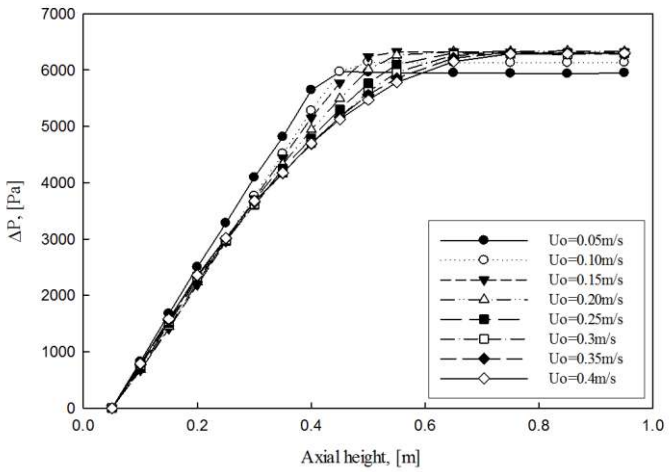

FIG.4. AXIAL PRESSURE DROPS OF ILMENITE-COKE MIXTURE

Fig. 5 shows the total bed pressure drop according to superficial gas velocity. In the figure, axial pressure drop was increased steadily according to superficial gas velocity up to Uo=0.05 m/s. Actually, fixed bed condition was maintained below Uo=0.05 m/s. When superficial gas velocity was in the range of Uo=0.05m/s to Uo=0.15 m/s, axial bed pressure drop was decreased slightly, and increased again. This is the region of partial fluidized beds, some particles were partially fluidized and other particles were remained in fixed bed. More increasing of superficial gas velocity above Uo=0.15 m/s, axial pressure drop was maximized, and no more increased according to gas velocity. From this result, complete fluidizing velocity of binary solid mixture of ilmenite and coke was found, that was Uo=0.15 m/s.

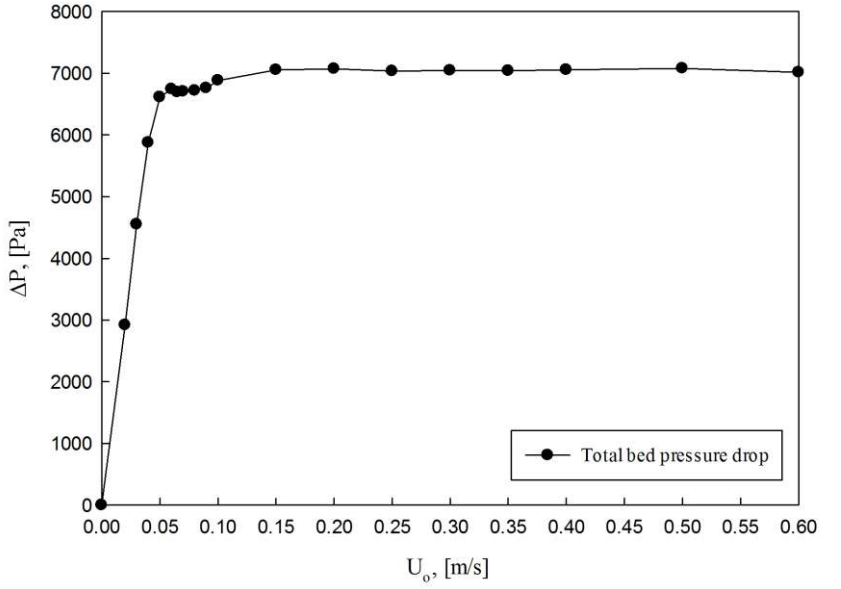

FIG.5. TOTAL BED PRESSURE DROP OF ILMENITE-COKE MIXTURE ACCORDING TO SUPERFICIAL GAS VELOCITY

Fig. 6 shows the mass fraction of ilmenite in each superficial gas velocity according to axial bed height. Axial mass fraction of ilmenite was measured in the range from Uo=0.05 m/s, minimum fluidizing velocity of binary mixture or ilmenite and coke, to Uo=0.33 m/s, takeover velocity, which was takeover velocity calculated by Eq. (1). All of the result was not significantly differed to 0.7 of mass ratio, which is the average mass fraction of ilmenite in the beds.

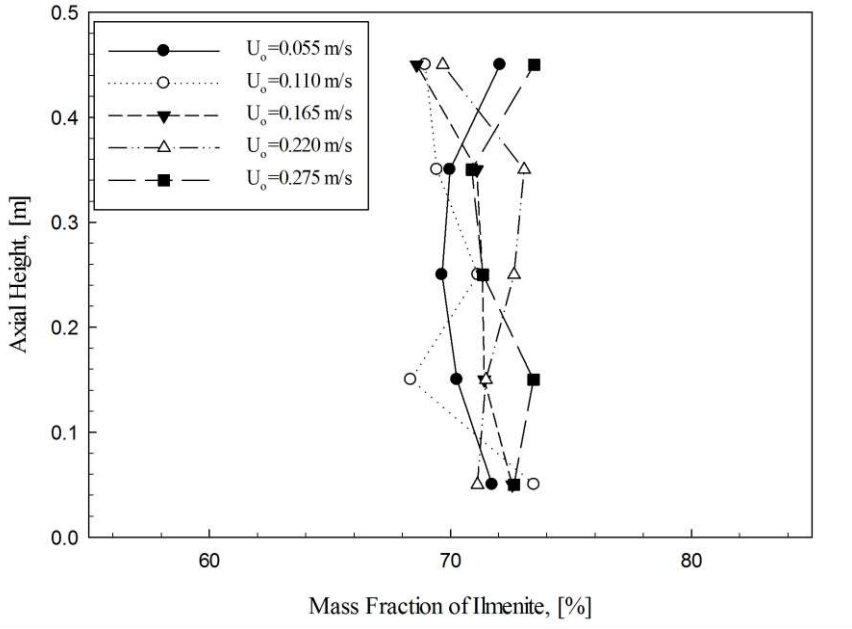

FIG.3. AXIAL MASS FRACTION OF ILMENITE

Fig. 7 shows mixing index calculated from axial mass fraction of ilmenite according to superficial gas velocity using Eq. (8). There were no significant tendency according to superficial gas velocity, and shown mixing index near to perfect mixing in entire gas velocity range. This result caused by very wide size distribution of two particles. Therefore, ilmenite and coke were partially fluidized at same superficial gas velocity, and they were not separated into jetsam and clearly.

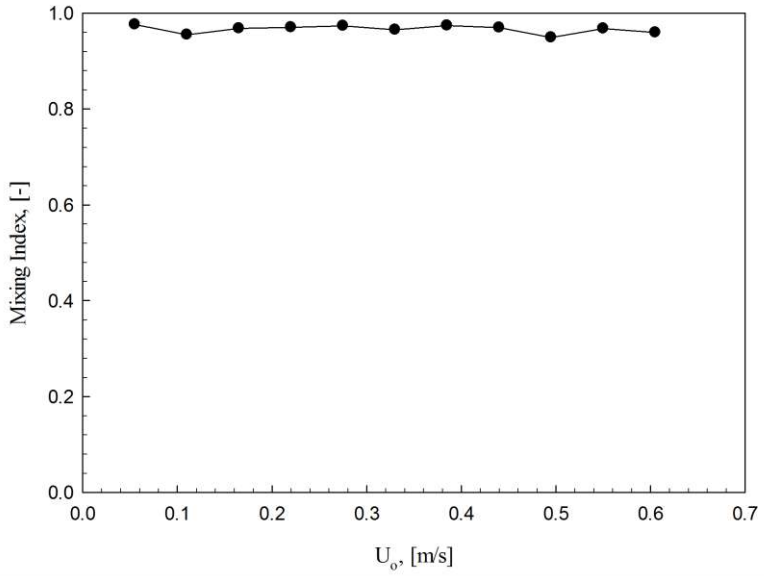

FIG.7. VARIATION OF MIXING INDEX OF ILMENITE-COKE MIXTURE BED WITH GAS VELOCITY

Fig. 8 shows axial pressure drop of alternated particle mixtures containing ceramic beads and plastic beads with narrow size distributions, which have similar particle density and average particle size of ilmenite and coke, respectively, according to axial bed height in each superficial gas velocities. Unlikely to ilmenite-coke mixture, in low gas velocity above Uo=0.02 m/s, gradient of pressure in the bottom of the bed was lower than in the top of the bed. Increasing gas velocity above Uo=0.02 m/s, gradient of pressure drop in the top of beds was decreased according to superficial gas velocity. Above Uo=0.05 m/s, gradient of pressure drop was uniform in entire beds.

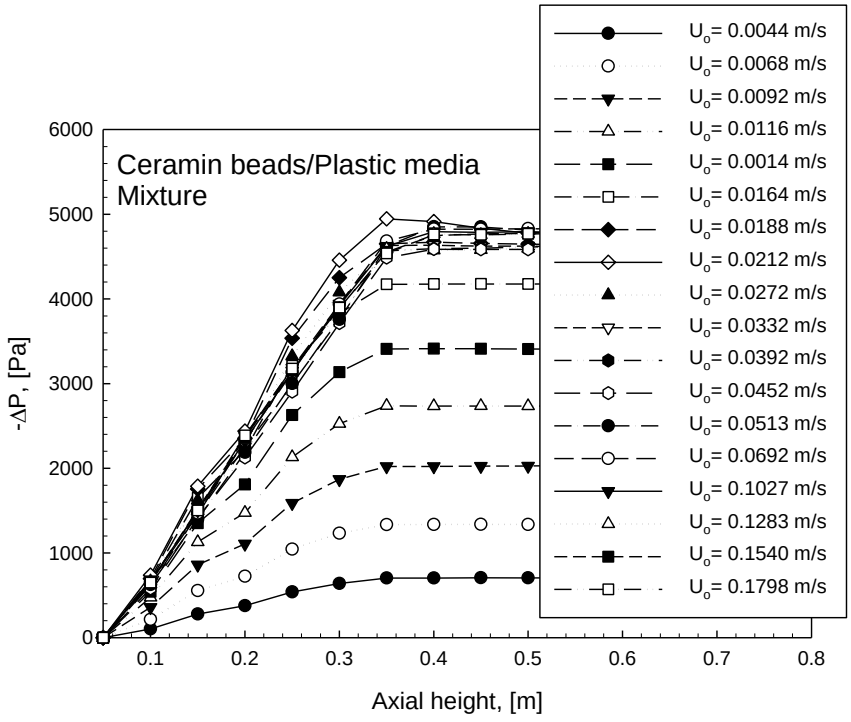

FIG.8. AXIAL PRESSURE DROPS OF CERAMIC BEADS-PLASTIC BEADS MIXTURE

Fig. 9 shows total bed pressure drop of ceramic beads-plastic plastic beads mixture. Comparing to total bed pressure drop in Fig. 9, gradient of pressure drop in the top of bed was decreased from Uo=0.02 m/s, which was minimum fluidizing velocity of ceramic beads-plastic beads mixture. Above Uo=0.05 m/s, in the complete fluidizing area, gradient was same in entire beds. From these results, flow regime in the bed could be classified to fixed, partial fluidized, and complete fluidized bed.

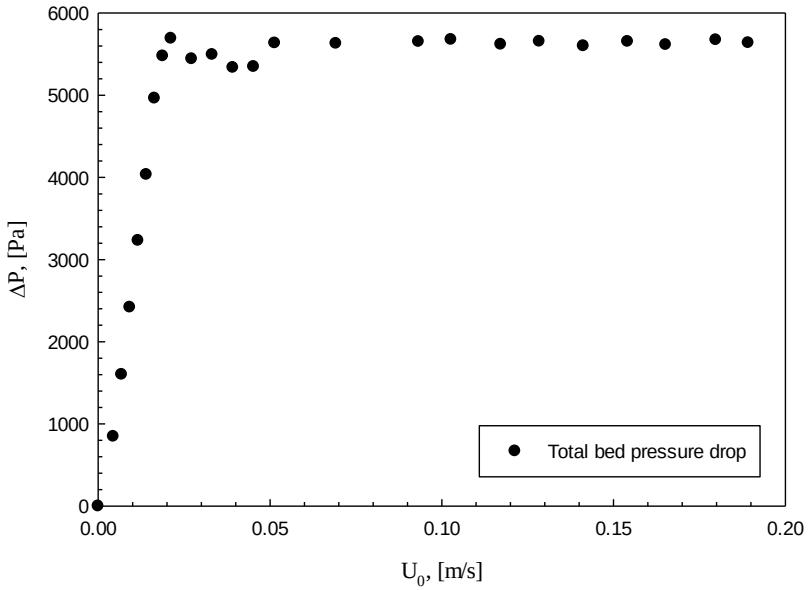

FIG.9. TOTAL BED PRESSURE DROP OF CERAMIC BEADS-PLASTIC BEADS MIXTURE

Fig. 10 shows the result of axial sampling experiments to ceramic beads-plastic media mixture. As different from ilmenite-coke mixture shown in Fig. 6, there was significant difference in the axial bed composition. Under Uo=0.057 m/s, mass fraction of ceramic beads in the bottom of bed was lower than that of the top of bed. Above Uo=0.057 m/s, mass fraction of ceramic beads was uniform in entire bed.

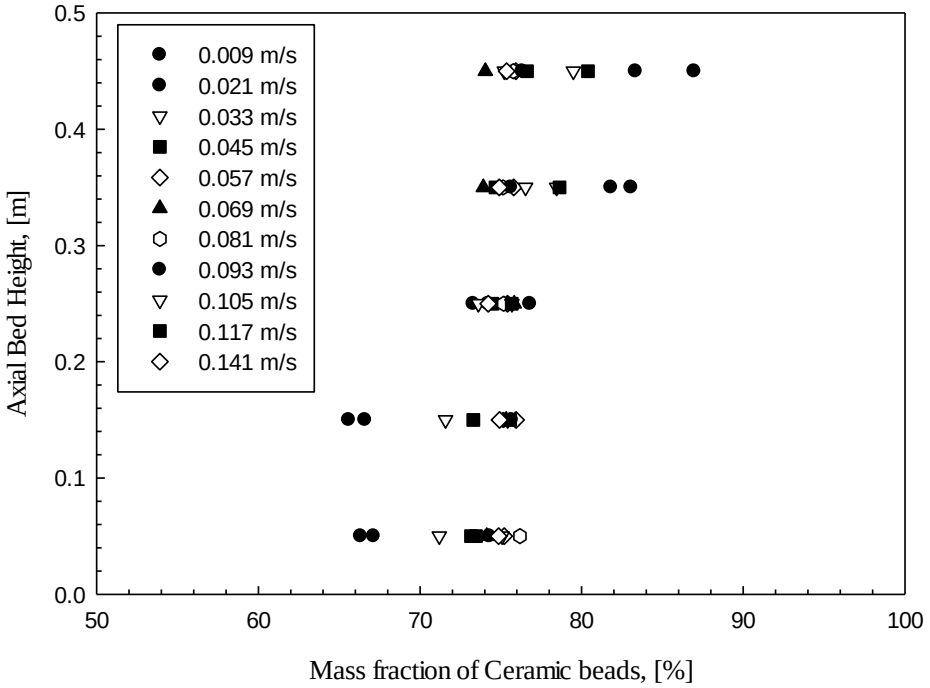

FIG.10. AXIAL MASS FRACTION OF CERAMIC BEADS

Fig. 11 shows mixing index calculated from the results in Fig. 10 according to superficial gas velocity. Mixing index was increased according to superficial gas velocity under Uo=0.057 m/s, and maximized at Uo=0.057 m/s. Thesis results indicate that there were the takeover velocity in the ceramic beads-plastic beads mixture, unlike to ilmenite-coke mixture.

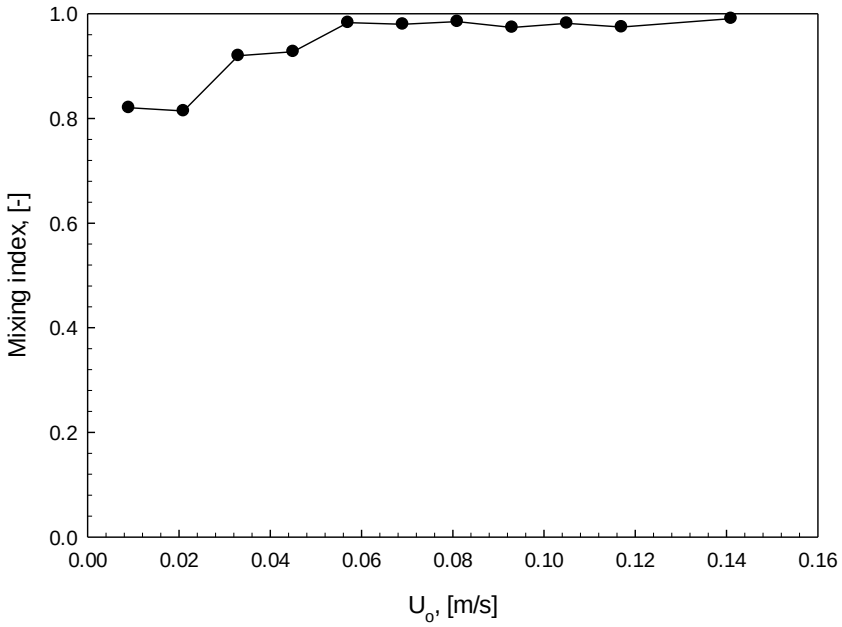

FIG.11. MIXING INDEX OF CERAMIC BEADS-PLASTIC BEADS MIXTURE

V. CONCLUSION

In the ilmenite-coke binary solid mixture, takeover velocity was not found significantly, because of their wide particle size distribution. However, in the ceramic beads-plastic beads mixture which has narrow size distribution, takeover velocity was found unlike to ilmenite-coke mixture. From these results, we figured out that particle size distribution of binary mixture strongly affect to mixing characteristics of beds.

ACKNOWLEDGEMENTS

This work was supported by the Technology Innovation Program (or Industrial Strategic Technology Development Program (10052751) funded By the Ministry of Trade, Industry & Energy (MOTIE, Korea). This work was partly supported by the Korea Institute of Energy Technology Evaluation and Planning (KETEP) grant (No.20163010050070) funded by the Ministry of Trade, Industry and Energy, Republic of Korea.

REFERENCES

[1] P.N. Rowe and A.W. Nienow, "Particle mixing and segregation in gas fluidized beds.A review." Powder Technol., vol.15, pp.141-147, 1976.

[2] P,N. Rowe, "A preliminary quantitative study of particle segregation in gas fluidized beds-binary systems of near-spherical particles" Trans. Inst. Chem. Eng., vol. 50, pp. 324-333, 1972.

[3] W.C. Yang, Hand book of fluidization and fluid-particle systems, 1st ed., Marcel Derkker, incl. New York-Basel, 2003, pp.92-111

[4] J. Baeyens and D. Geldart, "Gas fluidization technology" John Wiley & Sons, New York., 1986, pp. 97-122

[5] A.W. Nienow, P.N. Rowe and LY-L. Cheung, "A quantitative analysis of the mixing of two segregating powders of different density in a gas-fluidised bed" Powder Technol. vol.20, pp.89-97, 1986.

[6] C. M. H. Brereton and J.R. Grace, "Microstructural aspects of the behaviour of circulating fluidized beds" Chem. Eng. Sci., vol. 48, pp. 2565-2572, 1993.

Cold Photons in Space & Hot Photons in Atmosphere: A Review

Dr Bijay Kumar Parida (MS, FRCSG)

Associate Professor, Muthusamy Virtual University of Ophthalmology Post Graduation, Bhubaneswar, Odisha, India

Abstract— *Space is dark because the photons released from sun have lost energy and became cold photons during their passage towards earth. Because photons do not have energy in space, so space is cold. When photons reach atmosphere, it hits suspended particles and get annihilated. Thus these photons produce energy and light is seen. A definite quantum of energy must hit retina of eye to detect light which is absent in space. This article explains the phenomenon assuming dual nature of light. Retina can see the particular wavelengths of light ranging from 380nm to 780nm.*

Keywords— photon, space, energy, wavelength.

I. INTRODUCTION

Photons are released from sun have mass and definite quanta of energy. The energy associated with the photon is responsible for high speed. Gradually photon loses energy while it traverses through space towards earth. In spite of the temperature of the sun in excess of 1,000,000 Kelvin [1] the outer space is dark and very cold. This is a perplexing question for which the explanations proposed, are not exactly satisfactory. This article ventures to explain this phenomenon assuming dual nature of light as follows.

While travelling from sun photons lose energy and become cold. A definite quantum of energy is essential to be visible and felt as warm. Retina can see the particular wavelengths of light ranging from 380nm to 780nm.[2-6] So despite photons are present in sufficient amount in space, human eyes cannot detect it.

As photons enter atmospheres of earth, it hits the suspended particles present in atmosphere, explosion occurs and get annihilated. The presence of carbon particles and oxygen enhances the chance of explosion. The velocity of photons peaks up once more to moderate level. The energized photons as further moves, hit the larger and abundant suspended particles near the surface of earth. Here massive explosion results in higher energy of photons and wavelengths around ultra violet rays associated with photons emanate from photons. Gradually the energy is lost as it traverses through atmosphere. Ultra violet rays are abundant on surface of where carbon particles are plenty.

This questions the validity of ozone layer that filters out ultraviolet rays. Reduced carbon particles shall reduce ultraviolet load on earth surface.

II. DISCUSSION

Outer space is the expanse that exists beyond the Earth and between celestial bodies. Outer space is not completely empty, it is hardly a vacuum containing a low density of particles, predominantly a plasma of hydrogen and helium as well as electromagnetic radiation, magnetic fields, dust, and cosmic rays The baseline temperature, as set by the background radiation from the Big Bang, is 2.7 Kelvin.. There is no definite altitude above the Earth's surface where outer space begins. However, the Karman line, at an altitude of 100 km above sea level,[7] is conventionally used as the start of outer space for aerospace records. It contains few hydrogen atoms per cubic meter. The air humans breathe, contains about 1025 molecules per cubic meter.[8,9] A piece of bare metal in space, under constant sunlight can get hot. This is dangerous to astronauts who have to work outside the station. If they need to handle bare metal, they wrap it in special coatings or blankets to protect themselves. Astronauts can experience vast differences in temperature between the side facing the Sun, and the side in shadow.

This article explains above phenomenon as "photons liberated from sun, loses energy in its path. Photons, due to its higher energy liberated from sun have highest velocity in comparison to space, upper atmosphere and lower atmosphere of earth. In space the photon loses its energy and gains back in atmosphere. In upper atmosphere due to lesser suspended particle, energy content is medium, so also its velocity. But in lower atmosphere due to more of carbon particles and oxygen, photon gets annihilated and gains more energy. The velocity of light is 2nd highest in lower atmosphere of earth in comparison to other media."

At daytime sky is blue because light from the nearby sun hits molecules in the Earth's atmosphere and scatters off in all directions. The blue color of the sky is a result of this scattering process. At night, when the part of earth is facing away from the sun, space looks black because there is no nearby bright source of light.

This paper proposes that "photons after losing all its energy becomes cold and makes the space dark and cold. On entering into atmosphere, it hits few suspended particles and gains energy. Human eye is sensitive to a range of wavelengths which carry a quantum of energy. 'But the cumulative energy liberated in upper atmosphere is of blue wavelength range. So sky appears blue. In morning lesser number of cold photons enter the atmosphere, so lesser amount of energy is liberated which is around red wavelength'."

We know from experience that the space is black. This paradox is known as Obler's paradox. It is a paradox because of the apparent contradiction between the expectations that the night sky be bright. Many different explanations have been put forward to resolve Oblers' Paradox. The best solution at present is that the universe is not infinitely old; it is somewhere around 15 billion years old. That means one can only see objects as far away as the distance of light can travel in 15 billion years. The light from stars far away than that has not yet had time to reach us and can't contribute in making the sky bright.

Explanation proposed by this article is that "photons in space are devoid of energy. So these are not seen. Due to lack of particles in space, photons do not get annihilated. Hence photons are devoid of any energy. So the space is dark. If a photon have definite quantum of energy associated, then also it can be seen even there is no suspended particle in space. Space is cold because, the photon although having mass, does not have energy to keep the space warm. Entering into atmosphere of earth, photons hit particles and get energized. In morning and evening, lesser amount of photons hit particles, so the resultant energy is lesser and of red color range. At lower atmosphere, where suspended articles are there, more energy is being released, but never reaches a cumulative violet range, although violet and ultraviolet rays are emitted. Maximum ultraviolet rays are generated at most dense part of suspended and carbon particles."

"Photon after repeated annihilation, possibly losing its mass and subsequent chance of generating ultraviolet rays is reduced. So ultraviolet rays are maximum in middle of atmosphere."

III. CONCLUSION

Photon loses energy while it traverses through space towards earth. The paper provides an explanation on dual phenomena assuming photon having real mass and only energized photon is visualized by human retina. When photons reach atmosphere, it hit suspended particles and get annihilated producing energy and light is seen. The velocity of light is fastest near sun, slowest in space and gradually increases towards the surface of earth. A definite quantum of energy is essential to be visible and felt as warm.

REFERENCES

[1] Aschwanden, M. J. Physics of the Solar Corona. An Introduction. Praxis Publishing, 2004.
[2] Curtis, Barnes. Invitation to Biology: 5th Edition. New York: Worth Publishers, 1994: 163.
[3] Chambers Cambridge. Chambers Science & Technology Dictionary. New York: W & R Chambers Limited, 1940: 914.
[4] Freudenrich, Craig. How Light Works. www.Howstuffworks.com
[5] Lapedes, Daniel. Dictionary of Scientific & Technical Terms: Second Edition. New York: McGraw Hill, 1978: 954.
[6] Cesare, Emiliani. Dictionary of the Physical Sciences. New York: Oxford University Press, 1987: 124.
[7] Chuss, David T, Cosmic Background Explorer, NASA Goddard Space Flight Center, archived from original, 2013.
[8] Where does space begin? Aerospace Engineering, Aviation News. Archived from original, 2015.
[9] Tadokoro, M, A Study of the Local Group by Use of the Virial Theorem, Publications of the Astronomical Society of Japan, 1968, 20: 230.

Tracking down the Vehicle Collision Detection and Messaging System using GPS and GSM

S.Suganya[1], T.Divya[2], M.Subha Sankari[3], Dr.P.Gomathi[4]

[1,2,3]Department of Computer Science and Engineering, N.S.N college of Engineering and Technology, Karur-639003,TN, INDIA

[4]Department of Electrical and Electronic Engineering, N.S.N college of Engineering and Technology, Karur-639003,TN, INDIA

Abstract— *Security in travelling is a primary concern for everyone. Rising demand for automobile has increased the traffic, thereby causing more accidents on the road. People often lose their lives because of poor emergency facilities in the case of unattended accidents. Pre-emption of the accidents taking place on the roads is not possible, but at least the after effects can be minimized. The proposed system ensures making emergency facilities available to accident victims as early as possible by letting relatives; by the way of monitoring the car using its number plate recognizes the camera. Before that it can act through the tollbooth, the vehicle number plate was captured by this camera and stores it in a database. It will check out that the vehicle was authorized or not, if the number plate was registered one, then it passes the entry to the vehicle, otherwise buzzer alarm will rise. When the car met an accident sense by vibration sensor making an alert to hospital or a rescue team knows the accident spot with the help of this module embedded in the vehicle. Sensors are attached to the ARDUINO-Controller. In the event that there is a mishap, the sensor gets enacted and the GSM framework will send notices to the closest doctor's facility, police headquarters or sort of the casualty with the area organizes where the mischance has happened. With the assistance of room route framework GPS finds the position of the vehicle where a mischance has happened.*

Keywords— Collision Detection, messaging system, GPS, GSM, mobile communication, security issue, sensors, GSM framework.

I. INTRODUCTION

The popularity for automatic has likewise expanded the movement perils and the street mishaps. The life of the general population is under high hazard. This is a result of the absence of best crisis offices accessible in our nation. A programmed caution gadget for vehicle mishaps is presented in this paper. This outline is a framework which can distinguish mis-chances in fundamentally less time and sends the essential data to the medical aid focus inside a couple of moments covering topographical directions, the time and edge in which a vehicle mishap had happened. This alarm message is sent to the safeguard group in a brief span, which will help in sparing the profitable lives. A switch is likewise given with a specific end goal to end the sending of a message in the uncommon situation where there is no loss, this can spare the valuable time of the restorative save group. At the point when the mischance happens the alarm message is sent consequently to the save group and to the police headquarters. The message is sent through the GSM module and the area of the mischance is recognized with the assistance of the GPS module. The mishap can be distinguished definitely with the assistance of both Arduino controller and vibration sensor. The Angle of the moves over of the auto can likewise be known by the message through the vibration sensor. This application gives the ideal answer for poor crisis offices accommodated the street mishaps in the most possible way.

II. LITERATURE SURVEY

Proposes a develop once a vehicle meets with associate accident straight off Vibration device can set the signal or if an automobile roll over, and small Electro system (MEMS) device can detect the signal and sends it to ARM controller. Microcontroller sends the alert message through the GSM electronic equipment as well as the situation to police room or a rescue team. Therefore, the police will straight off trace the situation through the GPS electronic equipment, when receiving the data[1]. Proposes this paper implies a system that may be an answer to the present downside. The measuring device sensing element is utilized in automobile security system to sense vibrations in the vehicle and GPS to grant location by car, thus dangerous driving is detected. Once accident happens, measuring device can notice signal send signal to microcontroller will modify airbag to blow and message with accident location is shipped with pre-programmed numbers love automobile, station house, GSM[2]. Proposes a system consists of 2 units, particularly, Crash Detector Embedded Unit and automaton

management Unit. Crash Detector Embedded Unit is liable to detection the accident condition victimization three-axis measuring system detector, position encoder, bumper detector and one warning switch [3].A road accidents represent the main a part of the accident. The purpose of the project is the vehicle wherever it's and finds the vehicle by means that of causing a message employing a system that is placed within the vehicle system. Most of the day could not be ready to find accident location as a result of don't grasp wherever accident can happen[4]. The numerous techniques that are contributed from the electronic systems are embedded in automobile industry to minimize the accidents caused by the vehicles. It's focused on the automatic collision detection and warning system depending on the GPS and GSM. The vehicle secured is to be mounted with the system firmly confirming good mechanical oriented with the complete framework [5]. A framework guarantees making crisis offices accessible to mishap casualties as right on time as conceivable by letting relatives, healing centre or a protest group know the mischance spot with the assistance of this module inserted in the vehicle. Sensors are appended to the microcontroller. On the off chance that there is a mishap, the sensor gets initiated and the GSM framework will send notices to the closest healing centre, police headquarters or sort of the casualty with the area arranges where the mischance has happened[6]. Proposes a road accidents represent the key a part of the accident. The purpose of the project is to search out the vehicle wherever it's and find the vehicle by means that of causing a message employing a system that is placed within vehicle system, most of the day not be able to notice the accident location as a result of don't recognize wherever accident can happen[7].

2.1 Block Diagram

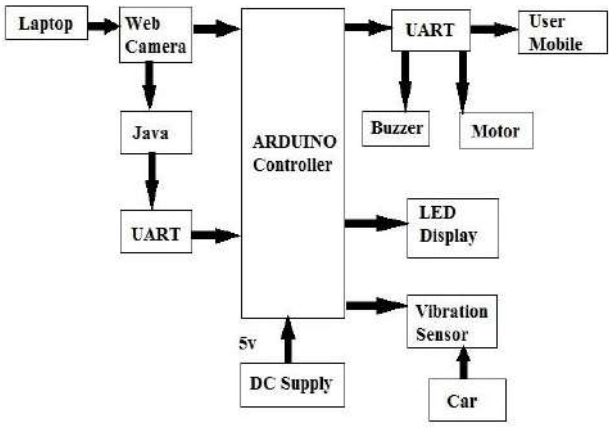

FIG.1.ARTCHITECTURE OF VEHICLE COLLISION

2.2 Existing System

About 1.3 million people kick the bucket in street crashes each year, on the normal three, 287 passing is every day. A further 20-50 million are debilitated or crippled. A very large portion of all street activity passing is happen between youthful grownups age's 15-44. Activity is on the expansion on the grounds that the interest in vehicles is getting higher step by step. In this way, transportation wants change as, since requests are expanding, there will be extra odds of auto crashes. Vehicle mishaps are one among the main sources of the casualty. Normally experience the established truth that once A mishap happens the people close got to physically choose the car that winds up in misuse of your chance.

A substantial assortment of valuable lives is a unit lost on account of streetcar crashes a day. The basic reasons are a unit driver's misstep and late reaction from crisis administrations. There is a need to have a decent street mishap discovery and information, correspondence framework in situation to abstain from squandering lack persons. A framework that sends data messages to close crisis administrations concerning the mischance for auspicious reaction is absolutely in might want. In examination writing, assortment of programs mishap recognition frameworks is a unit anticipated by changing scientists.

2.3 Disadvantages

It will be a serious consequence if people can't get help on right time. Poor emergency incident is a major cause of death rate in our country. Hence there is a delay for emergency services to arrive at the location of the accident.

III. METHODOLOGY

Figure [1] shows that the block diagram for car accident detection and monitoring process. Here first of all we have used power supply of +5V for Arduino controller. Arduino controller is the heart of our project. The inputs are taken from various sensors which is given to Arduino controller. The main objective is to reduce the road side accident, while the vehicle enter into toll booth its need a pass entry to move out.

The web camera capture the image of the number plate the way of conversion of java. That move a Universal Asynchronous Receiver/Transmitter(UART). UART transmit into the Arduino controller handle the power from the DC supply; transmitter can act as in two different paths as authorized and unauthorized vehicle alert it's like to monitoring about buzzer and motor for entry. After passing the booth, whether the accident occurred, they can sense by vibration sensor pass the information with a second. Displays the accident detection using the LED display. Finally, its pass into the emergency service and relatives.

IV. PROPOSED SYSTEM

Consistently around the globe, a huge level of individuals kicks the bucket from car crash wounds. A successful approach for diminishing movement, casualty is first building programmed auto collision location framework, second, decreasing the time between when a mischance happens and when first crisis responders are dispatched to the scene of the mishap. Late methodologies are utilizing are working in vehicle programmed mishap discovery and warning framework. While these methodologies work fine, they are costly, upkeep complex errand, and are not accessible in all autos.

The proposed framework comprises of two stages; the identification stage, which is utilized to identify fender bender in low and high speeds. The notice stage, and quickly after a mishap is shown, is utilized to send definite data, for example, pictures, video, mischance area, and so on to the crisis responder for quick recuperation. The framework was essentially trying in genuine reproduced condition and accomplished very great execution comes about. It is a need of acquainting a framework with diminished the death toll because of mischance and the time taken by the rescue vehicle to achieve the healing centre.

To conquer the downside of existing framework will execute the new framework in which there is a programmed recognition of mishap through sensors gave in the vehicle. A primary server contains a rundown of all doctor's facilities in the city. The principle and sends the exact accident location to the emergency vehicle.

4.1 Flow Chart

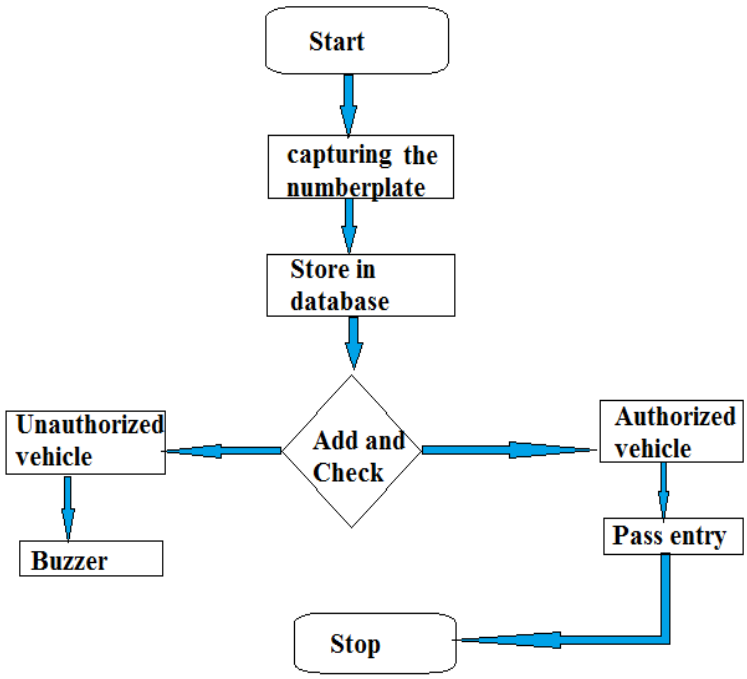

FIG.2. TOLL BOOTH ENTRY

V. LIST OF MODULES

5.1 Checking Number Plate

The ETC (Electronic Toll Collection) aims to eliminate the delay on toll roads by cashless tolling and it is rapidly becoming the most innovative technology for the commuters who pass through the toll plaza. Focuses on an ETC system using ANPR (Automated Number Plate Recognition) technology. The Automated Number Plate is used for detecting crime through intelligence monitoring.

5.2 Vibration Sensor Analysis

Vibration sensor (Piezo elements) comes in handy when you need to detect vibration or a knock. Can use these for tap or knock sensors pretty easily by reading the voltage on the output. Vibration sensor helps to send the signal to Arudino controller. Arudino controllers send the alert message through GSM modem with location. If the person meets a small accident, the driver can inform attention is not required by terminating the message using switch. This is to avoid wasting the time of the medical and police team.

5.3 Sending the Message

GPS stands for Global Positioning System and used to detect the Latitude and Longitude of any location on the Earth, with exact UTC time (Universal Time Coordinated). GPS module is used to track the location of accident in our project. This device receives the coordinates from the satellite for each and every second, with time and date. Previously extracted string in Vehicle Tracking System to find the Latitude and Longitude Coordinates. GSM modem is similar to mobile phone without any display, keypad and speakers. This accepts a SIM card, and operates over a subscription to a mobile operator.

5.4 Tracking Location

Automatic vehicle location could be suggests that for mechanically decisive and transmittal the geographic location of a vehicle. This vehicle location knowledge, from one or a lot of vehicles, could then be collected by a vehicle following system to manage a summary of auto travel. As of 2017, GPS technology has reached the purpose of getting the transmittal device is smaller than the dimensions of an individual's thumb ready to run half-dozen months or a lot of between batteries charging, straightforward to speak with smart phones merely requiring a replica SIM card from one's. Most commonly, the location is determined using GPS and the transmission mechanism is SMS, GPRS, or a satellite or terrestrial radio from the vehicle to a radio receiver. A single antenna unit covering all the needed frequency bands can be employed. GSM most common services applied, because of the low data rate needed for AVL, and the low cost and near-ubiquitous nature of these public networks.

VI. HARDWARE DESCRIPTION

6.1 Arduino

Arduino controller is the brain of our project. UNO SMD R3 used. It is a 14 digital pin and 6 analog pin that may be interfaced to various expansion boards and other circuits. Arduino is Associate in Nursing open supply component and code organization, and client group that styles and fabricates single-board microcontrollers.

6.2 Vibration Sensor

Vibration sensor is used to detect the particular environment area. The three parameters representing motion detected by vibration monitors are displacement, velocity, and acceleration.

FIG.3.ARDUINO UNO

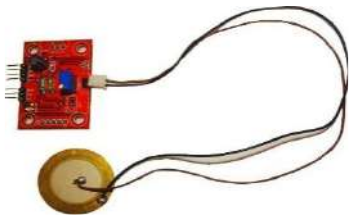

FIG.4.VIBRATION SENSOR

FIG.5.RELAY

6.3 Relay

A relay is an associate magnetic attraction switch operated by a comparatively tiny current that may activate or off a far larger current in our project. The center of a relay is associate magnet. Relays are switches that open and shut circuits electromechanical or electronically. Arduino is controlling a 5V Relay to operate high voltage AC appliances and devices.

6.4 Buzzer Alarm

A buzzer or pager is AN audio signalling device, which can be mechanical, mechanical device, or electricity. Typical uses of buzzers and beepers embrace alarm devices, timers, and confirmation of user input reminiscent of a depression or keystroke.

FIG.6.BUZZER ALARM

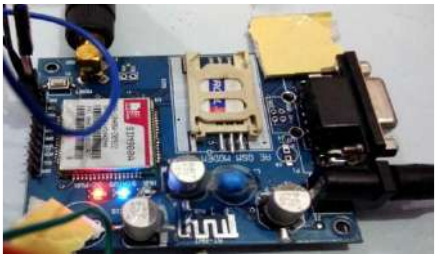

FIG.7.GSM

FIG.8.GPS MODULE

6.5 GSM Module

GSM is employed as a medium that is employed to manage and monitor the electrical device to load from any place by causation a message.M95 QUECTEL Modem used. It's own settled character. Thereby, here GSM is employed to watch and manage the DC motor, Stepper motor, Temperature detector and Solid State Relay by causation a message through GSM electronic equipment.

6.6 GPS Module

GPS is employed in vehicles for each trailing and navigation. SIM900A Modem used. Trailing systems alter a base station to stay track of the vehicles while not the intervention of the driving force wherever, as navigation system helps the driving force to achieve the destination.

VII. RESULT AND DISCUSSION

In proposing system it enhances this problem by using messaging and tracking system. First, it is used to manage the vehicle number plate in a toll booth. If it is authorized there if capture the number plate and store it in a database. After that, if the accident was occurring in-between booths, the message alert is intimated to the nearby police station and hospital using GSM, by using GPS location is tracked.

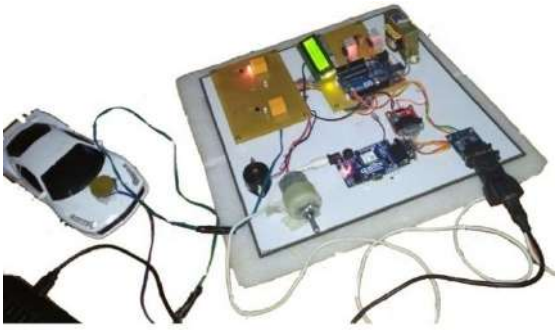

FIG.9. OUTPUT OF THE PROPOSED SYSTEM

VIII. CONCLUSION

In this mode, the modernizing supported the reduction of road facet accident. Ordinarily it has associate expertise concerning passing vehicle through the tollbooth, there it's want to pay a fee then our vehicle number plate was trying to next step of entry. Around this idea, modernizing was enhanced by the preceding session, if the accident arose in association spot there a

machine use to make a salve for the delay. However, here change return by the electronic messaging system to their relatives and machine by victimization GSM, to understand the position of the vehicle by victimization GPS.

IX. FUTURE WORK

In future, the public person can know to drive the car carefully, but if there is any unfortunate accident happens it is useful to find out the location and alert SMS send to a nearby police station and hospital within a second. It will decrease the death rate through the process of "Right Information at Right Time". While it works in every place definitely it's a peak achievement to save our people live.

REFERENCES

[1] Khyati Shah, Vile Parle, Swati Bairagi,Vile Parle "Accident Detection and Conveyor System using GSM and GPS Module" International journal of Computer Applications (0975-8887) Voluma-176-No.2,October 2017.

[2] Pooja Shindalkar, Aasiya Fatema Shaikh, Chaitanya Mate, "Arduino Based Vehicle Accident Detection System", International journal of Innovative Research in Computer and Communication Engineering (An 3297:2007 certified organization) Vol.5, Issue 4,April 2017.

[3] E.Krishna Priya, P.Manju, V.Mythra, "IoT Based Vehicle Tracking and Accident Detection System" International journal of Innovative Research in Computer and Communication Engineering, (An ISO 3297:2007 Certified organization) Vol.5,Issue 3, March 2017.

[4] Surekha Pinnapati, Manjunath Kamath K, Carmal Joseph, "Automatic Accident Detection and Alerting System Based on IOT" International Journal of Innovative Research in Computer and Communication Engineering (An ISO 3297:2007 Certified organization) Vol.5,Issue5, May 2017.

[5] Jazim Baramy, Pragya Singh, Aryasheel Jadhav, " Accident Detection & Alerting System", International journal of Technical Research and Application e-ISSN 2320-8163, March 2016.

[6] A.Vairavan, S.Karalika, "An Automatic Warning Alert System for Accident Detection using GPS and GSM " SSRG International journal of Industrial Engineering (SSRG-IJIE)- Volume 3 Issue 6 – Nov to Dec 2016

[7] Namrata H. Sane Damini S. PatilSnehal D. "Real Time Vehicle Accident Detection and Tracking Using GPS and GSM" International journalon Recent and Innovation Trends in Computing and Communication, Issue-4,Vol.4 April 2016.

[8] Vikram singh Kushwaha, Abusayeed Topinkatti, "Car Accident Detection System Using GPS and GSM", International journal of Emerging Trend in Engineering and Basic Science(IJEEBS) Vol.2, Feb 2015

[9] Aboli Ravindra Wakure, Apurva Rajendra Patkar, "Vehicle Accident Detection and Reporting System Using GPS and GSM" International Journal of Engineering research and Development, Vol.10, Issue 4, April 2014

[10] C.Prabha, R.Sunitha, R.Anitha, "Automatic Vehicle Accident Detection and Messaging System Using GSM and GPS Modem", International Journal of Advanced Research in Electrical and Electronic and Instrumentation Engineering (An ISO 3297:2007 Certified organization) Vol.3, Issue 7, July 2014.

AD Publications
Sector-3, MP Nagar, Bikaner,
Rajasthan, India
www.adpublications.org, info@adpublications.org